LBL-6094
c.1

SIMULTANEOUS REACTIONS ON A ROTATING-DISK ELECTRODE

Ralph Edward White
(Ph. D. thesis)

March 1977

Prepared for the U. S. Energy Research and Development Administration under Contract W-7405-ENG-48

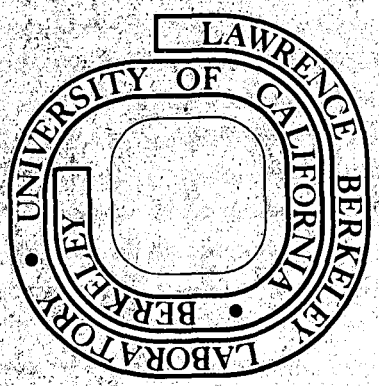

LBL-6094
c.1

DISCLAIMER

LBL-6094

SIMULTANEOUS REACTIONS ON A ROTATING-DISK ELECTRODE

Ralph Edward White

Materials and Molecular Research Division, Lawrence Berkeley Laboratory,
and Department of Chemical Engineering, University of California,
Berkeley, California 94720

March 1977

for Carolyn

Simultaneous Reactions on a Rotating-Disk Electrode

Contents

Simultaneous Reactions on a Rotating-Disk Electrode

Ralph Edward White

Materials and Molecular Research Division, Lawrence Berkeley Laboratory, and Department of Chemical Engineering, University of California, Berkeley, California 94720

Abstract

Multiple reactions at a rotating-disk electrode are modeled in this dissertation for two cases. In the first case, the governing equations, which do not include the effect of ionic migration but do include the radial dependence of the concentrations and potential, are used to generate a parameter which characterizes the effect of a side reaction on the limiting-current curve of a main reaction. Various predicted current-potential curves illustrate the importance of this parameter for copper deposition with simultaneous formation of dissolved hydrogen at a disk electrode rotating in a copper sulfate solution containing sulfuric acid.

Predicted and measured limiting-current curves for this system are compared. In addition, distributions of current, potential, and surface concentration on the disk indicate that in some cases the main reaction can be below its limiting rate at the center of the disk while hydrogen gas bubbles may be formed near the edge.

In the second case, deposition of copper from an aqueous solution containing cupric and ferric chloride is modeled. The potential distribution and concentration profiles within the diffusion layer are predicted for given potential differences between the electrode and the solution.

A cuprous ion, which is formed by the reduction of the complexed cupric ion at the electrode, is stabilized in the chloride solution and can react either at the electrode or with ferric species within the diffusion layer. The assumptions that this homogeneous reaction is fast and irreversible generates a reaction plane, whose position is shown in the concentration and potential profiles. In addition, the position of the reaction plane is plotted as a function of the potential difference between the electrode and the adjacent solution. Predicted current-potential and current efficiency-potential curves are also reported. Finally, the iron contamination of the deposited copper is estimated to be less than 10^{-5} atom percent for some cases.

However, because some of the partial current densities are below their limiting values, the analysis is strictly valid only at the center of the disk.

Work performed under the auspices of the U. S. Energy Research and Development Administration.

Chapter 1. Copper Deposition from an Aqueous, Acidic Copper Sulfate Solution

Introduction

The rotating-disk electrode is a popular experimental tool.[1-6] It has been used, for example, to measure diffusion coefficients, investigate metal deposition and organic synthesis, determine bulk concentrations of electroactive species, and study corrosion. Multiple electrode reactions occur invariably to some extent in all of these cases. To help understand better their effect, a model of an electrochemical cell consisting of a rotating-disk electrode on which multiple reactions can occur, a distant counterelectrode, and a reference electrode of a given kind is presented.

A similar model[7] is presented in chapter 2, which includes multiple electrode reactions and the effect of ionic migration but neglects the nonuniformity of the ohmic potential drop in solution. The present model includes this effect but neglects that due to ionic migration within the diffusion layer.

The model is similar to ones presented earlier.[8-28]

Model

Assumptions

The following assumptions apply to the model:

1. There are two types of species: major and minor. The major species are the dissociation products of the supporting electrolyte; all other species are minor. The concentration of supporting electrolyte is constant. Minor species are transported according to the theory of transport processes in infinitely dilute electrolytic solutions.[22]

Diffusion coefficients and other physical properties of the solution depend only on the bulk composition.

2. The diffusion potential difference across the diffusion layer is negligible. Also, the potential in a separate reference-electrode compartment is assumed to be the same as that in the bulk solution at the entrance to the connecting capillary tube.

3. The local current density just outside the diffuse double layer on the rotating-disk electrode is the same as that at the outer edge of the diffusion layer.

4. The surface of the disk remains uniformly smooth during metal deposition.

5. The system is isothermal and operated at steady state, so that charging currents are negligible.

6. The Schmidt number of each minor species is large.

Bulk solution

The potential distribution in the solution outside the diffusion layer is governed by Laplace's equation. For the disk geometry, the general solution satisfying the condition of an insulating plane surrounding a disk electrode of radius r_o and remaining finite on the axis of the disk, can be expressed as[10,21]

$$\tilde{\Phi}(\eta,\xi) = \sum_{n=0}^{\infty} B_n P_{2n}(\eta) M_{2n}(\xi) \quad , \qquad (1\text{-}1)$$

where η and ξ are rotational elliptic coordinates, natural to the disk geometry, and are related to cylindrical coordinates r and z by the relationships

$$z = r_o \xi \eta \tag{1-2}$$

and

$$r = r_o[(1 + \xi^2)(1 - \eta^2)]^{1/2} . \tag{1-3}$$

$P_{2n}(\eta)$ is the Legendre polynomial of order $2n$, and $M_{2n}(\xi)$ is a corresponding Legendre function of imaginary argument[10,29] normalized in such a way that $M_{2n} = 1$ at $\xi = 0$. The potential distribution in equation 1 also approaches zero as ξ approaches infinity, corresponding to a distant placement of the counterelectrode.

Diffusion layer

When the effect of ionic migration is ignored, the concentrations of minor species are found to satisfy the equation of convective diffusion. For the high values of the Schmidt number ν/D_i commonly enountered in electrolytic solutions, the velocity profiles can be approximated by their forms close to the disk surface, and this equation can be solved even though the concentration of a species is not constant along the surface. The resulting normal component of the flux density at the surface can be expressed as an integral over this variation of the surface concentration:[11,30,31]

$$N_i(r) = -D_i \left.\frac{\partial c_i}{\partial z}\right|_{z=0} = \frac{-(D_i^2 D_R)^{1/3}}{\delta_d \Gamma(4/3)} \left[c_{i,\infty} - c_{i,o}(0) - r \int_o^r \frac{dc_{i,o}(x)}{dx} \frac{dx}{(r^3 - x^3)^{1/3}} \right] , \tag{1-4}$$

where δ_d is the diffusion-layer thickness,

$$\delta_d = \left(\frac{3D_R}{a\nu}\right)^{1/3} \left(\frac{\nu}{\Omega}\right)^{1/2} , \qquad (1\text{-}5)$$

based on the diffusion coefficient D_R of the principal reactant, the rotation speed Ω, and the kinematic viscosity ν of the fluid.

Current densities and multiple reactions

An electrochemical reaction j can be written abstractly as

$$\sum_i s_{ij} M_i^{z_i} \rightarrow n_j e^- , \qquad (1\text{-}6)$$

where n_j denotes the number of electrons transferred and M_i represents species i, z_i its charge number, and s_{ij} its stoichiometric coefficient. Let the rate of each possible reaction be represented by the value i_j of its contribution to the total (local) electrode current density i_T. Then the flux of a solution species at the electrode surface is given in the steady state by Faraday's law:

$$N_i(r) = - \sum_j \frac{s_{ij} i_j}{n_j F} . \qquad (1\text{-}7)$$

It has furthermore been assumed that the diffusion layer is so thin that the total current density can be obtained either from the sum of partial current densities for the electrode reactions or from the derivative of the potential distribution (equation 1) prevailing outside the diffusion layer:

$$i_T(r) = \sum_j i_j = -\kappa_\infty \left.\frac{\partial \tilde{\Phi}}{\partial z}\right|_{z=0} , \qquad (1\text{-}8)$$

where κ_∞ is the conductivity of the bulk solution. The orthogonality of the Legendre polynomials and the values[10,21] of $M'_{2n}(0)$ permit the coefficient B_n in equation 1 to be expressed as an integral over the electrode current density i_T :

$$B_n = [P_{2n}(0)]^2 \frac{(4n+1)\pi r_o}{2\kappa_\infty} \int_0^1 \eta i_T P_{2n}(\eta) d\eta . \qquad (1\text{-}9)$$

The local current density due to reaction j is related to the surface overpotential for reaction j and the surface concentrations of the species by the Butler-Volmer equation

$$i_j = i_{oj,ref} \prod_i \left(\frac{c_{i,o}}{c_{i,ref}}\right)^{\gamma_{ij}} \left[\exp\left(\frac{\alpha_{aj} F}{RT} \eta_{sj}\right) - \exp\left(-\frac{\alpha_{cj} F}{RT} \eta_{sj}\right)\right] , \qquad (1\text{-}10)$$

where $c_{i,ref}$ is a reference concentration, $i_{oj,ref}$ is a value of the exchange current density for reaction j calculated at the composition $c_{i,ref}$, and γ_{ij} is an exponent expressing the composition dependence of the exchange current density.

The surface overpotential η_{sj} for reaction j can be expressed as

$$\eta_{sj} = V - \Phi_o - U_{j,o} , \qquad (1\text{-}11)$$

that is, it is the difference between the electrode potential V and

the potential $\Phi_o(r)$ in the solution just outside the diffuse part of the double layer, minus the theoretical open-circuit potential $U_{j,o}$ for reaction j. Both Φ_o and $U_{j,o}$ are measured by a reference electrode of a given kind, corrected for any liquid-junction potential which might exist between the solution in question and that within the reference-electrode compartment (see section 40 of reference 22). $U_{j,o}(r)$ is related to the local solution composition as well as the nature of the reference electrode. In the dilute-solution approximation used here, activity-coefficient corrections can be ignored, and this relationship becomes

$$U_{j,o} = U_j^\theta - U_{re}^\theta - \frac{RT}{n_j F} \sum_i s_{ij} \ln \left(\frac{c_{i,o}}{\rho_o} \right) + \frac{RT}{n_{re} F} \sum_i s_{i,re} \ln \left(\frac{c_{i,re}}{\rho_o} \right) . \quad (1\text{-}12)$$

If the usual tabulations of standard electrode potentials are used for U_j^θ and U_{re}^θ, the concentrations in equation 12 must be expressed in moles/liter. Alternatively, the pure solvent density ρ_o can be expressed in kg/cm^3 instead of g/cm^3. (See Appendix A.)

If we set ξ equal to zero in equation 1, we obtain $\tilde{\Phi}_o$, the potential in the bulk solution extrapolated to the electrode surface as if the current distribution was unchanged but there were no concentration variation in the diffusion layer. With the supporting-electrolyte approximation used here, Φ_o in equation 11 is indistinguishable from $\tilde{\Phi}_o$ because any diffusion potential and any conductivity variation across the diffusion layer are neglected.

Parameters

It is frequently useful to introduce a dimensionless formulation of the problem because in this manner it is possible to identify a small number of dimensionless parameters which govern a system. These may specify laws of similitude which show how the system depends on size or rotation speed, and in favorable situations it may be possible to compute general solutions which apply to a number of different chemical systems over a range of compositions and temperatures. These are very useful for instruction, scale-up, and for drawing general conclusions about system behavior.

However, the reduction in the number of parameters is limited for complex systems where there are several relevant species in solution and several possible electrode reactions. For example, if the potentials, including overpotentials and open-circuit potentials, are made dimensionless with RT/F, there remain as dimensionless parameters the transfer coefficients of the electrode reactions. Even if one recognizes that cathodic processes with a main reaction m are most important and makes the potentials dimensionless with $RT/\alpha_{cm}F$, there remain the ratios of the transfer coefficients to α_{cm}. Furthermore, there are the exponents γ_{ij} and the ratio of the stoichiometric coefficients s_{ij} to n_j. For the minor species, there are the bulk composition, the reference concentrations $c_{i,ref}$, and the ratios D_i/D_R of diffusion coefficients to that of the principal reactant. (One cannot generally set $c_{i,ref}$ equal to $c_{i,\infty}$ because some species may not be present in the bulk solution.) These considerations suggest that we must deal with specific chemical systems or a narrow class of systems.

Nevertheless, even for specific systems it will be instructive to introduce parameters related to the size and the rotation speed. When we are concerned with the effects of a nonuniform ohmic potential drop in the solution, current densities should be made dimensionless with $RT\kappa_\infty/Fr_o$, or with $|s_{Rm}/n_m|\ RT\kappa_\infty/Fr_o$ to be consistent with previous work.[10] The dimensionless average current density is then

$$\delta = \frac{-n_m Fr_o}{s_{Rm} RT\kappa_\infty} i_{avg} , \tag{1-13}$$

and dimensionless exchange current densities are

$$J_j = -\frac{n_m}{s_{Rm}} \frac{Fr_o}{RT\kappa_\infty} i_{oj,ref} . \tag{1-14}$$

According to the Levich equation,[32] the limiting current density for the principal reactant is

$$i_{m,lim} = \frac{n_m F D_R c_{R,\infty}}{s_{Rm} \Gamma(4/3) \delta_d} . \tag{1-15}$$

This leads to the dimensionless limiting-current density*

$$N = \Gamma(4/3) \frac{n_m Fr_o}{s_{Rm} RT\kappa_\infty} i_{m,lim} = \frac{n_m^2 F^2 D_R c_{R,\infty}}{s_{Rm}^2 RT\kappa_\infty} \left(\frac{a\nu}{3D_R}\right)^{1/3} \left(\frac{r_o^2 \Omega}{\nu}\right)^{1/2} , \tag{1-16}$$

which can also be thought of as a dimensionless (square root of) rotation speed.

*To be consistent with earlier work,[10] $\Gamma(4/3)$ is inserted as shown.

Let us also identify a single parameter which will characterize the manner in which a side reaction tends to obscure the limiting-current plateau for a main, or desired, reaction. It is the magnitude of the side reaction relative to the main reaction at potentials in the neighborhood of the limiting-current plateau which is important (see figure 1). At these potentials, it is unlikely that the backward terms in the Butler-Volmer equation 10 have a major influence, and a Tafel approximation could be applied for both the main and side reactions. For our example, the cathodic processes are involved.

The electrode potential V_m for which the main reaction is beginning to reach the limiting current is, in the absence of an ohmic potential drop, approximately equal to

$$V_m = U_{m,ref} - \frac{RT}{\alpha_{cm} F} \ln\left(-\frac{i_{m,lim}}{i_{om,ref}}\right) , \qquad (1\text{-}17)$$

where $U_{m,ref}$ is given by equation 12 but with reference concentrations in place of the surface concentrations. At this potential defined by equation 17, the current density for the side reaction j divided by the limiting current density for the main reaction (see equation 15) is proportional to $\exp(-\alpha_{cj} F \Delta U_j / RT)$, where

$$\Delta U_j = U_{m,ref} - U_{j,ref} - \frac{RT}{\alpha_{cj} F} \ln\left(-\frac{i_{oj,ref}}{i_{m,lim}}\right) + \frac{RT}{\alpha_{cm} F} \ln\left(-\frac{i_{om,ref}}{i_{m,lim}}\right) . \qquad (1\text{-}18)$$

This parameter makes it clear that it is neither the exchange current density nor the open-circuit potential alone which determines the

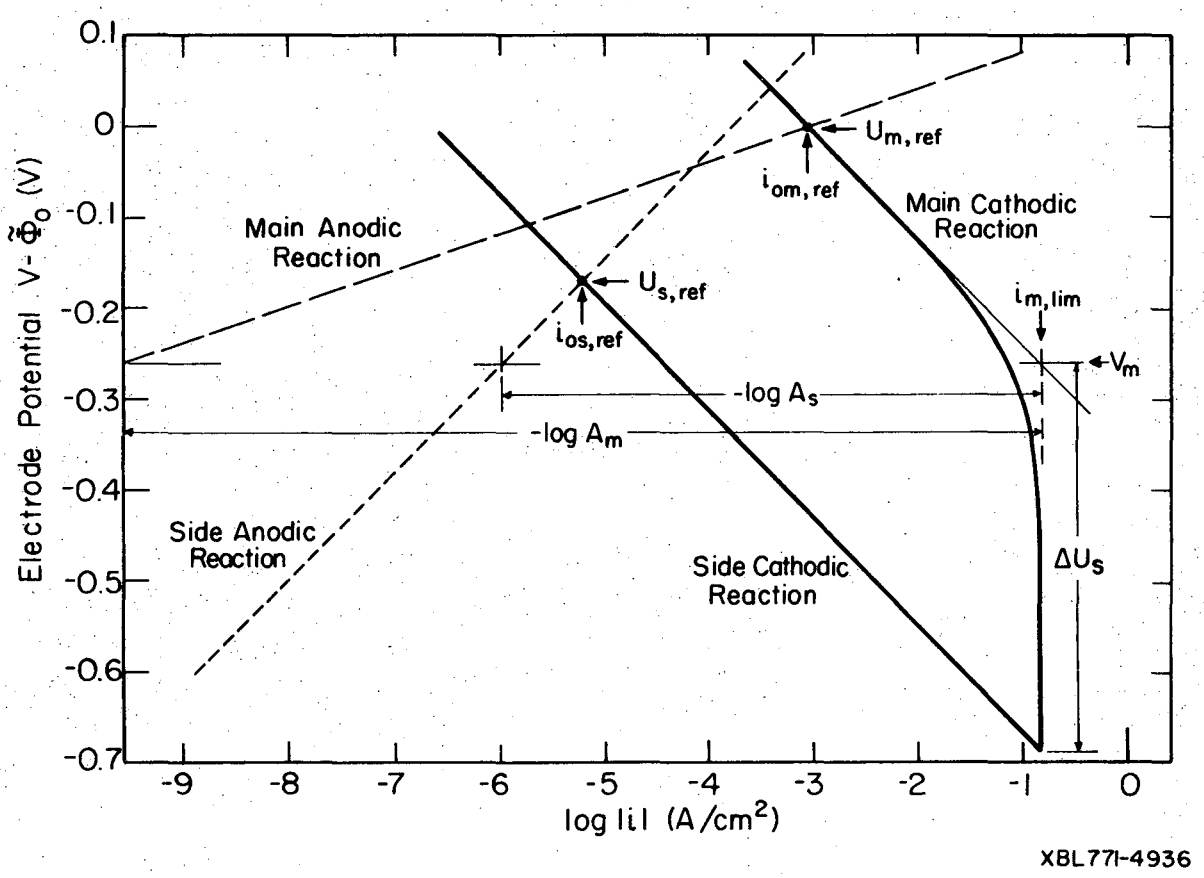

Figure 1-1. Qualitative sketch of the current-potential curves for a main and a side reaction showing some of the parameters defined in the text.

relative significance of a side reaction. If either the exchange current density is very small or the open-circuit potential is quite negative, the side reaction will not obscure the limiting-current plateau.

In the case of a corrosion process, a different selection of parameters would be appropriate, one placing emphasis on the anodic part of one reaction and the cathodic part of another reaction.

If equations 7, 10, and 11 are substituted into equation 4 and use is made of the definitions in equations 12, 15, 17, and 18, one obtains the equation (one for each minor species i)

$$\frac{s_{Rm}}{n_m}\frac{(D_i/D_R)^{2/3}}{c_{R\infty}}\left[c_{i,\infty} - c_{i,o}(0) - r\int_o^r \frac{dc_{i,o}}{dx}\frac{dx}{(r^3-x^3)^{1/3}}\right]$$

$$= \sum_j \frac{s_{ij}}{n_j} \exp\left(-\frac{\alpha_{cj}F}{RT}\Delta U_j\right) \exp\left[-\frac{\alpha_{cj}F}{RT}(V - V_m - \tilde{\Phi}_o)\right] \prod_k \left(\frac{c_{k,o}}{c_{k,ref}}\right)^{q_{kj}}$$

$$- \sum_j \frac{s_{ij}}{n_j} A_j \exp\left[\frac{\alpha_{aj}F}{RT}(V - V_m - \tilde{\Phi}_o)\right] \prod_k \left(\frac{c_{k,o}}{c_{k,ref}}\right)^{p_{kj}}, \quad (1\text{-}19)$$

where the cathodic and anodic reaction orders are

$$q_{kj} = \gamma_{kj} - \alpha_{cj}\frac{s_{kj}}{n_j} \quad \text{and} \quad p_{kj} = \gamma_{kj} + \alpha_{aj}\frac{s_{kj}}{n_j} \quad (1\text{-}20)$$

and the parameter

$$A_j = \left|\frac{i_{oj,ref}}{i_{m,lim}}\right|^{1+\alpha_{aj}/\alpha_{cj}} \exp\left(\frac{\alpha_{aj}F}{RT}\Delta U_j\right) \quad (1\text{-}21)$$

characterizes the magnitude of the anodic part of reaction j at an electrode potential related to the limiting-current plateau for the main reaction. The influence of the parameter A_m for a main reaction alone on the shape of limiting-current curves was investigated in 1955 by Gerischer[33] (see also references 5 and 34). (See Appendix B.)

Solution Technique

As in earlier work,[12] one alternates between revising the surface concentrations and improving the potential distribution, iterating between the two until no further improvement is noticed.

For a given distribution of $V - \tilde{\Phi}_o$, equation 19 (one for each minor species i) governs the surface concentration distributions $c_{i,o}$. For calculational convenience, we specify $c_{R,o}$ at the center of the disk. Equation 19 is solved by a multidimensional Newton-Raphson iteration method for the value of $V - \tilde{\Phi}_o$ and the other values of $c_{i,o}$ at the center of the disk. As a start, it is assumed that this potential difference applies across the whole surface of the electrode.

More generally, with the best possible radial distribution of $V - \tilde{\Phi}_o$, equation 19 is solved for the surface concentration distributions by a generalization of the technique of Acrivos and Chambré.[35] This involves evaluation of the integrals by means of discrete mesh points evenly spaced in r^3. One proceeds from the center of the electrode toward its edge, and at each mesh point he solves the coupled equations 19 by the multidimensional Newton-Raphson method. This procedure gives implicitly the distribution of current density for each reaction j and hence for the total current density i_T.

From the current-density distribution determined above, one next calculates a new distribution of potential $\tilde{\Phi}_o$ from equation 1 after first calculating a finite number of values of B_n by means of equation 9. (A damping technique, whereby $\tilde{\Phi}_o$ values are averaged with previously estimated values, can be used here to speed overall convergence.) The value of V is adjusted so that $V - \tilde{\Phi}_o$ at the center of the disk is the same as that originally calculated.

The procedure in the last two paragraphs is repeated until a convergence criterion is satisfied. (See Appendix B.)

Results and Discussion

The utility of the model is demonstrated by the simulation of copper deposition

$$Cu^{++} + 2e^- \rightarrow Cu \ , \qquad (1\text{-}22)$$

as the main reaction and the formation of dissolved hydrogen

$$H^+ + e^- \rightarrow \frac{1}{2} H_2 \ , \qquad (1\text{-}23)$$

as the side reaction. Table 1 gives parameters for these processes in a cupric sulfate solution containing sulfuric acid, where the kinematic viscosity* is $\nu = 0.010795$ cm^2/s and the bulk conductivity** is $\kappa_\infty = 0.54373$ $ohm^{-1} - cm^{-1}$. The cathodic transfer coefficients were set equal to 0.5; the anodic transfer coefficients were set equal

*Average value for the polarograms shown in figure 2.[36]
**Determined from Hsueh's correlation.[37]

Table 1. Parameter values for copper deposition at 298.15 K. The exchange current densities and the diffusion coefficient of cupric ions were determined by fitting the model to the data. The reference concentration for H_2 corresponds to the solubility in water at one atmosphere partial pressure.

Species	$10^6 D_i$	$c_{i,\infty}$	$c_{i,ref}$	γ_{im}	γ_{is}
	cm^2/s	mol/l	mol/l		
Cu^{++}	7.5	5.81×10^{-3}	$c_{R,\infty}$	0.42[b]	0
H_2	38[a]	4.155×10^{-10}	8.31×10^{-4}	0	0.25
H^+	——	1.5[c]	1.5[c]	0	0.5

Reaction	$U_j^\ominus$	$i_{oj,ref}$
	V	A/cm^2
main	0.337	9.08×10^{-4}
side	0	6.124×10^{-6}

[a] Arbitrarily selected for this work. (See reference 38).

[b] Taken from reference 22 (see also reference 39).

[c] It is assumed here that the dissociation products of H_2SO_4 are H^+ and HSO_4^- and that the bisulfate ion does not dissociate.

to 1.5 and 0.5 for the main and side reactions, respectively.

Predicted and measured[40] current-potential curves for this system are shown in figure 2. The comparison was used to determine some of the parameters in table 1. For the choice of transfer coefficients used here, ΔU_s is independent of the rotation speed.

Figure 3 shows how the shape of the current-potential curves depends on N and ΔU_s, where the bulk concentration of the principal reactant and the supporting electrolyte concentration were set equal to 0.1 and 1.0 M, respectively. ΔU_s and N were varied by changing the exchange current density of the side reaction and the disk size, respectively. Hsueh's correlations[37] were used to determine the solution density, viscosity, conductivity, and the cupric ion diffusion coefficient as a function of the bulk concentration of $CuSO_4$ and H_2SO_4, and the rotation speed was set at 2500 rpm (261.8 rad/s). In this case, the anodic portion of the side reaction is negligible in the potential range shown, and the anodic portion of the main reaction is significant only near the open-circuit potential (an abscissa value of 0.19 V). The results are therefore applicable to other systems with similar values of the cathodic transfer coefficients and reaction orders, and they illustrate qualitatively the expected behavior for systems with different parameters.

In figure 4, the desired values of ΔU_s were obtained by varying the bulk concentration of the principal reactant, thereby increasing A_m, while holding $c_{H_2SO_4} = 1.0$ M. Where the anodic

portion of the main reaction is not negligible, figure 4 must be used; otherwise, for values of $V - \tilde{\Phi}_o(r = 0)$ more negative than about -0.025 V , the curves would agree with those of figure 3 if plotted against the same abscissa.

The maximum variation of the potential $\tilde{\Phi}_o$ in the solution across the surface of the disk occurs when the current density distribution is uniform (as, for example, at the limiting current for a single reaction) and then has the value[10,41]

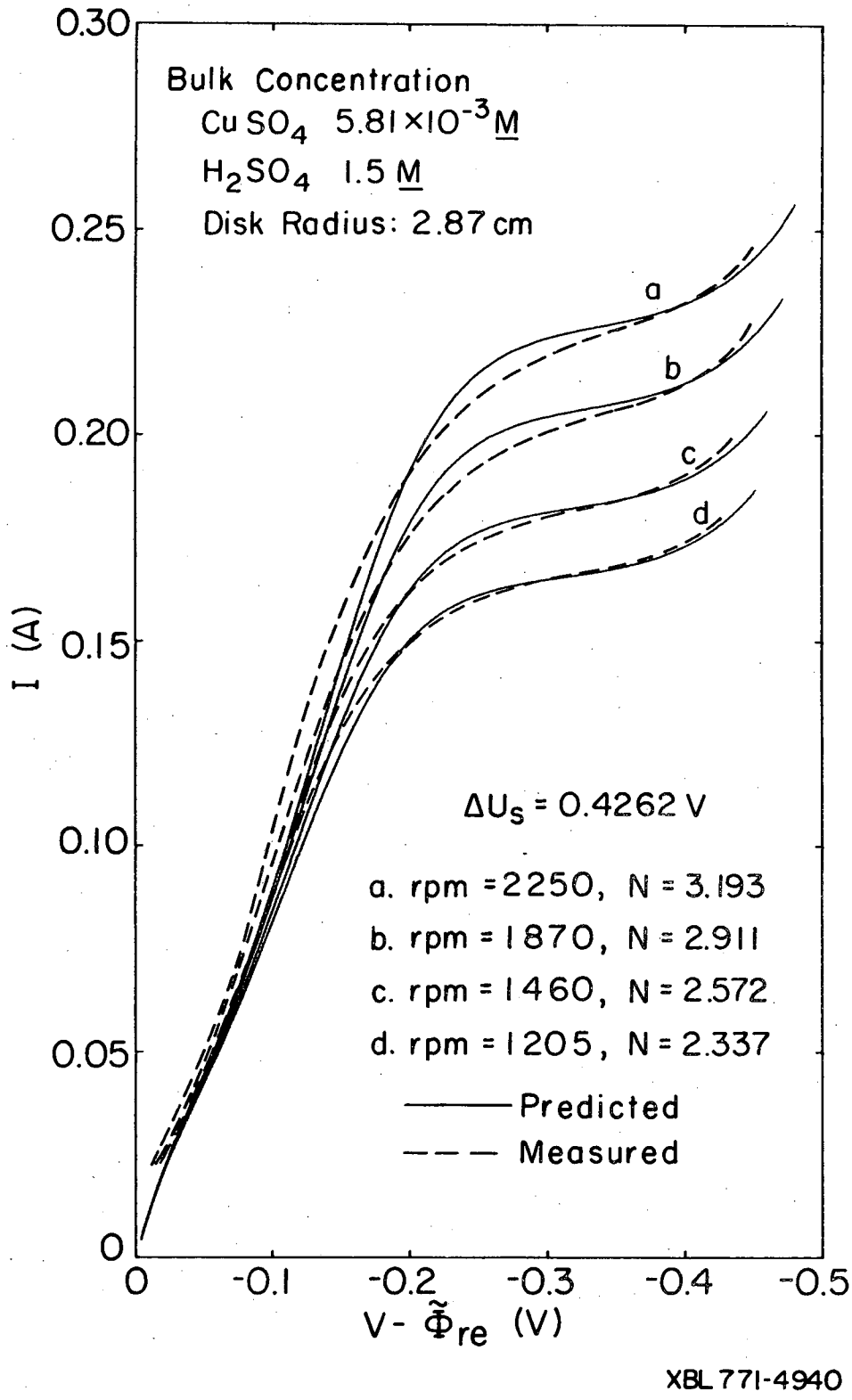

Figure 1-2. Comparison of predicted and measured[40] limiting current curves for copper deposition with simultaneous formation of dissolved hydrogen. The reference electrode was a copper wire located in the bulk solution; its position in the experimental cell was approximated in the model by placing it in the plane of the disk, 5 cm from the axis of rotation.

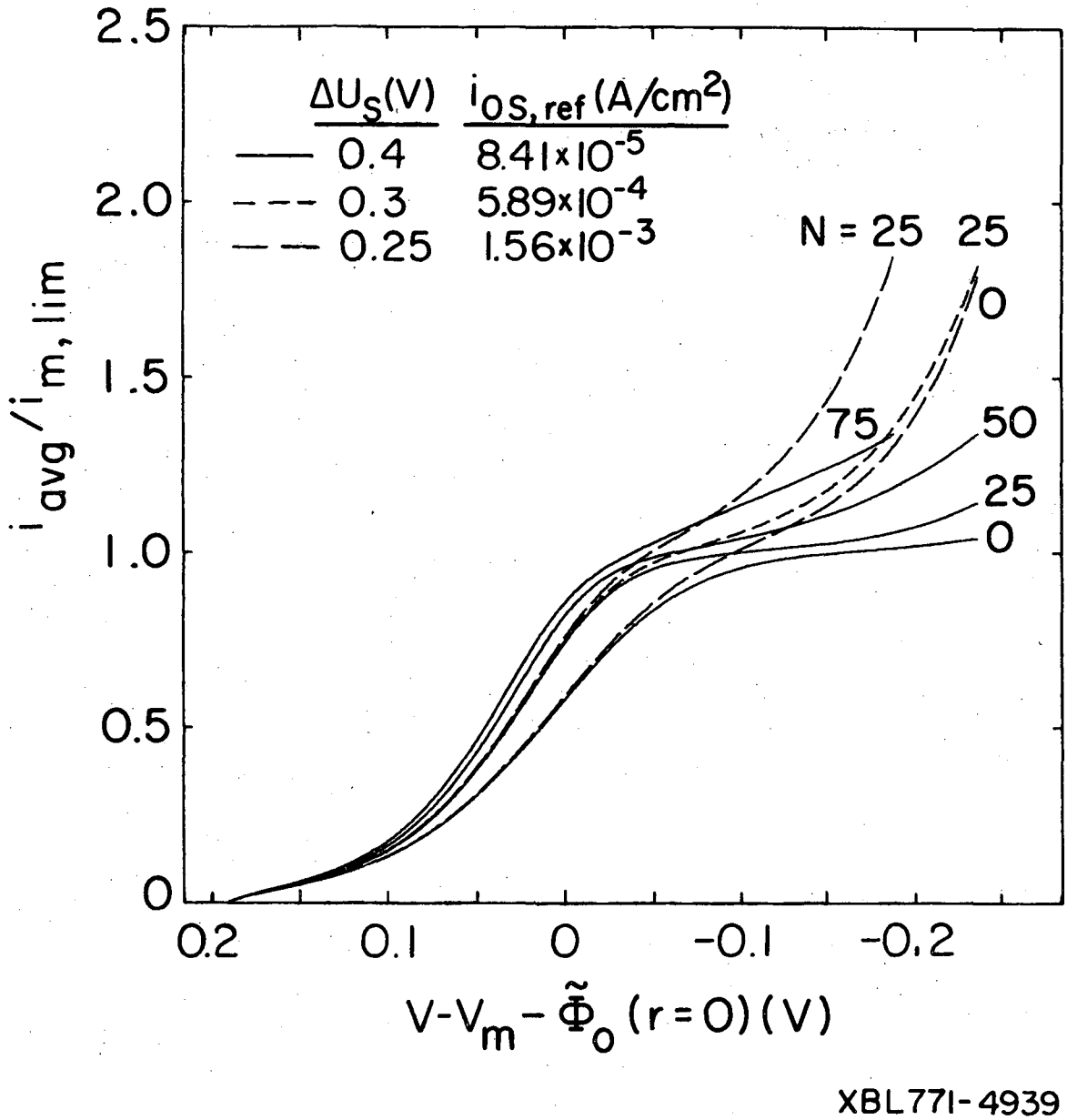

Figure 1-3. Simulated current-potential curves for copper deposition with simultaneous dissolved hydrogen formation, where the anodic portion of the side reaction is negligible and the anodic portion of the main reaction is significant only near the open-circuit potential. The reference exchange current density for the main reaction is $i_{om,ref} = 3\times10^{-3}$ A/cm^2 and $A_m = 3.52\times10^{-7}$.

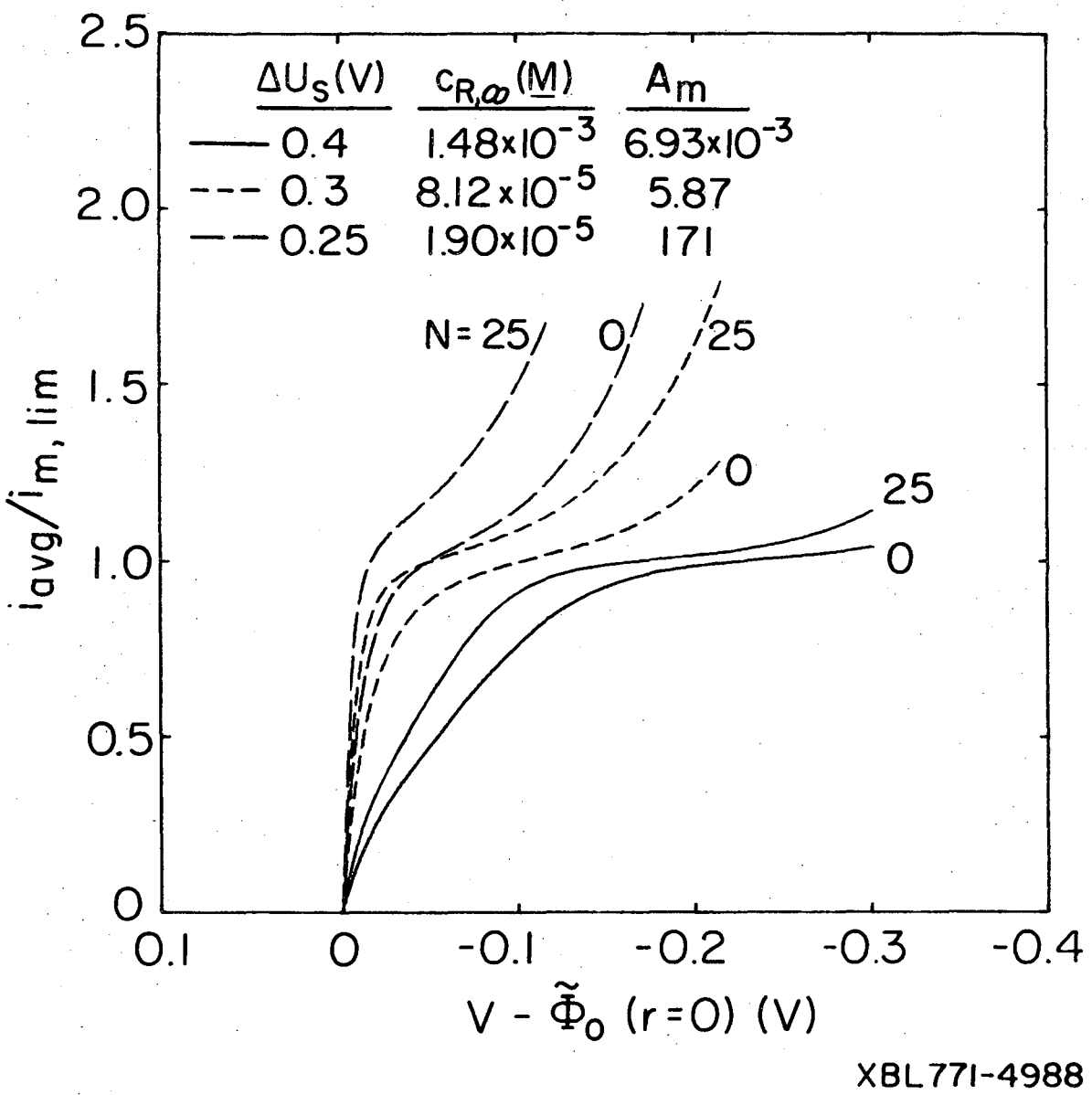

Figure 1-4. Simulated current-potential curves for copper deposition with simultaneous dissolved hydrogen formation, where the anodic portion of the side reaction is negligible. The reference exchange current density of the side reaction is $i_{os,ref} = 5\times10^{-6}$ A/cm^2 .

$$\Delta\tilde{\Phi}_o = 0.363 \frac{r_o \bar{i}_{avg}}{\kappa_\infty} . \qquad (1\text{-}24)$$

The current densities of interest here are approximately equal to $i_{m,lim}$. Thus, the parameter N provides a measure of the potential variation in the solution to be expected at the limiting current, expressed in units of RT/F .

Curves for N = 0 in figures 3 and 4 thus describe a situation where the disk is so small that the entire electrode is at a uniform potential relative to the adjacent solution. The shape of these curves shows how the side reaction occurs at the same potential as the main reaction and obscures the limiting-current plateau more as ΔU_s becomes smaller. Figure 2 also illustrates that distortion of the limiting-current plateau can occur even for a relatively small value of N and a large value of ΔU_s .

Since ΔU_s depends on the reference concentrations, they should be chosen appropriately (see table 1) to ensure that ΔU_s is characteristic of the physical system under study. For example, lowering the bulk concentration of the principal reactant to reduce N would also lower ΔU_s .

The value of A_m also influences the shape of current-potential curves, as discussed by Gerischer[33] in the abscence of a side reaction. Comparison of the curves for N = 0 on figure 4 shows that below the limiting current the importance of the anodic portion of the main reaction increases as A_m increases.

Distortion of the limiting-current plateau (see figure 3) becomes more pronounced as N increases for a given value of ΔU_s. (The disk sizes necessary to make $N = 25$ for the $c_{R,\infty}$ values shown in figure 4 are unrealistically large from an experimental standpoint.) As discussed above, for large N there can be an appreciable variation of $V - \tilde{\Phi}_o$ from the center to the edge of the electrode. The curve on figure 3 for $N = 50$ is expanded upon in figures 5 and 6. These figures show the radial distributions of current densities, surface

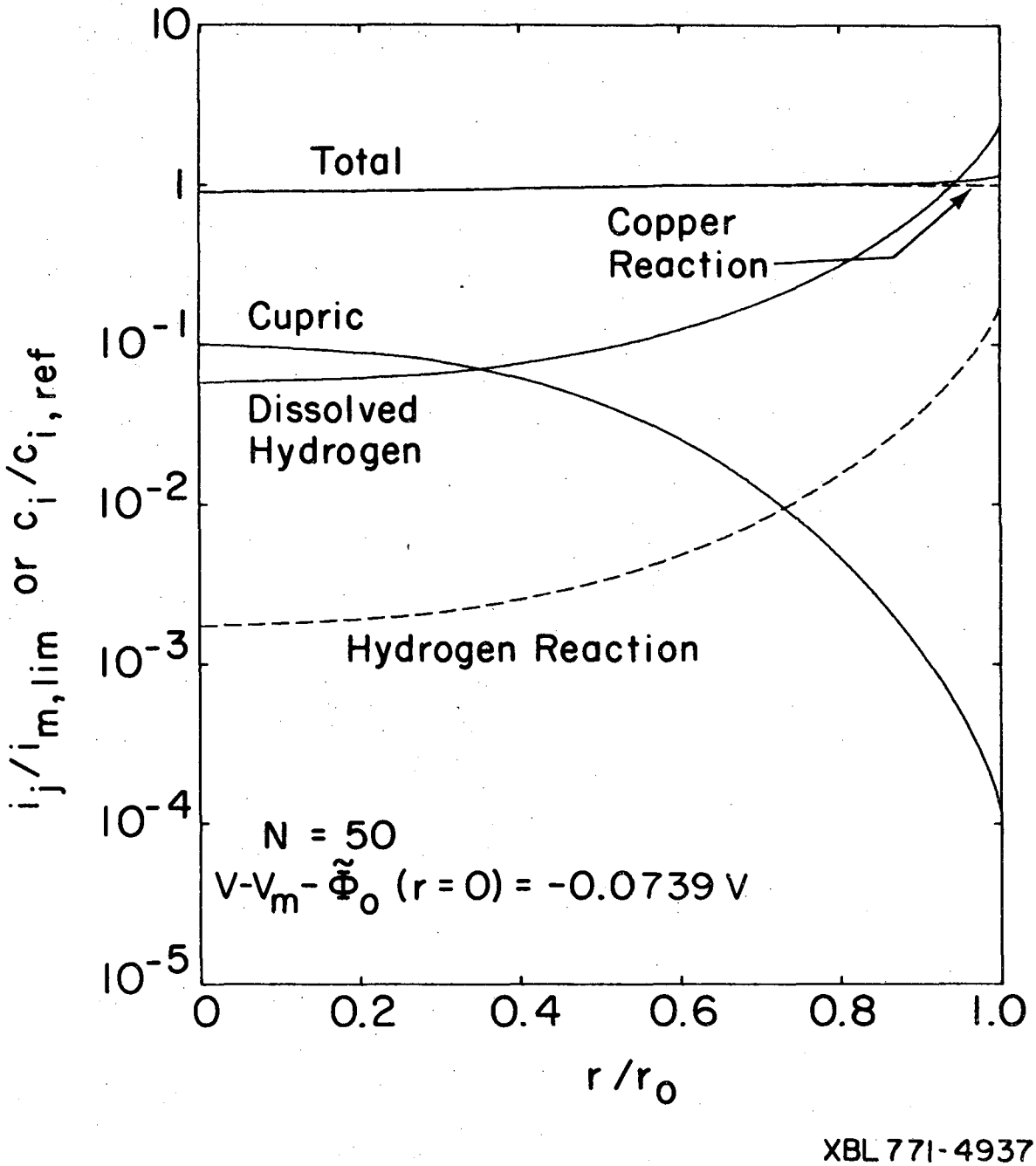

Figure 1-5. Radial current and surface concentration distributions. The reference concentration of the cupric species is the bulk value; that for hydrogen is the solubility. Hence, the solution is somewhat supersaturated in hydrogen toward the edge of the electrode.

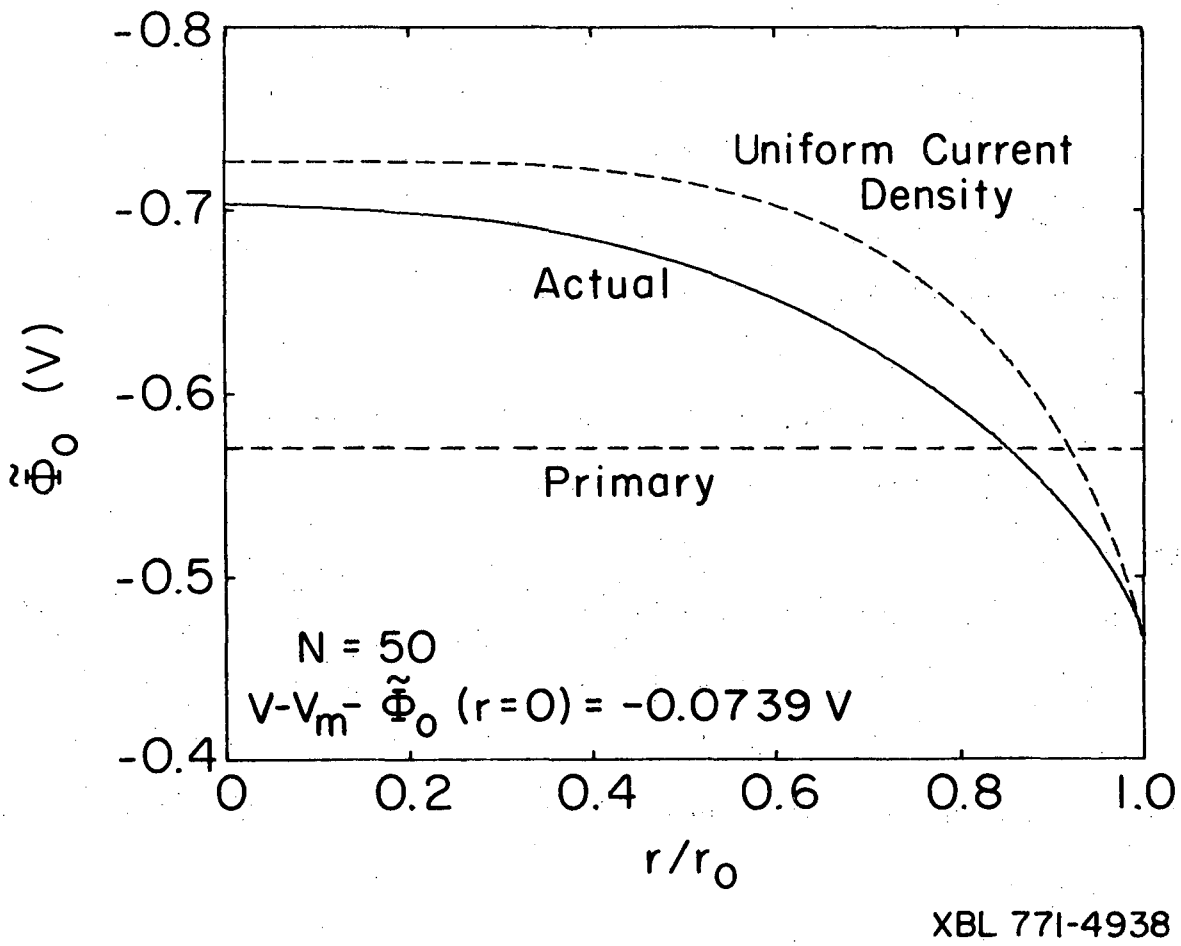

Figure 1-6. Radial potential distributions.

concentrations, and solution potential for a point well up on the limiting-current curve.

Figure 5 demonstrates that the main reaction current density can be below its limiting value at the center of the disk while hydrogen gas bubbles may be formed at the edge of the disk, since the dissolved hydrogen concentration exceeds its saturation value there by a factor of 2.388. However, larger supersaturation values of dissolved hydrogen with no bubble formation have sometimes been observed.[42]

The potential distribution labeled "Actual" in figure 6 gives rise to the nonuniform distributions in figure 5. The potential changes by about 0.236 V from the center to the edge of the disk because of its nonuniform accessibility from an ohmic standpoint. The potential labeled "Primary" was obtained from[43]

$$\tilde{\Phi}_o = I/4\kappa_\infty r_o \ . \qquad (1\text{-}25)$$

The nonuniformity of the ohmic drop across the disk, as measured by N, can be an important cause of plateau distortion. On this basis, the distortion will be increased by increasing the rotation speed (or flow rates in general), disk size, or bulk concentration of the principal reactant. Some of these influences can be seen clearly in published sets of limiting-current curves. However, lowering $c_{R,\infty}$ can also lead to plateau distortion. This is the case because the magnitude of the main and side reactions approach one another as the bulk concentration of the principal reactant is lowered, as can be seen

by considering figure 1. The effect of $c_{R,\infty}$ is thus ambiguous -- a large value of $c_{R,\infty}/\kappa_\infty$ leads to distortion while a large value of $c_{R,\infty}/i_{os,ref}$ leads to a distinct plateau. For a reasonable value of $c_{R,\infty}$, the nonuniform ohmic effects can contribute significantly to plateau distortion for large disks or high rotation speeds. The competition of these several effects is adequately reflected in the definitions of the parameters N and ΔU_s and in the curves in figures 3 and 4 showing the resulting behavior.

Actually, with small disk electrodes and well-supported solutions, plateau distortion is primarily due to the occurrence of the side reaction at the same potential as the main reaction (the ΔU_s effect). However, in technical applications where large systems become involved, one can be assured that the effect of nonuniform ohmic potential drop will be of great importance.

Summary

A model of the rotating-disk electrode with simultaneous reactions is presented. Predicted and measured current-potential curves are compared for copper deposition with simultaneous formation of dissolved hydrogen on a disk electrode rotating in a well-supported cupric sulfate solution.

Distortion of the limiting-current plateau for the main reaction by a side reaction can occur for two reasons. First, the side reaction can be in close proximity to the main reaction, as indicated by a small value of ΔU_s, and, second, a nonuniform ohmic potential drop, as

characterized by a large value of N, can promote the onset of a side reaction near the edge of the disk before the limiting-current condition is attained at the center.

Chapter 2. Copper Deposition from an Aqueous, Acidic Copper Chloride Solution Containing Iron

Introduction

Among the numerous hydrometallurgical schemes for extraction and recovery of copper currently under consideration there are several which employ an aqueous chloride solution as a lixiviant.[45-54] The tendency of chloride to form metal complexes provides high metal solubilities; and, in conjunction with a suitable oxidizing agent such as chlorine, oxygen, ferric ions, or cupric ions, excess chloride facilitates rapid leaching of not only scrap metal but also sulfide ores such as chalcopyrite, $CuFeS_2$.[55-58]

The possibility of regenerating a leaching agent such as ferric ions at an anode while depositing copper cathodically makes the prospect of direct electrolysis of copper chloride leach liquors attractive. There are, however, two major difficulties with this approach. First, copper deposits from chlorides in a rough, porous, or even powdery form under most operating conditions so that the copper product would probably require remelting.[54,59,60] The second problem is that the pregnant leach liquors may contain oxidized species that could react in the electrolysis cell and cause low current efficiencies for metal deposition. For example, iron occurring in an ore, or as the leaching agent, may appear in the electrolysis cell as ferric ion and be reduced to ferrous ion at the cathode. This latter problem can be avoided by assuring reduction of the electrolyte prior to electrolysis, or by precipitating iron, to eliminate ferric ions, while using a diaphragm to prevent transport of ferric ions from the anode to the cathode. Nevertheless, it is interesting to investigate the quantitative effect of ferric ions

on the deposition of copper from chloride solutions to determine whether removal of ferric ions prior to electrolysis is necessary. In this paper we compute the cathodic current efficiency for deposition of copper from a copper chloride solution which contains high levels of ferric ions and identify some interesting phenomena that can occur in this situation. The current efficiency for a cupric chloride solution which contains no ferric ions is considered elsewhere.[61]

The process stream that results when copper ore containing iron is leached under mildly oxidizing conditions is presumed to contain the following ionic species in water at 25°C: $CuCl^+$, $FeCl^{2+}$, H^+, and Cl^-. Available stability constant data[62,63] indicate that these are the most stable forms of the possible cupric-chloride and ferric-chloride complex ions in chloride solutions. Subsequently, these complex ions will be referred to as the cupric and ferric species, respectively.

Deposition of copper from the process stream is assumed to involve two steps. The first step is the reduction of the cupric species:

$$CuCl^+ + e^- + 2Cl^- \rightarrow CuCl_3^{2-} \quad . \qquad (2\text{-}1)$$

The second step is the reduction of the resulting cuprous-chloride complex ion (hereafter referred to as the cuprous species) to copper:

$$CuCl_3^{2-} + e^- \rightarrow Cu + 3Cl^- \quad . \qquad (2\text{-}2)$$

Stability constant data[62,64] also indicate that this cuprous species is the most stable form of those possible in the solution considered here. It should be emphasized that the stability of the cuprous species enables it to exist at a much higher concentration than its counterpart could in other solutions, such as copper sulfate in aqueous sulfuric acid (see reference 22, for example).

Two additional electrode reactions are the cathodic deposition of iron

$$FeCl^{+} + 2e^{-} \rightarrow Fe + Cl^{-} \qquad (2\text{-}3)$$

by reduction of a ferrous-chloride complex ion, which is produced within the diffusion layer (see reaction 5), and the reduction of hydrogen ions to form dissolved hydrogen gas

$$H^{+} + e^{-} \rightarrow \frac{1}{2} H_2 \, . \qquad (2\text{-}4)$$

This ferrous species, $FeCl^{+}$, is also considered to be the most stable form that could exist in this solution.[62]

One could also conceive of the direct reduction of ferric to ferrous species on the electrode, and this would occur at quite positive electrode potentials (where copper and iron would, in fact, dissolve). However, the presence of the ferric species is incompatible with the simultaneous presence of the cuprous species, and the ferric species cannot exist in the region near the electrode in the range of potentials where reactions 1 and 2 may occur. Instead, in addition to its participation in reactions 1 and 2 at the rotating-

disk electrode, the cuprous species can diffuse away from the electrode and react with the ferric species, which is being transported toward the working electrode from the bulk solution, according to the following oxidation-reduction reaction:

$$CuCl_3^{2-} + FeCl^{2+} \rightleftarrows CuCl^{+} + FeCl^{+} + 2Cl^{-} \quad . \qquad (2\text{-}5)$$

This reaction occurs within the diffusion layer adjacent to the rotating-disk electrode. Since such ionic reactions are usually relatively rapid, reaction 5 is essentially equilibrated locally, and the treatment is similar to that for partial dissociation of bisulfate ions within a diffusion layer.[65]

The ferrous species produced by reaction 5 diffuses back into the bulk solution and is also transported toward the electrode (where it may react according to reaction 3).

The equilibrium constant K for reaction 5 can be estimated to be 1.55×10^{5} $(kg/mole)^2$ by using standard electrode potentials as well as the stability-constant data referred to above. Because this is a large number, the analysis can be simplified by assuming that K is infinitely large. (Further work on this problem in which K is not set equal to infinity is contemplated.) As a consequence of the assumption that reaction 5 has an infinitely large equilibrium constant, a reaction plane forms within the diffusion layer and thereby separates it into two regions (see figure 1). Furthermore, because of this assumption the ferric species is absent in region 1 and the cuprous species is absent in region 2.

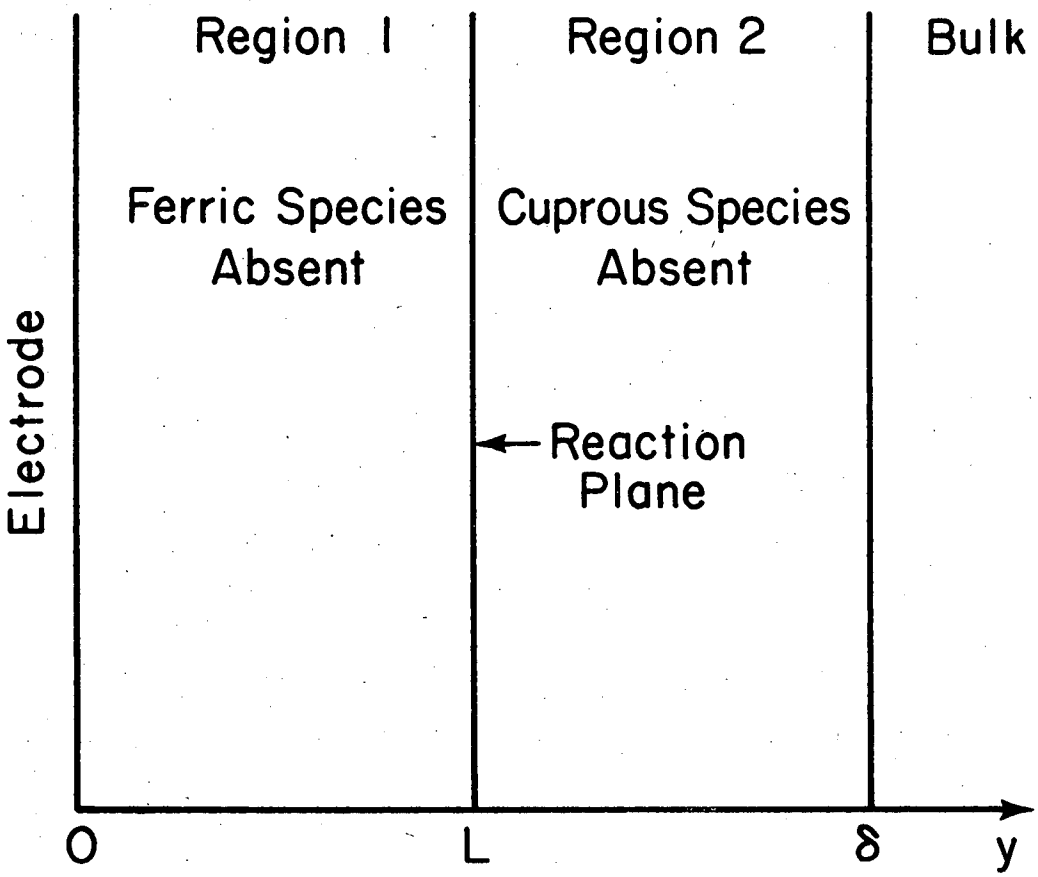

Figure 2-1. The separation into regions of a diffusion layer within which a fast oxidation-reduction reaction occurs with an infinitely large equilibrium constant.

The formation of a reaction plane by an instantaneous, irreversible bimolecular reaction was treated first by Hatta[66] within the context of simultaneous gas absorption and chemical reaction. Van Krevelen and Hoftijzer,[67] Danckwerts,[68] Perry and Pigford,[69] Olander,[70] and others have applied this concept in similar work. Recent treatment of reaction planes can be found in books by Sherwood and Pigford,[71] Astarita,[72] Danckwerts,[73] Albery and Hitchman,[4] Sherwood, Pigford, and Wilke,[74] and Carberry.[75] Friedlander and Litt[76] and Acrivos[77] used the reaction plane concept in their analyses of laminar boundary layer flows with a homogeneous reaction. Others[78-92] have also studied this subject.

Also of concern with this system is the possibility that the chloride complexing will stabilize the cuprous species to such an extent that iron is deposited in preference to copper. The standard electrode potentials of reactions with the chloride-complexed species were calculated from those of reactions of noncomplexed species and the stability constants from the literature. Table I shows that, at the potentials at which copper will begin to be plated, the ferrous ion is more stable than either the ferric ion or metallic iron, and this is true in both the complexed and noncomplexed systems.

The desired process in the electrochemical cell is the reduction of cupric species to deposited copper, which requires two electrons per copper atom deposited. The current efficiency will therefore be defined as the number of copper atoms deposited for each two electrons passed through the cell. The principal process which tends to reduce the current efficiency is the diffusion of cuprous species back into the solution where it can escape or lead to the indirect reduction of ferric species to ferrous according to reaction 5. Any reduction of ferrous ions to iron at the electrode will also lower the current efficiency as well as contaminate the deposit. In addition, the current efficiency is lowered by the reduction of hydrogen ions according to reaction 4.

The electrochemical cell used to model the physical phenomena discussed above consists of a rotating-disk electrode (the active portion of which is made either of copper or of an inert material such as platinum), a normal calomel reference electrode (whose standard electrode potential is 0.2676 V), a distant counterelectrode,

Table I. Standard electrode potentials with and without complexing by chloride, at 25°C, see Appendix C.

	U^{θ}, volt	
reaction	noncomplexed	with chloride
ferrous/ferric	0.771	0.745
cuprous/copper	0.521	0.233
cupric/copper	0.337	0.3355
cuprous/cupric	0.153	0.438
ferric/iron	-0.036	-0.0523
ferrous/iron	-0.440	-0.451

and a bulk solution of the same composition as the process stream. Deposition of copper from this electrochemical cell can be analyzed by applying dilute-electrolytic-solution theory with constant physical properties.[22,93] The results of this analysis include concentration profiles of the ionic species within the diffusion layer on the electrode, current-potential curves, and current efficiencies for this system.

For convenience, the current density distribution was assumed to be uniform on the surface of the electrode. Newman[10] showed how one should calculate the current distribution on a rotating-disk electrode, but consideration of the problem treated here at that level of sophistication is beyond the scope of this work. However, the results to be presented are applicable at the center of the disk.

Newman[9] also showed that for the rotating-disk electrode, on which one electrode reaction occurs at its limiting value, the governing equations for electrolytic mass transfer are the same as those for other flow configurations. Consequently, the assumption that the results reported here are also applicable to other flow configurations[9] should be a reasonable first approximation.

Governing Equations

Material-balance equations for species within the diffusion layer on a rotating-disk electrode are[94]

$$(D_i/D_R)c_i'' + 3\xi^2 c_i' + (z_i u_i F/D_R)(c_i\Phi'' + c_i'\Phi') = 0 \ , \quad (2\text{-}6)$$

where the prime denotes differentiation with respect to the dimensionless distance ξ. For the rotating disk

$$\xi = y/\delta \ , \tag{2-7}$$

where y is the normal distance from the surface and δ is the thickness of the diffusion layer, expressed as

$$\delta = \left(\frac{3D_R}{a\nu}\right)^{1/3} \left(\frac{\nu}{\Omega}\right)^{1/2} \ , \tag{2-8}$$

with $a = 0.51023262$.[44] The position of the reaction plane, the ionic species concentration profiles, and the potential distribution can be determined by solution of these equations together with the condition of electroneutrality

$$\sum_i z_i c_i = 0 \ , \tag{2-9}$$

and the following boundary conditions.

The boundary conditions in the bulk solution are that

$$c_i \rightarrow c_{i,\infty} \text{ as } \xi \rightarrow \infty \ .$$

At an arbitrary position, Φ can be specified, corresponding to the arbitrary zero of potential. At the reaction plane the boundary conditions are:

a. The total flux of each element (Cu, Fe, and Cl) as well as the flux of H^+ and dissolved H_2 is continuous.

b. The concentration of both the cuprous and the ferric species is zero.

c. The fluxes of ferric and cuprous species to the reaction plane are equal.

The boundary conditions at the rotating-disk electrode are that the normal component of the flux of species i evaluated at the electrode surface is equal to the sum of its reaction rates:

$$N_i = -z_i u_i F c_i \frac{d\Phi}{dy} - D_i \frac{dc_i}{dy}$$

$$= - \sum_{j=1}^{m} \frac{s_{ij} i_j}{n_j F} , \qquad (2\text{-}10)$$

where m is the number of reactions occurring at the electrode and s_{ij} and n_j are the stoichiometric coefficient of species i and the number of electrons transferred in electrode reaction j when written in the abstract form

$$\sum_i s_{ij} M_i^{z_i} \rightarrow n_j e^- . \qquad (2\text{-}11)$$

The current density due to reaction j was approximated by the Butler-Volmer equation:

$$i_j = i_{oj} \left[\exp \left(\frac{\alpha_{aj} F}{RT} \eta_{sj} \right) - \exp \left(- \frac{\alpha_{cj} F}{RT} \eta_{sj} \right) \right] , \qquad (2\text{-}12)$$

where the composition dependence of the exchange current density was assumed to have the form

$$i_{oj} = i_{oj,ref} \prod_i \left(\frac{c_{i,o}}{c_{i,ref}}\right)^{\gamma_{ij}} \prod_k a_k^{\gamma_{kj}} \quad . \qquad (2\text{-}13)$$

The symbol $i_{oj,ref}$ represents the exchange current density evaluated at the reference concentration of the ionic species, with $c_{i,ref} = 1\ \underline{M}$, and at unit relative activity of the metallic species. In equation 13, i ranges over the ionic species and k over the metallic species. The relative activity of iron was taken to equal its mole fraction in the deposit, and the relative activity of copper was set equal to unity since little iron was expected to be deposited. Thus, a_{Fe} was set equal to $0.5\ i_3/i_2$, and the activity coefficient was ignored. The activity coefficient of iron should be greater than unity since iron and copper are not completely miscible, and consequently the deposition rate of iron should be even lower than that calculated here.

The transfer coefficients α_{aj} and α_{cj} are taken to sum to n_j. The exponents for both ionic and metallic species were given the values

$$\gamma_{ij} = q_{ij} + \frac{\alpha_{cj}}{n_j} s_{ij} \quad , \qquad (2\text{-}14)$$

where $q_{ij} = -s_{ij}$ for a cathodic reactant and is zero otherwise.

The surface overpotential for reaction j is

$$\eta_{sj} = V - \Phi_o - U_{j,o} \quad , \qquad (2\text{-}15)$$

where V is the potential of the rotating disk, Φ_o is the potential of the solution just outside the diffuse part of the double layer as measured by a reference electrode of a given kind, and $U_{j,o}$ is the theoretical open-circuit potential for reaction j at the composition prevailing at the electrode surface -- again relative to the reference electrode of a given kind. For a normal calomel reference electrode,

$$U_{j,o} = U_j^\theta - U_{cal}^\theta - \frac{RT}{n_j F}\left[\sum_i s_{ij} \ln\left(\frac{c_{i,o}}{\rho_o}\right) + \sum_k s_{kj} \ln a_k\right] + \frac{RT}{F} \ln\left(\frac{c_{Cl^-}^\lambda}{\rho_o}\right) . \qquad (2\text{-}16)$$

Here, $c_{Cl^-}^\lambda$ is the concentration of chloride ion in the reference electrode compartment, and the concentrations must be expressed in moles/liter if the usual tabulations of standard electrode potentials U_j^θ are to be used. Note that possible activity-coefficient corrections to the concentrations of the ionic species have been ignored. (See Appendix A.)

Solution Technique

Equations 6 and 9 together with the above boundary conditions constitute a boundary-value problem involving coupled, ordinary, nonlinear, differential equations. The governing equations and boundary conditions were cast in finite-difference form accurate to order h^2, where h is the dimensionless distance between mesh

points, and solved by a numerical solution technique developed by Newman.[22] An interesting aspect of this problem is the unknown reaction plane position. In conditions b and c there is one more boundary condition than would be needed for a fixed plane position. Consequently, the plane position L must be treated as an unknown constant. To use the same computer subroutines, the treatment of this unknown constant was similar to that used by Newman[21] for the eigenvalues of the Graetz problem. (See Appendix D.)

Parameter values used to obtain numerical results are presented in table II. Mobilities were calculated from the tabulated diffusion coefficients by means of the Nernst-Einstein relation, $u_i = D_i/RT$. For the transfer coefficients, $\alpha_{cj} = 0.5$, and the exchange current densities, $i_{oj,ref}$, for reactions 1 and 3 were given the value 10^{-3} A/cm^2 while values of 5×10^{-3} and 5.89×10^{-7} A/cm^2 were used for reactions 2 and 4, respectively.

Results

Results are presented for four cases. In case one, only reaction 1, the reduction of the cupric species to cuprous species, is permitted to occur at the electrode (see table II). In the remaining cases, reactions 1, 2, 3, and 4 occur at the electrode. These separate cases emphasize the significance of multiple electrode reactions and the significance of the ratio of the bulk concentration of cupric species to ferric species. Table II gives the bulk concentrations for each case.

Figure 2 displays the dependence of the electric potential Φ on the dimensionless distance from the electrode ξ for case one.

Table II. Parameter values.

species	$10^5 D_i$ cm^2/s	$c_{i,\infty}$ mol/l cases 1 and 2	case 3	case 4
$CuCl_3^{2-}$	0.6[a]	0	0	0
$CuCl^+$	0.6[a]	3	2.25	1.5
$FeCl^+$	0.739[b]	0	0	0
$FeCl^{2+}$	0.896[b]	1.5	2.25	3
Cl^-	2.032[c]	6.1	6.85	7.6
H^+	9.312[c]	0.1	0.1	0.1
H_2	3.8[d]	$4.155 \cdot 10^{-10}$	⟶	⟶

$T = 298.15$ K $\quad \nu = 0.010049$ cm^2/s

$\rho_o = 0.99707$ g/cm^3 $\quad \Omega = 261.8$ rad/s

---

[a] Taken from reference 95.

[b] Because of a lack of data, the diffusion coefficients of the ferrous and ferric species were taken to be the same as those of ferrocyanide and ferricyanide ions, respectively, as given in table 75-1 of reference 22.

[c] Taken from table 75-1 of reference 22.

[d] This value was arbitrarily selected for this work (see John Newman and Limin Hsueh, "Currents Limited by Gas Solubility," Industrial and Engineering Chemistry Fundamentals, 9 (1970), 677-679).

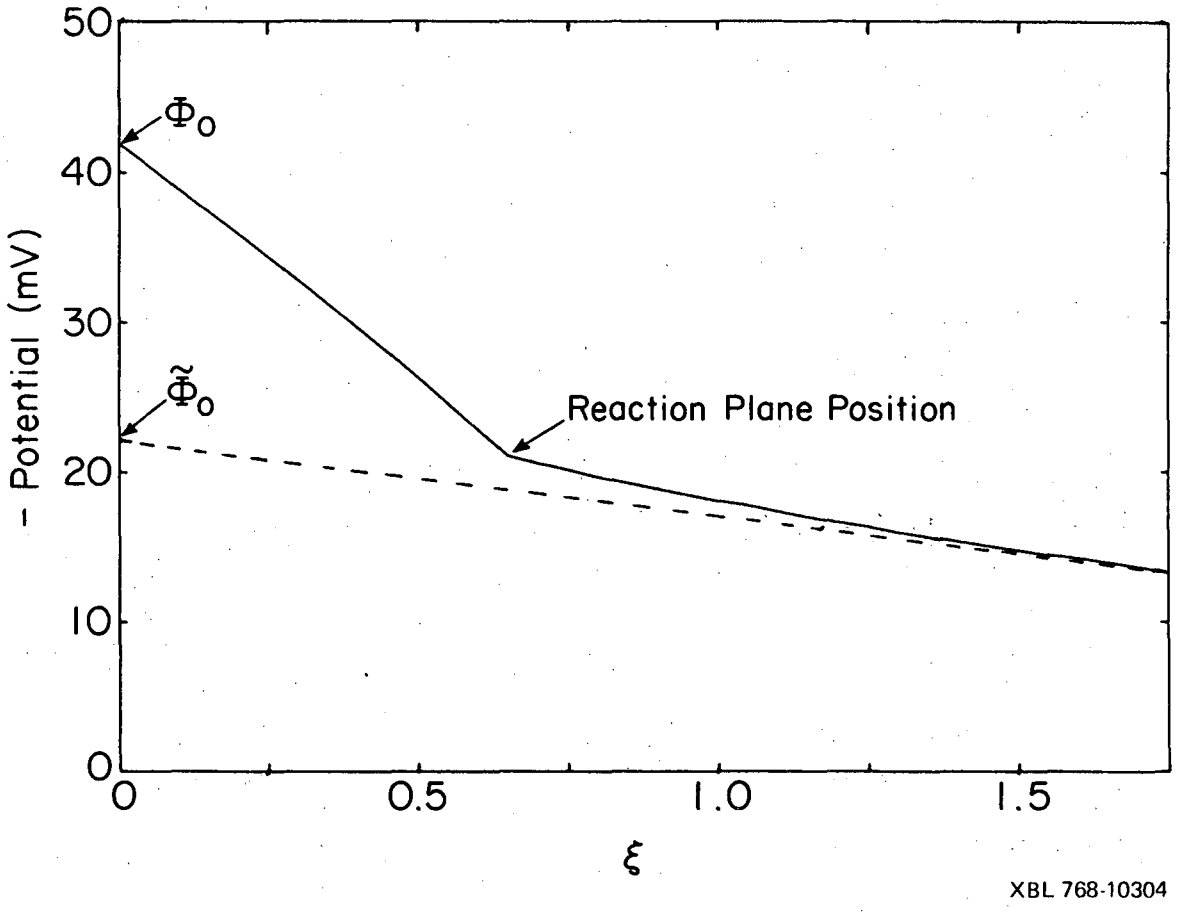

Figure 2-2. Dependence of the electric potential on the dimensionless distance from the electrode when $V - \tilde{\Phi}_o = -0.3545$ V and reaction 1 alone occurs at the electrode.

Two quantities of interest, Φ_o and $\tilde{\Phi}_o$, are illustrated in this figure. The potential in the solution at the electrode surface (just outside the diffuse double-layer) Φ_o and the potential of the working electrode V are used to form the potential difference $V - \Phi_o$, which is related to the driving force for the electrode reaction (see equation 15).

The electric potential in the solution outside of the diffusion layer, $\tilde{\Phi}$, extrapolated to the electrode surface is designated as $\tilde{\Phi}_o$. Its value may be obtained by extrapolating Ohm's law,

$$i_T = \sum_{j=1}^{m} i_j = -\kappa_\infty \frac{d\tilde{\Phi}}{dy} , \qquad (2\text{-}17)$$

to the electrode surface from the bulk by using the previously calculated value of i_T and the conductivity κ_∞ of the bulk solution. The potential difference $V - \tilde{\Phi}_o$ represents an alternative driving force for the electrode reaction. We might write for the total overpotential

$$\eta_{sj} + \eta_{cj} = V - \tilde{\Phi}_o - U_{j,\infty} , \qquad (2\text{-}18)$$

where η_{cj} is the concentration overpotential for reaction j and $U_{j,\infty}$ is the theoretical open-circuit potential for reaction j at the bulk solution composition and the alloy composition of the deposit.

There is a difference between $\tilde{\Phi}_o$ and Φ_o because the conductivity varies with position in the diffusion layer and is not equal to κ_∞ and because there exists a diffusion potential due to

the concentration variations and the different diffusion coefficients of the various species (see equation 125-7 of reference 22). These factors are accounted for when one solves simultaneously the coupled equations 6 and 9 across the diffusion layer to obtain the potential distribution in figure 2.

Figure 3 depicts the calculated concentration profiles of the ionic species within the diffusion layer that were obtained at the same potential difference. In this figure, the dimensionless distance from the electrode at which the concentration of both the cuprous and the ferric species is zero indicates the position of the reaction plane.

The calculated current density due to reaction 1 alone, i_1, normalized by the current density predicted by the Levich equation[32]

$$i_{LD} = 0.62048 \frac{n_1 F c_{R\infty}}{s_{R1}} (\Omega\nu)^{1/2} \left(\frac{D_R}{\nu}\right)^{2/3} , \qquad (2\text{-}19)$$

is presented in figure 4, as a function of the potential differences $V - \tilde{\Phi}_o$ and $V - \Phi_o$.

Figure 5 displays the calculated concentration profiles for case two with $V - \tilde{\Phi}_o = -0.3493$ V.

In figure 6 the dimensionless position of the reaction plane L/δ is presented as a function of the potential difference $V - \tilde{\Phi}_o$ for cases 1 and 2.

The total predicted dimensionless current density for case 2 is plotted in figure 7 as a function of the potential difference $V - \tilde{\Phi}_o$.

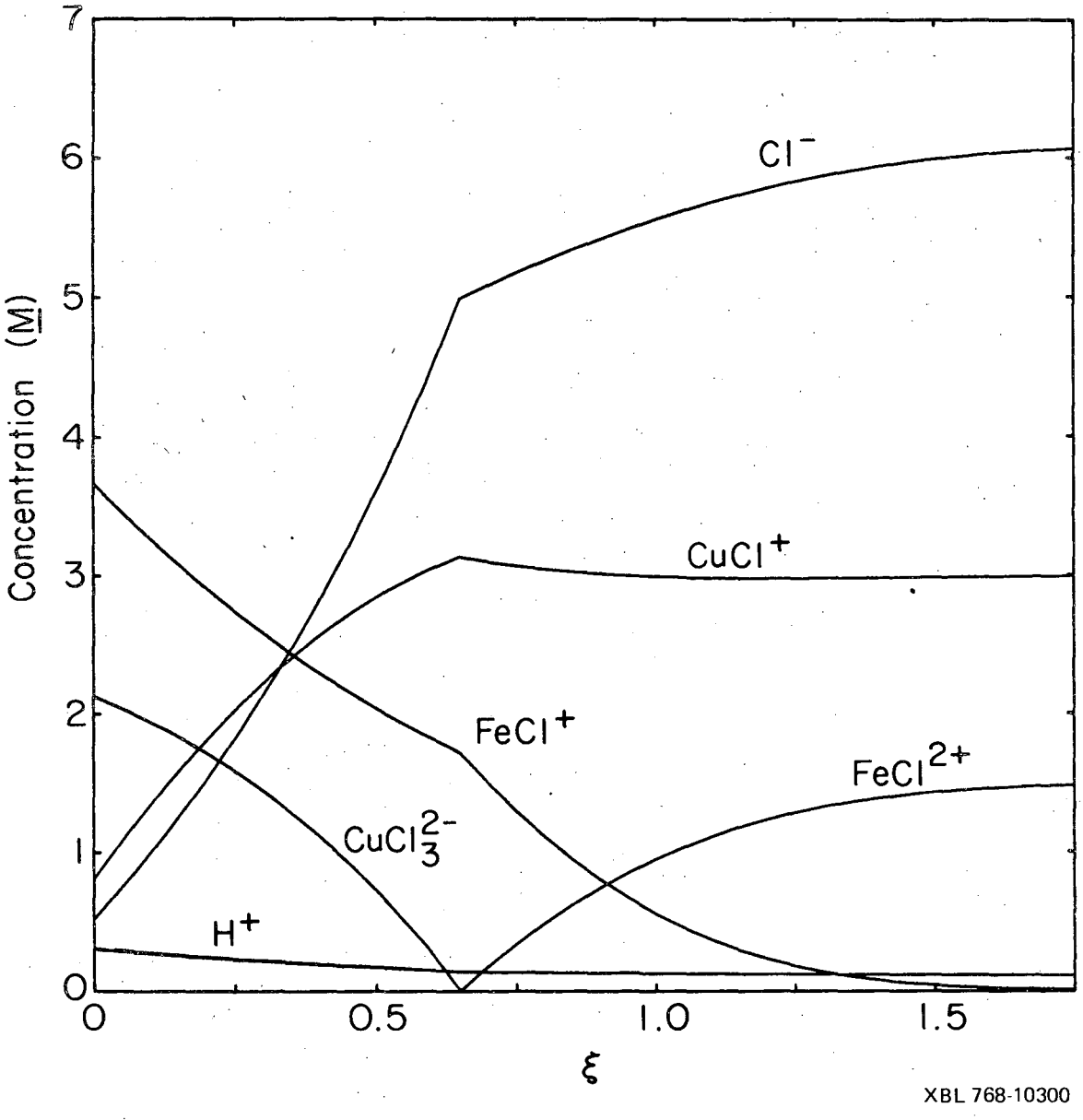

Figure 2-3. Dependence of the concentration of the various species on the dimensionless distance from the electrode for case 1 with $V - \tilde{\Phi}_o = -0.3545$ V.

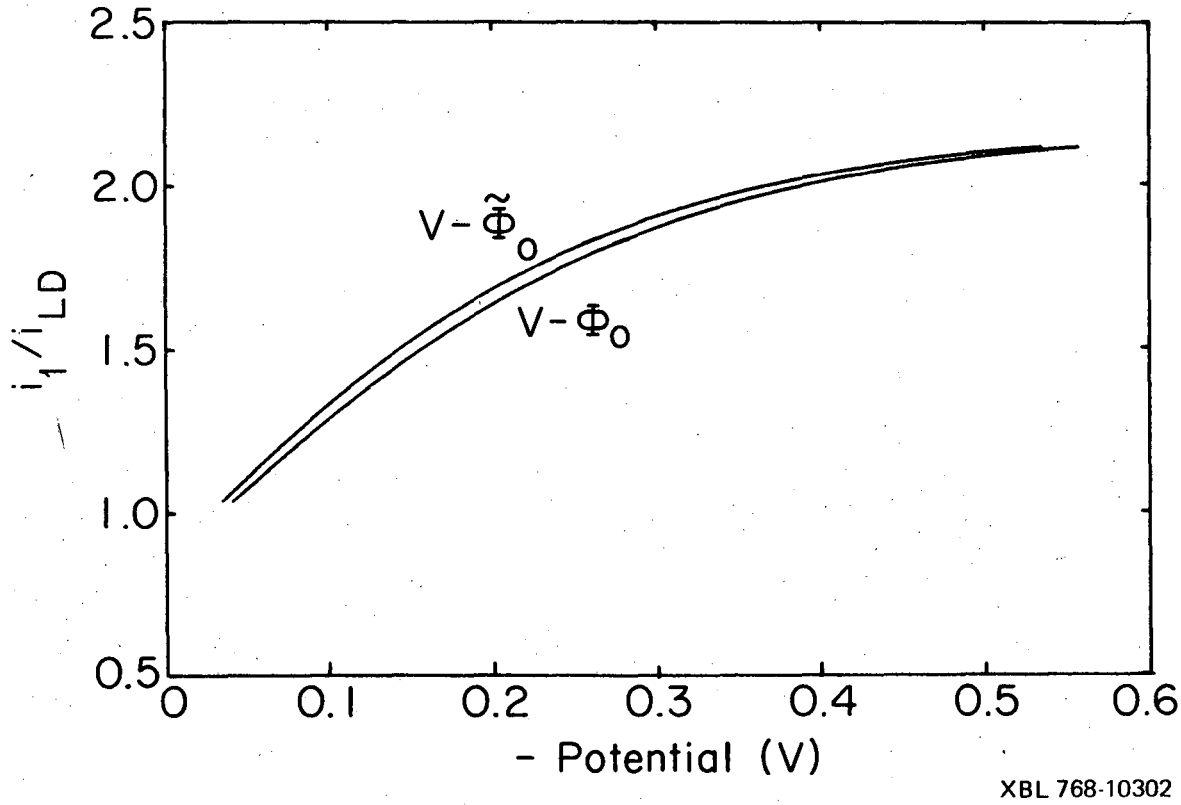

Figure 2-4. The dimensionless current density when reaction 1 alone occurs at the electrode as a function of the potential differences $V - \tilde{\Phi}_o$ and $V - \Phi_o$.

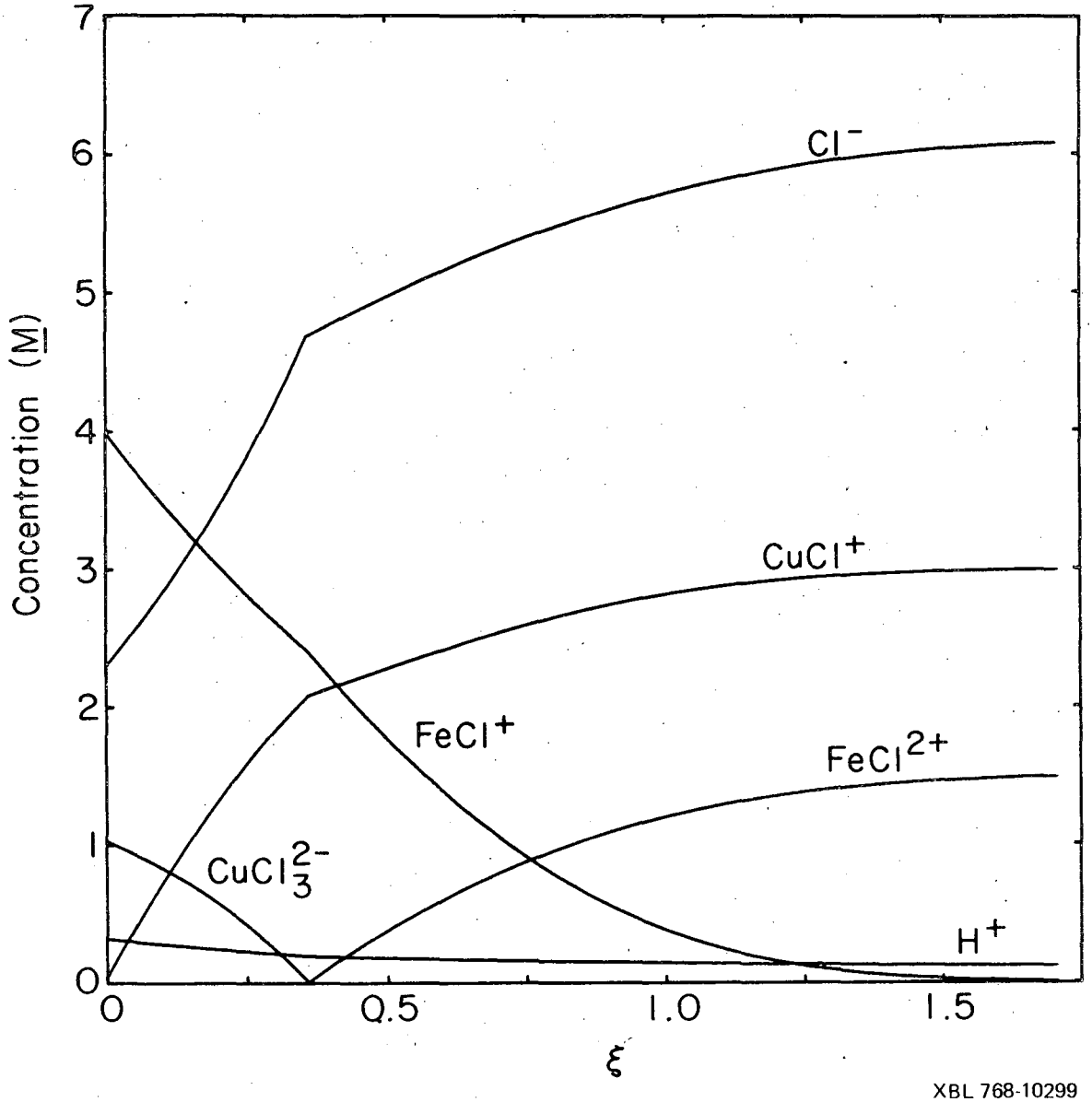

Figure 2-5. Concentration profiles of the various species near the electrode for case 2 with $V - \tilde{\Phi}_o = -0.3493$ V.

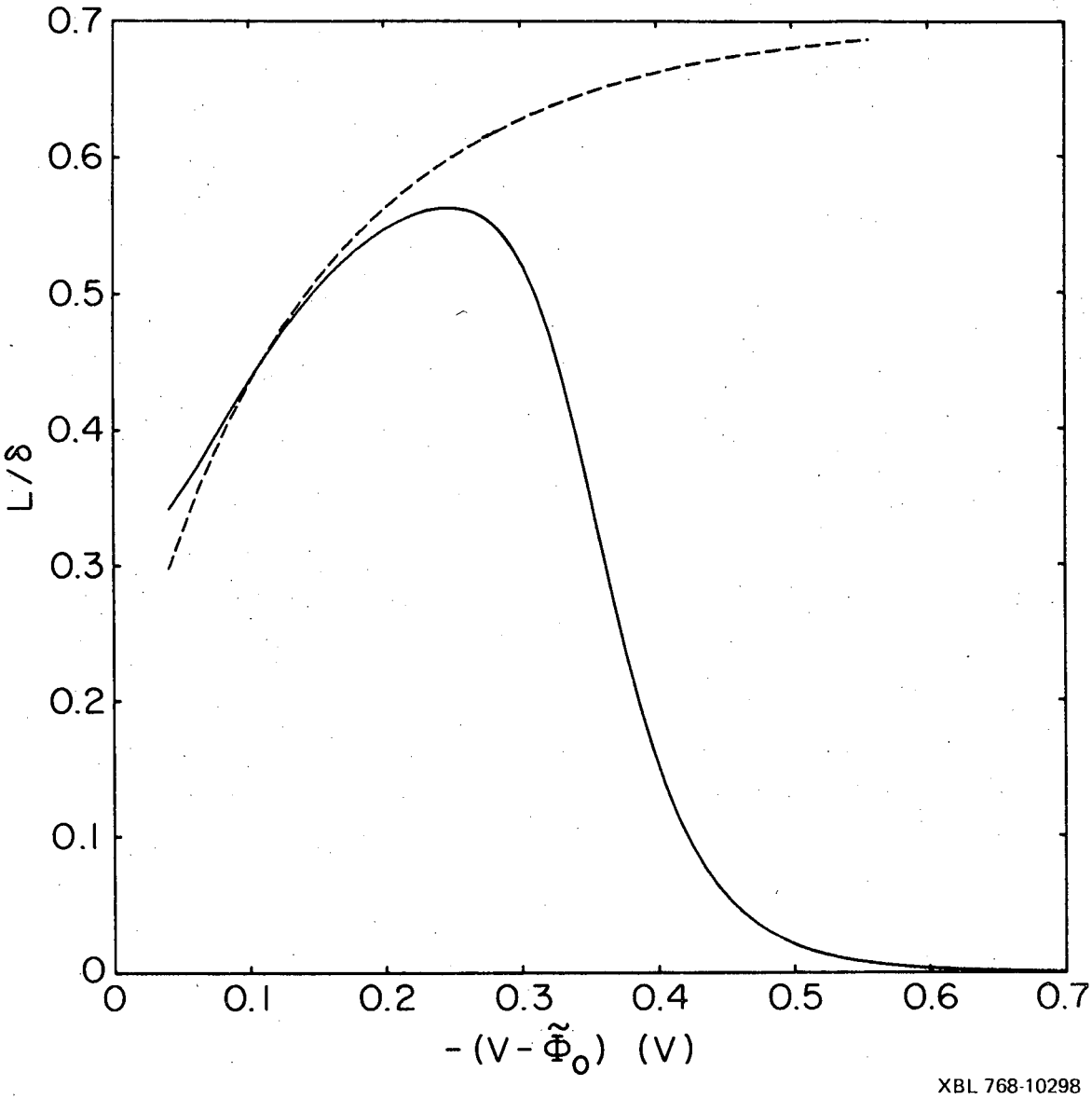

Figure 2-6. Dependence of the dimensionless reaction plane position on $V - \tilde{\Phi}_o$ for cases 1(---) and 2(——).

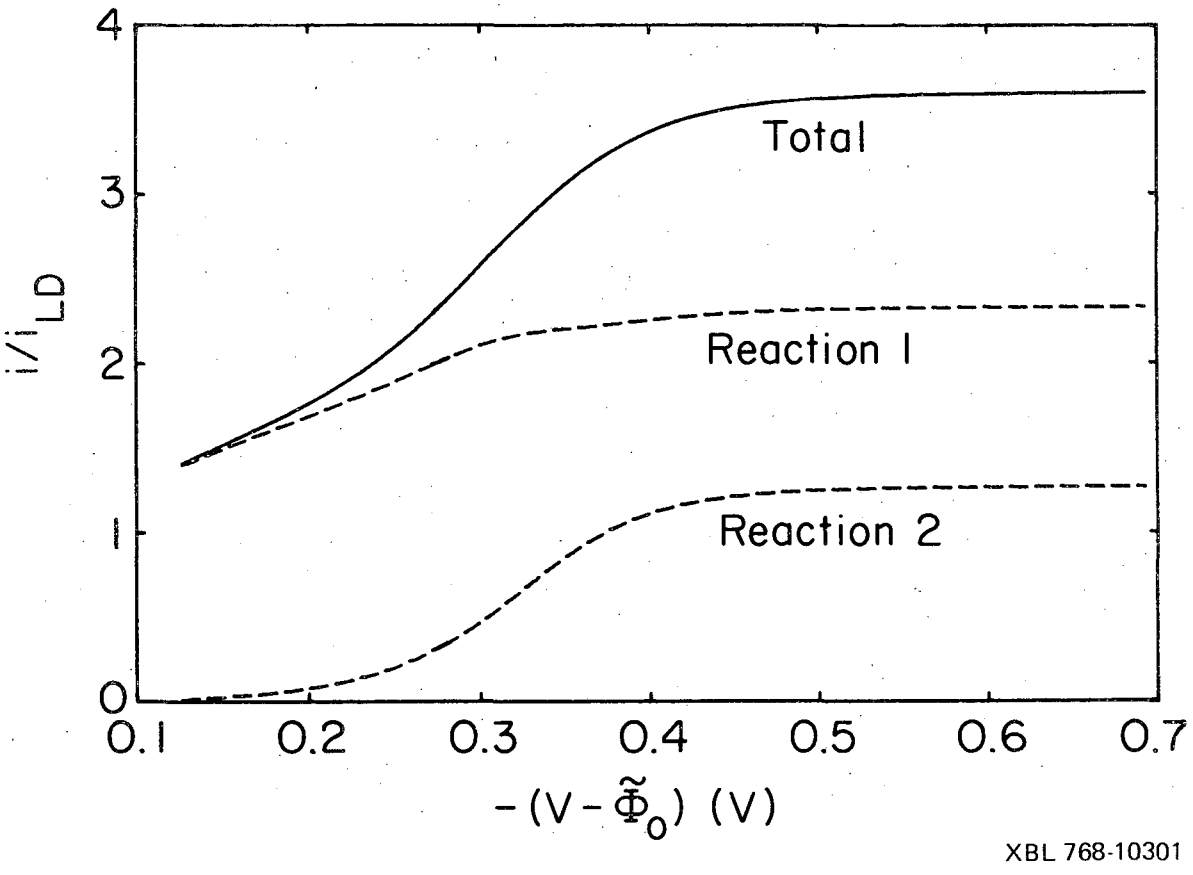

Figure 2-7. Dependence of the dimensionless current densities on $V - \tilde{\Phi}_o$ for case 2.

The current densities due to reactions 1 and 2 for case 2 are also plotted in figure 7. (The current density due to reactions 3 and 4 were too small to be plotted conveniently on figure 7.)

These calculated current densities were used to calculate the current efficiency, $100 \times 2i_2/i_T$, as a function of the potential difference $V - \tilde{\Phi}_o$, which is plotted in figure 8. Also shown in figure 8 are the current efficiencies for cases 3 and 4.

Finally, the dependence of the relative surface concentration of the cupric, cuprous, and chloride species on $V - \tilde{\Phi}_o$ is presented in figure 9.

Discussion

The potential profile and the concentration profiles shown in figures 2, 3, and 5 are not smooth at the reaction plane because of the assumption that K is infinite.

Consider first case one, where the only electrode reaction is the reduction of cupric to cuprous ions. The latter diffuse away from the electrode to the reaction plane, where they reduce ferric to ferrous ions, with regeneration of cupric. Some of the cuprous species also escapes by radial convection. The concentration profiles in figure 3 illustrate these processes. As the electric driving force is increased, the concentration of the limiting reactant, the cupric species, approaches zero, and the concentration of the product cuprous species at the electrode increases. Consequently, the position of the reaction plane moves away from the electrode, as also shown in figure 6. The position of the reaction plane is determined by a

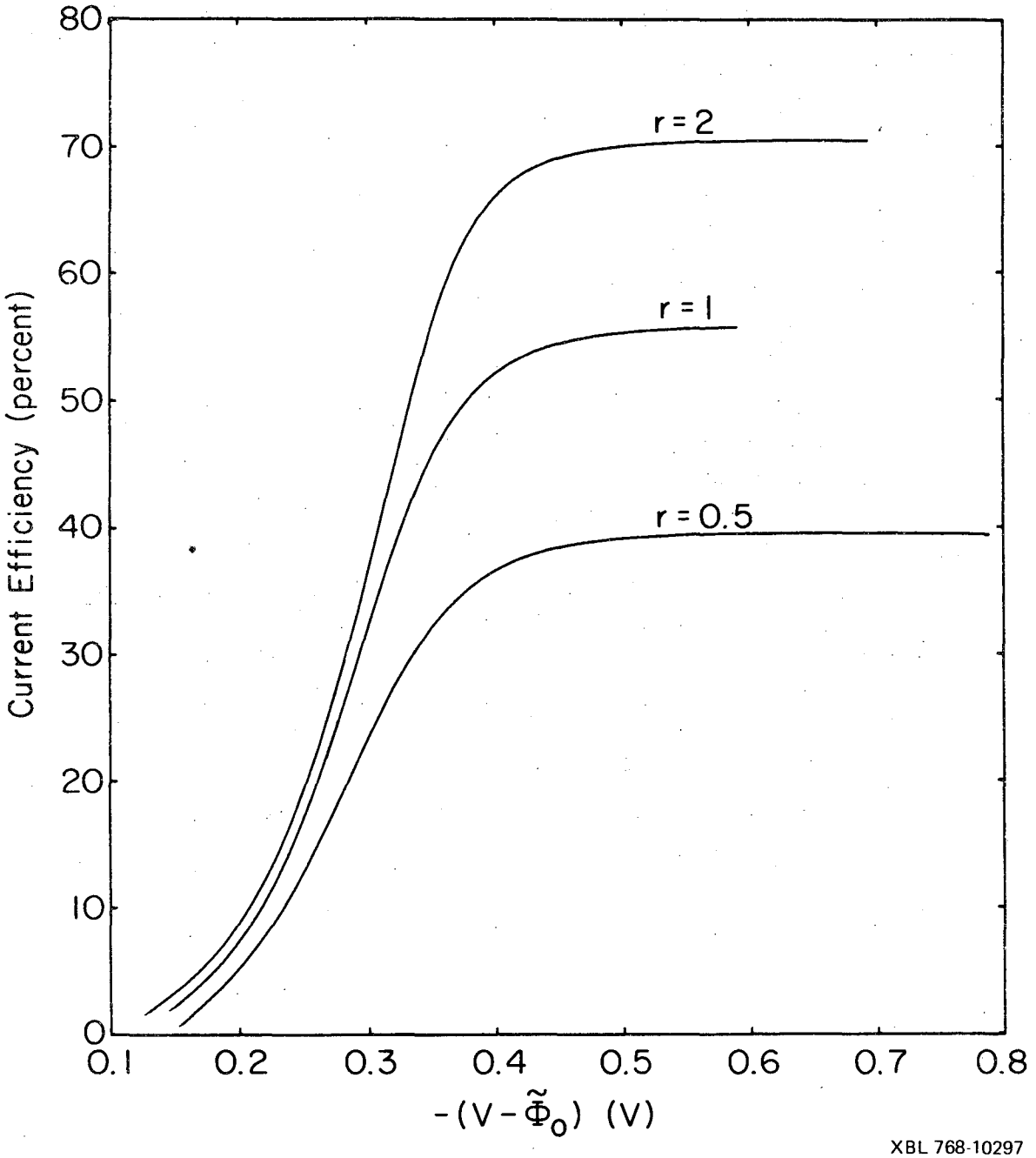

Figure 2-8. Dependence of the current efficiency on $V - \tilde{\Phi}_o$. $r = c_{CuCl^+,\infty} / c_{FeCl^{2+},\infty}$. r = 2, 1, and 0.5 for cases 2, 3, and 4, respectively.

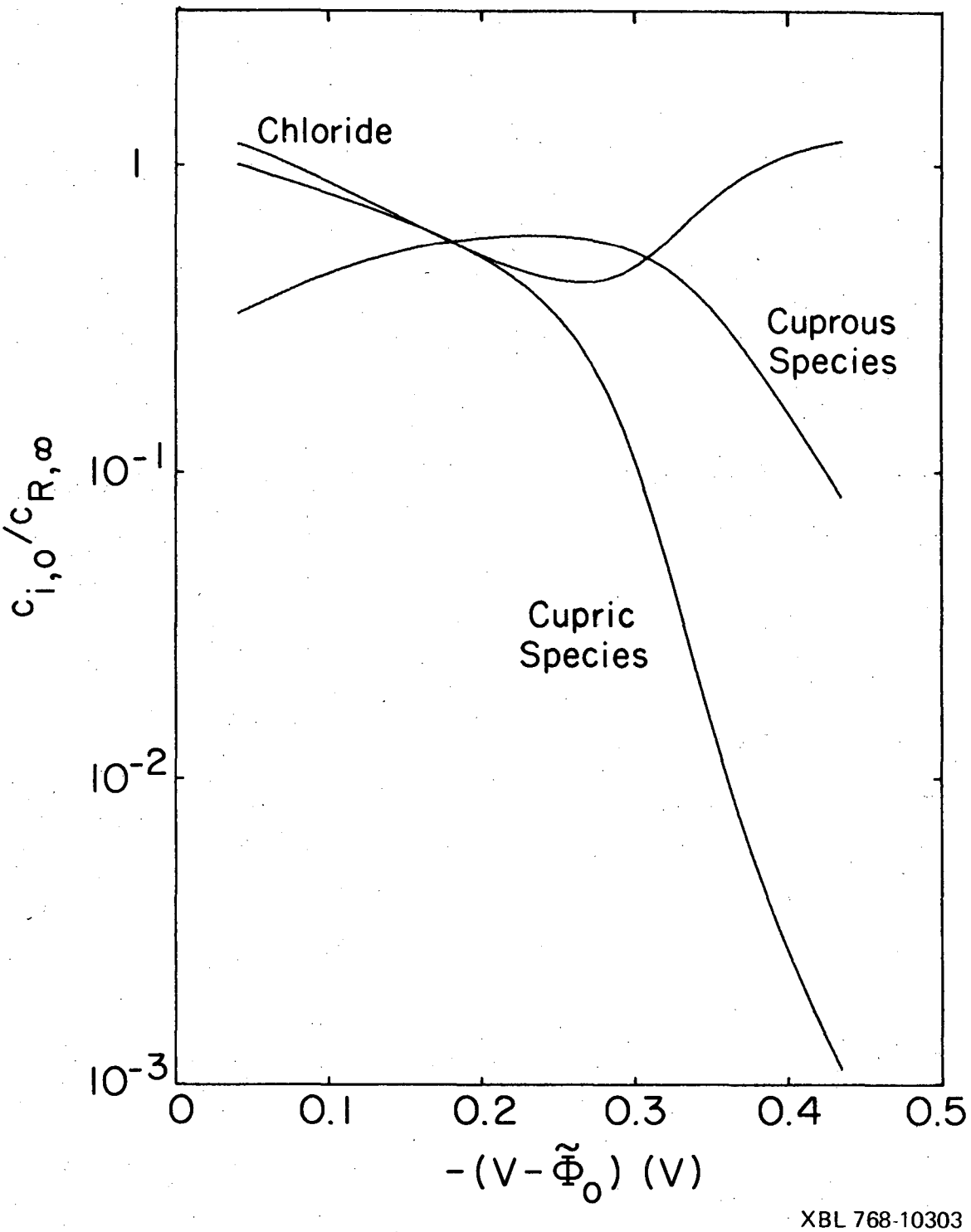

Figure 2-9. Dependence of the relative surface concentration of some of the ionic species present in the system on $V - \tilde{\Phi}_o$ for case 2.

balance of the transport of cuprous species from the electrode and the transport of ferric species from infinity. The ferrous species, the product of the plane reaction, also has accumulated toward the disk surface. The chloride ion is produced by reaction 5 at the plane and consumed by reaction 1 at the electrode, and the consequences of this are observed in the concentration profiles.

The current density for reaction 1 can exceed substantially the limiting value for convection and diffusion of the cupric species as given by the Levich equation. Figure 4 shows ratios as high as 2.12. This enhancement is due to ionic migration of the limiting reactant[94] and the regeneration of the cupric species at the reaction plane. Since the cupric species is positively charged, it is attracted toward the cathode according to the potential distribution in figure 2. This effect of migration also accounts for the maximum in the concentration of the cupric species at the reaction plane and for the increase of concentration of the ferrous species toward the electrode (see figure 3), where this species is neither produced nor consumed. The effect of the reaction plane is, in essence, to bring the bulk concentration of the limiting reactant closer to the electrode, since the cupric species is produced at the plane by reaction 5, and this serves to increase the concentration gradient at the electrode.

Another way to think about this effect is to realize that the reduction of ferric to ferrous, which occurs at the plane, requires a supply of electrons from the electrode. The indirect supply of these electrons through the transport of cuprous species from the electrode to the plane contributes to a higher current density for

reaction 1. In fact, the reduction of ferric to ferrous requires a smaller electric driving force than the reduction of cupric to cuprous (see table I). When the reaction-plane distance has decreased to zero, the reduction of ferric to ferrous can proceed directly on the electrode, and the analysis would actually become simpler.

Figure 4 shows that $\tilde{\Phi}_o - \Phi_o$, the difference between the potential drop through the diffusion layer and that obtained by extrapolation with the bulk conductivity, is relatively small compared with the scale of potentials over which the current rises toward its limiting value. For the situation in figure 2, $\tilde{\Phi}_o - \Phi_o$ has the value of 19.9 mV.

For case two, we must now consider the additional effects associated with the possibility of depositing copper and iron on the electrode and also the possibility of evolving hydrogen gas at the electrode. The deposition of copper by reaction 2 consumes cuprous ions produced through reaction 1, and consequently less of the cuprous species remains to diffuse back into the solution. Comparison of the concentration profiles in figures 3 and 5 shows this reduction of the cuprous concentration at the surface. The reaction plane is now much closer to the electrode, as also depicted in figure 6. Comparison of the predicted reaction plane positions at small values of $-(V - \tilde{\Phi}_o)$ for cases 1 and 2, as shown in figure 6, reveals that the reaction plane is further from the electrode in case 2, a result which is due to the dissolution of deposited copper according to reaction 2.

The current densities in figure 7 reflect the difference in the potentials of the two copper reactions (see table I). The current density due to reaction 1 is well along toward a limiting current -- the same limit shown in figure 4 -- before the current density due to reaction 2 becomes significant. The slight increase in the current density due to reaction 1 above the initial plateau is due to the increasingly larger concentration gradient of the limiting reactant as the reaction plane moves closer to the electrode (compare figures 3 and 5). The cupric species produced at the reaction plane can no longer escape by radial convection. Furthermore, the current density due to reaction 2 will increase the potential gradients and enhance further the migration of cupric ions toward the electrode from the bulk solution.

In order to avoid contamination of the deposit with iron, the electric driving force should not be made too large, according to the standard electrode potentials in table I. For example, the current density for reaction 3 is very small and can be used to estimate that less than 10^{-5} atom percent of the deposit is iron for values of $V - \tilde{\Phi}_o$ more positive than about -0.51 V. However, this estimate is probably high because the activity of iron was taken to equal the atom fraction, with neglect of the activity coefficient. Since the activity coefficient is greater than unity, the deposition of iron would be further impeded.

For such low rates of reaction 3, the low current efficiencies in figure 8 are mainly due to two causes: (1) "leakage" of cuprous

species away from the electrode by radial convection and (2) consumption of cuprous species at the reaction plane. The latter is equivalent to the indirect current required for reduction of ferric to ferrous at the plane. Because the reduction of cupric and ferric species occurs at a lower electric driving force than reaction 2, the current efficiency increases with an increase in the electric driving force and approaches about 70.5, 55.7, and 39.5 percent for cases 2, 3, and 4, respectively. The maximum possible current efficiency is determined mainly by the ratio of ferric and cupric concentrations in the bulk solution. At still larger values of the electric driving force, the current efficiency would decrease due to the deposition of iron by reaction 3 and the evolution of hydrogen according to reaction 4.

For some cases the range of acceptable operating potential differences may be determined by the solubility limit of the cuprous species (approximately 1 M in the solutions studied here) and the maximum tolerable iron contamination of the deposit or hydrogen gas evolution. For case 2, figure 9 (also see figure 5) shows that operating at potential differences more positive than about -0.35 V could lead to undesirable precipitation of cuprous species. (For cases 3 and 4, $\tilde{\Phi}_o - V$ should be at least 0.32 and 0.275 V, respectively, to avoid CuCl precipitation.) At the other extreme in the range of acceptable operating potential differences for case 2, the current density due to reaction 3 may be used to predict that the iron contamination of the deposited alloy would exceed 10^{-5} atom percent for $V - \tilde{\Phi}_o$ values more negative than about -0.52 V. Further

reduction of $V - \tilde{\Phi}_o$ would lead eventually to hydrogen gas evolution. (The value of $V - \tilde{\Phi}_o$ at which this may begin to occur for case 4 was predicted to be approximately -0.789 V , for example.)

Another limiting situation is associated with the bulk chloride concentration. Since chloride ions are consumed and liberated at the electrode at rates which depend on $V - \tilde{\Phi}_o$, a minimum in the surface concentration of chloride ions exists, as shown in figure 9. The implication of this minimum is that, for some bulk compositions, the chloride ion concentration would vanish at the electrode, a condition which may be considered undesirable because the complexing of the species would be no longer ensured.

Summary and Conclusion

The results of this work are that one can predict for this system: 1) the location of a hypothesized reaction plane; 2) reasonable concentration profiles for the ionic species; 3) realistic current-potential curves; 4) current efficiencies of about 70.5, 55.7, and 39.5 percent for cases 2, 3, and 4, respectively; and 5) a copper product that can be at least 99.99999 percent pure. Consequently, the design of an electrochemical cell to remove the copper directly from the model process stream appears to be feasible provided that problems with the physical structure of the copper deposit can be avoided.

Again, the analysis is strictly valid only at the center of the disk.

Acknowledgement

It is a pleasure to acknowledge those who contributed to this work.

Professor John Newman, my research director, contributed significantly to this work and to my professional development for which I shall be forever grateful.

James A. Trainham aroused my interest in the topic discussed in chapter 2 and contributed his unfinished computer program for treating the problem. I would also like to thank Jim for his many helpful discussions about electrochemical systems.

Professor Thomas W. Chapman of the University of Wisconsin conceived the physical phenomena analyzed in chapter 2. He contributed part of the introduction to chapter 2 and many helpful suggestions about the results and discussion sections.

Thomas J. Edwards and Clarence G. Law, Jr., contributed by reading and discussing with me parts of this work.

Linda Betters transformed handwritten manuscripts into attractive typed copy in her usual efficient, courteous manner.

Appendix A. Overpotentials

Purpose

Concentration, surface, and total overpotential expressions are developed for a working electrode on which multiple charge-transfer reactions occur. The derivations follow closely those given by Newman[22] for a single electrode reaction (see also Appel[96] and Nisancioğlu[97]).

Concentration Overpotential

The concentration overpotential is the potential difference between a reference electrode of the same kind as the working electrode located adjacent to it (just outside the diffuse double layer) and one of the same kind located in the bulk solution (see figure 1), minus the potential drop between these reference electrodes in the absence of concentration variations.

The development of an expression for the concentration overpotential for the general electrode reaction j,

$$\sum_i s_{ij} M_i^{z_i} \rightarrow n_j e^- , \qquad \text{(A-1)}$$

begins by considering the equilibrium expression for reaction j,

$$\sum_i s_{ij} \mu_i = n_j \mu_{e^-} . \qquad \text{(A-2)}$$

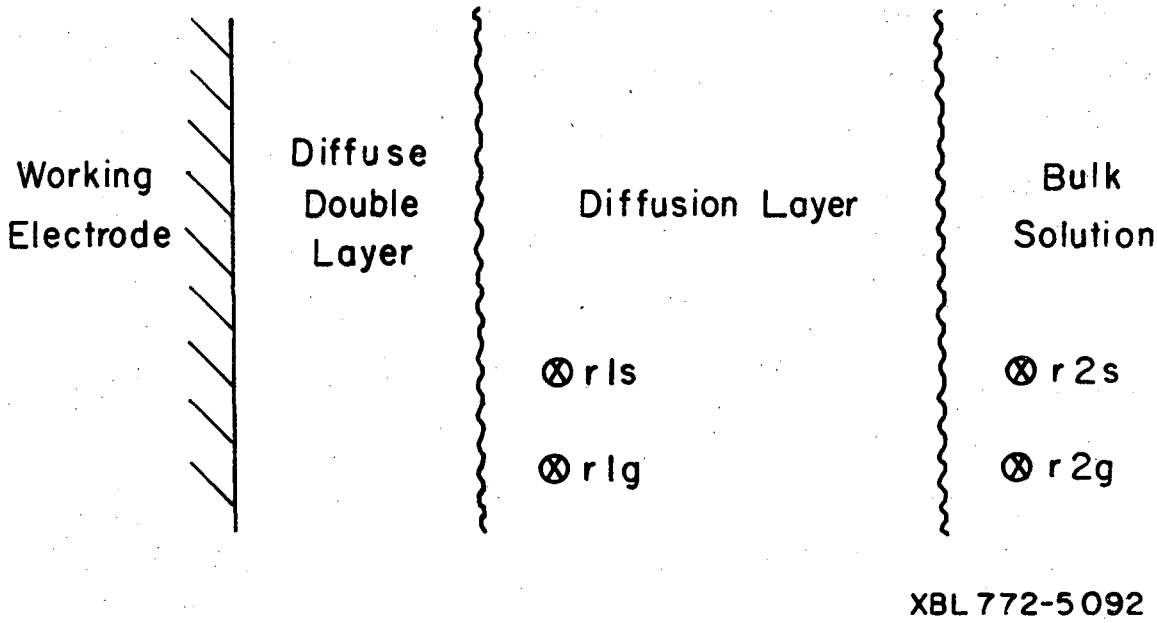

Figure A-1. Reference electrodes, which may be imaginary, positioned in the bulk solution and within the diffusion layer. The reference electrodes labeled r1s and r2s are of the same kind as the working electrode. The reference electrodes r1g and r2g are of a given kind.

Equation 2 can be used to obtain an expression relating the normal component of the gradient of the potential of a reference electrode of the same kind to that of the electrochemical potential of the species participating in reaction j by the limiting process:

$$\frac{\mu_{\underline{e}rs}(y + \Delta y) - \mu_{\underline{e}rs}(y)}{\Delta y} = -F \frac{V_{rs}(y + \Delta y) - V_{rs}(y)}{\Delta y}$$

$$= \sum_i \frac{s_{ij}}{n_j} \left[\frac{\mu_i(y + \Delta y) - \mu_i(y)}{\Delta y}\right] , \qquad \text{(A-3)}$$

and as $\Delta y \to 0$

$$\frac{\partial V_{rs}}{\partial y} = - \sum_i \frac{s_{ij}}{n_j F} \frac{\partial \mu_i}{\partial y} , \qquad \text{(A-4)}$$

or in general

$$\nabla V_{rs} = - \sum_i \frac{s_{ij}}{n_j F} \nabla \mu_i . \qquad \text{(A-5)}$$

The next step is to select a reference ion n and, since

$$\sum_i s_{ij} z_i = -n_j , \qquad \text{(A-6)}$$

transform equation 5 into

$$\nabla V_{rs} = \frac{1}{z_n F} \nabla \mu_n - \sum_i \frac{s_{ij}}{n_j F} \left(\nabla \mu_i - \frac{z_i}{z_n} \nabla \mu_n\right) . \qquad \text{(A-7)}$$

The current $\underline{i}$ can be introduced into equation 7 by using equation 16-1 of reference 22,

$$\frac{F}{\kappa}\underline{i} = -\sum_i \frac{t_i^o}{z_i}\nabla\mu_i \ , \qquad \text{(A-8)}$$

which, since

$$\sum_i t_i^o = 1 \ , \qquad \text{(A-9)}$$

can be written as

$$\frac{1}{z_n}\nabla\mu_n = -\frac{F}{\kappa}\underline{i} - \sum_i \frac{t_i^o}{z_i}\left(\nabla\mu_i - \frac{z_i}{z_n}\nabla\mu_n\right) . \qquad \text{(A-10)}$$

Combining equations 7 and 10 yields

$$\nabla V_{rs} = -\frac{\underline{i}}{\kappa} - \sum_i \frac{s_{ij}}{n_j F}\left(\nabla\mu_i - \frac{z_i}{z_n}\nabla\mu_n\right)$$

$$- \sum_j \frac{t_j^o}{z_j F}\left(\nabla\mu_j - \frac{z_i}{z_n}\nabla\mu_n\right) . \qquad \text{(A-11)}$$

Next, introduce the quasi-electrostatic potential Φ, which is defined by

$$\mu_n = RT \ln c_n + z_n F\Phi \ , \qquad \text{(A-12)}$$

so that the electrochemical potential of species i is given by

$$\mu_i = RT \ln c_i f_{i,n} a^{\theta}_{i,n} + z_i F\Phi \ , \tag{A-13}$$

where

$$f_{i,n} = f_i / f_n^{z_i/z_n} \tag{A-14}$$

and

$$a^{\theta}_{i,n} = a^{\theta}_i / \left(a^{\theta}_n\right)^{z_i/z_n} \ . \tag{A-15}$$

Then, by using equations 6, 9, and 13, equation 11 becomes

$$\nabla V_{rs} = -\frac{i}{\kappa} - \frac{RT}{n_j F} \sum_i s_{ij} \nabla \ln c_i f_{i,n}$$

$$- \frac{RT}{F} \sum_j \frac{t^o_j}{z_j} \nabla \ln c_j f_{j,n} \ . \tag{A-16}$$

Finally, an expression for the concentration overpotential for reaction j can be obtained by integrating equation 16 with respect to the normal distance y :

$$\eta_{cj} = V_{rls} - V_{r2s} - (V_{rls} - V_{r2s})_{\text{constant } c_i}$$

$$= \int_o^{y_{re}} i\left(\frac{1}{\kappa} - \frac{1}{\kappa_\infty}\right) dy$$

$$+ \frac{RT}{n_j F} \sum_i s_{ij} \ln \left(\frac{c_{i,\infty} f_{i,n,\infty}}{c_{i,o} f_{i,n,o}}\right)$$

$$+ \frac{RT}{F} \int_{o}^{y_{re}} \sum_{j} \frac{t_j^o}{z_j} \frac{\partial \ln (c_j f_{j,n})}{\partial y} dy \ , \qquad \text{(A-17)}$$

where

$$(V_{r1s} - V_{r2s})_{\text{constant } c_i} = \tilde{\Phi}_{r1s} - \tilde{\Phi}_{r2s} = \Delta\tilde{\Phi}_{\text{ohmic}} = \frac{1}{\kappa_\infty} \int_{o}^{y_{re}} i \, dy \ . \qquad \text{(A-18)}$$

Equation 17 can be simplified by neglecting activity coefficients, using equation 70-5 of reference 22,

$$t_j^o = \frac{z_j^2 u_j c_j}{\sum_i z_i^2 u_i c_i} \ , \qquad \text{(A-19)}$$

and the Nernst-Einstein equation,

$$D_i = RT \, u_i \ , \qquad \text{(A-20)}$$

as follows:

$$\eta_{cj} = \int_{o}^{y_{re}} i\left(\frac{1}{\kappa} - \frac{1}{\kappa_\infty}\right) dy + \frac{RT}{n_j F} \sum_i s_{ij} \ln \left(\frac{c_{i,\infty}}{c_{i,o}}\right) + F \int_{o}^{y_{re}} \sum_j \frac{z_j D_j}{\kappa} \frac{\partial c_j}{\partial y} dy \ . \qquad \text{(A-21)}$$

These approximations are valid for infinitely dilute solutions.

When an abundance of supporting electrolyte exists in solution, κ is approximately equal to κ_∞, and equation 21 simplifies to

$$\eta_{cj} = \frac{RT}{n_j F} \sum_i s_{ij} \ln \left(\frac{c_{i,\infty}}{c_{i,o}} \right) . \qquad \text{(A-22)}$$

(The last term in equation 21 is negligible in this case because it is on the order of $\sum_j (c_{j,\infty} - c_{j,o}) / \sum_i c_{i,\infty}$.)

Surface Overpotential

The surface overpotential for reaction j is the potential difference between the working electrode and an imaginary reference electrode of the same kind as the working electrode placed just outside the diffuse double layer with reaction j only equilibrated on the imaginary reference electrode,

$$\eta_{sj} = V - V_{rls} . \qquad \text{(A-23)}$$

Since multiple reactions can occur on the working electrode, it is convenient to introduce a reference electrode of a given kind so that equation 23 becomes

$$\eta_{sj} = V - V_{rlg} - (V_{rls} - V_{rlg}) . \qquad \text{(A-24)}$$

or

$$\eta_{sj} = V - \Phi_o - U_{j,o} , \qquad \text{(A-25)}$$

where

$$\Phi_o = V_{rlg} \qquad \text{(A-26)}$$

and

$$U_{j,o} = V_{rls} - V_{rlg} \quad . \tag{A-27}$$

The open-circuit potential of reaction j relative to a reference electrode of a given kind, $U_{j,o}$, can be expressed in terms of the relative activity of pertinent species:

$$U_{j,o} = \frac{1}{F}\left(\mu_{e^-}^{rlg} - \mu_{e^-}^{rls}\right) =$$

$$U_j^\theta - U_{re}^\theta + \frac{RT}{n_{re}F}\sum_i s_{i,re} \ln a_{i,re}$$

$$- \frac{RT}{n_j F}\sum_i s_{ij} \ln a_{i,o} + \Phi^{rec} - \Phi^s \quad , \tag{A-28}$$

where

$$FU_j^\theta = \frac{1}{2}\mu_{H_2}^* - RT \ln \lambda_{H^+}^\theta$$

$$- \frac{1}{n_j}\left(\sum_k s_{kj}\mu_k^o + \sum_\ell s_{\ell j}\mu_\ell^* + RT\sum_i s_{ij} \ln \lambda_i^\theta\right) \quad , \tag{A-29}$$

and the relative activity of species i is defined according to type:

species type	relative activity	
solid, amalgam, solvent	$a_i = \lambda_i/\lambda_i^o$	(A-30)
gaseous	$a_i = p_i\phi_i$	(A-31)
solute	$a_i = \frac{c_i f_{i,n}}{\rho_o}$.	(A-32)

The superscripts rec and s refer to the solution in the reference electrode compartment and the solution of interest, respectively, and the superscripts o , * , and θ designate a pure species, the ideal-gas secondary reference state (see reference 98 and problem 2-14 of reference 22), and the infinitely dilute secondary reference state, respectively. The subscripts k , ℓ , and i used in equation 29 denote solid, amalgam, or solvent, gaseous, and dilute species, respectively.

The expression for $U_{j,o}$ used in chapters 1 and 2 can be obtained from the above equations by subtracting the potential difference $\Phi^{rec} - \Phi^{s}$ from both sides of equation 28, thereby generating an expression for an open-circuit potential corrected for any liquid-junction potential which might exist between the solution in question and that within the reference electrode compartment, and by setting $f_{i,n} = 1$.

Total Overpotential

The total overpotential for reaction j is the sum of the concentration and surface overpotentials:

$$\eta_j = \eta_{cj} + \eta_{sj} \quad , \tag{A-33}$$

which, according to equations 17, 18, and 23 can be rewritten as

$$\eta_j = V - V_{r2s} - (\tilde{\Phi}_{r1s} - \tilde{\Phi}_{r2s}) \tag{A-34}$$

or, since

$$\tilde{\Phi}_{r1g} - \tilde{\Phi}_{r2g} = \tilde{\Phi}_{r1s} - \tilde{\Phi}_{r2s} \ , \qquad \text{(A-35)}$$

as

$$\eta_j = V - \tilde{\Phi}_o - U_{j,\infty} \ , \qquad \text{(A-36)}$$

where

$$\tilde{\Phi}_o = \tilde{\Phi}_{r1g} \qquad \text{(A-37)}$$

and

$$U_{j,\infty} = V_{r2s} - \tilde{\Phi}_{r2g} = U_j^{\theta} - U_{re}^{\theta} - \frac{RT}{n_j F} \sum_i s_{ij} \ln a_{i,\infty}$$

$$+ \frac{RT}{n_{re} F} \sum_i s_{i,re} \ln a_{i,re} + \tilde{\Phi}^{rec} - \tilde{\Phi}^{s} \ , \qquad \text{(A-38)}$$

with $a_{i,\infty} = a_{i,o}$ for solid or amalgam components.

Finally, an expression for the difference between Φ_o and $\tilde{\Phi}_o$ can be obtained from equation 84-3 of reference 22:

$$\Phi_o - \tilde{\Phi}_o = \int_o^{y_{re}} \left[i\left(\frac{1}{\kappa} - \frac{1}{\kappa_\infty}\right) + \frac{RT}{F} \sum_j \frac{t_j^o}{z_j} \frac{\partial \ln (c_j f_{j,n})}{\partial y} \right] dy \ . \qquad \text{(A-39)}$$

Equation 39 shows that in a well-supported solution there is a negligible difference between Φ_o and $\tilde{\Phi}_o$.

Appendix B. Parameter Development and Solution Technique for Chapter 1

Purpose

This appendix presents a derivation of the parameters in the governing equations for the surface concentration and potential distributions, as presented in chapter 1, and the solution technique used to obtain those distributions.

Parameters

The parameters N , J_j , A_j , ΔU_s , and V_m presented in chapter 1 can be developed from the governing equations for the potential and surface concentration distributions by introducing dimensionless parameters and variables that arise naturally for this problem. The potential in solution and that of the rotating-disk electrode can be made dimensionless most simply with F/RT :

$$\tilde{\Phi}^* = F\tilde{\Phi}/RT \qquad \text{(B-1)}$$

and

$$V^* = FV/RT \ . \qquad \text{(B-2)}$$

The surface concentration of species i referred to a reference concentration for species i is natural and convenient; thus, let

$$\Theta_{i,\infty} = c_{i,\infty}/c_{i,ref} \qquad \text{(B-3)}$$

and

$$\Theta_{i,o} = c_{i,o}/c_{i,ref} \ . \qquad \text{(B-4)}$$

(One should not use the bulk concentration of species i for this purpose, since species i may not exist in the bulk.) The dimensionless parameters

$$c^*_{i,ref} = c_{i,ref}/c_{R,\infty} \tag{B-5}$$

and

$$D^*_i = D_i/D_R \tag{B-6}$$

arise naturally from the governing equations if the established parameter N (developed earlier by Newman[10,22]) is introduced into the formulation of the dimensionless governing equations. Finally, equation 1-4 suggests the dimensionless radial coordinate

$$\zeta = (r/r_o)^3 . \tag{B-7}$$

First, by using equations 1 and 1-2, equation 1-8 becomes

$$i^*_T = - \frac{1}{\eta} \frac{\partial \tilde{\Phi}^*}{\partial \xi}\bigg|_{\xi=0} , \tag{B-8}$$

where

$$i^*_T = \frac{r_o F}{RT \kappa_\infty} i_T , \tag{B-9}$$

as suggested in chapter 1. Consequently, equation 1-9 can be written as

$$B^*_n = [P_{2n}(0)]^2 \frac{(4n+1)\pi}{2} \int_0^1 \eta i^*_T P_{2n}(\eta) d\eta , \tag{B-10}$$

where

$$B_n^* = FB_n/RT \ , \tag{B-11}$$

and, since $M_{2n}(0) = 1$, equation 1-1 reduces to

$$\tilde{\Phi}_o^*(\eta) = \sum_{n=0}^{\infty} B_n^* P_{2n}(\eta) \ . \tag{B-12}$$

The next step is to equate the expression for the normal component of the flux of species i given by equation 1-4 to that given by equation 1-7 and to use equation 9:

$$\sum_j \frac{s_{ij}}{n_j} i_j^* = \frac{\left(D_i^2 D_R\right)^{1/3}}{\delta_d \Gamma(4/3)} \frac{F^2 r_o}{RT\ \kappa_\infty} \left[c_{i,\infty} - c_{i,o}(0) - r \int_o^r \frac{dc_{i,o}(x)}{dx} \frac{dx}{(r^3 - x^3)^{1/3}} \right] , \tag{B-13}$$

which, by using equations 3 through 7, can be rewritten as

$$\sum_j \frac{s_{ij}}{n_j} i_j^* = \frac{c_{i,ref}^* D_i^{*2/3} N'}{\Gamma(4/3)} \left[\Theta_{i,\infty} - \Theta_{i,o}(0) - \zeta^{1/3} \int_o^1 \frac{d\Theta_{i,o}(x)}{dx} \frac{dx}{(\zeta - x)^{1/3}} \right] , \tag{B-14}$$

where

$$N' = \frac{F^2 D_R c_{R,\infty}}{RT\, \kappa_\infty\, \delta_d} \,. \tag{B-15}$$

N' is related to the parameter N (see equation 1-16):

$$N' = \frac{n_m^2}{s_{Rm}^2} N \tag{B-16}$$

Let us rewrite equation 14 using N and equations 1-10, 1-11 (recalling that for this case there is a negligible difference between Φ_o and $\tilde{\Phi}_o$, since the solution is well supported), and 1-12:

$$\frac{n_m^2}{s_{Rm}^2} \sum_j \frac{s_{ij}}{n_j} J_j' \left\{ \prod_k \Theta_{k,o}^{p_{kj}} \exp\left[\frac{\alpha_{aj} F}{RT} (V - \tilde{\Phi}_o - U_{j,ref})\right] \right.$$

$$\left. - \prod_k \Theta_{k,o}^{q_{kj}} \exp\left[-\frac{\alpha_{cj} F}{RT} (V - \tilde{\Phi}_o - U_{j,ref})\right] \right\}$$

$$= \frac{c_{i,ref}^* D_i^{*2/3} N}{\Gamma(4/3)} \left[\Theta_{i,\infty} - \Theta_{i,o}(0) \right.$$

$$\left. - \zeta^{1/3} \int_o^1 \frac{d\Theta_{i,o}(x)}{dx} \frac{dx}{(\zeta - x)^{1/3}} \right] , \tag{B-17}$$

where $U_{j,ref}$ is given by equation 1-12 with the surface concentrations replaced with reference concentrations, and (according to equation 1-14)

$$J_j' = \frac{Fr_o}{RT\, \kappa_\infty} i_{oj,ref} = - \frac{s_{Rm}}{n_m} J_j \,. \tag{B-18}$$

Equation 17, which is solved in the computer program CURDMR (to be discussed), can be simplified by moving the ratio $\Gamma(4/3)J_j/N$ into the exponential terms and then by collecting and redefining parameters:

$$\frac{s_{Rm}}{n_m} D_i^{*2/3} c_{i,ref}^{*} \left[\Theta_{i,\infty} - \Theta_{i,o}(0) - \zeta^{1/3} \int_o^1 \frac{d\Theta_{i,o}(x)}{dx} \frac{dx}{(\zeta - x)^{1/3}}\right]$$

$$= \sum_j \frac{s_{ij}}{n_j} \exp\left(-\frac{\alpha_{cj}F}{RT} \Delta U_j\right) \exp\left[-\frac{\alpha_{cj}F}{RT} (V - V_m - \tilde{\Phi}_o)\right]$$

$$\prod_k \Theta_{k,o}^{q_{kj}} - \sum_j \frac{s_{ij}}{n_j} A_j \exp\left[\frac{\alpha_{aj}F}{RT} (V - V_m - \tilde{\Phi}_o)\right]$$

$$\prod_k \Theta_{k,o}^{p_{kj}} , \qquad \text{(B-19)}$$

where equation 19 has been written for convenient comparison to equation 1-19 and

$$A_j = \left(\frac{\Gamma(4/3)J_j}{N}\right)^{1 + \frac{\alpha_{aj}}{\alpha_{cj}}} \exp\left(\frac{\alpha_{aj}F}{RT} \Delta U_j\right) , \qquad \text{(B-20)}$$

$$V_m = U_{m,ref} - \frac{RT}{\alpha_{cm}F} \ln\left(\frac{N}{\Gamma(4/3)J_m}\right) , \qquad \text{(B-21)}$$

and

$$\Delta U_j = U_{m,ref} - U_{j,ref} - \frac{RT}{\alpha_{cj}F} \ln\left(\frac{\Gamma(4/3)J_j}{N}\right)$$

$$+ \frac{RT}{\alpha_{cm}F} \ln\left(\frac{\Gamma(4/3)J_m}{N}\right) . \qquad \text{(B-22)}$$

These expressions for A_j , V_m , and ΔU_j are the same as those given in chapter 1. (Substitute $U_{j,ref}$ from equation 22 into equation 17 to verify equation 19.) See chapter 1 for a discussion of the parameters A_j , V_m , and ΔU_j .

The governing equation for $\tilde{\Phi}_o$ comes from combining equations 10 and 12 and using equation 1-10, made dimensionless as before:

$$\frac{F\tilde{\Phi}_o}{RT} = \frac{n_m^2}{s_{Rm}^2} \frac{N}{\Gamma(4/3)} \frac{\pi}{2} \sum_{n=o}^{\infty} (4n + 1)[P_{2n}(0)]^2$$

$$\int_o^1 \sum_j A_j \exp\left[\frac{\alpha_{aj}F}{RT}(V - V_m - \tilde{\Phi}_o)\right] \prod_k \Theta_{k,o}^{p_{kj}}$$

$$- \exp\left(-\frac{\alpha_{cj}F}{RT}\Delta U_j\right) \exp\left[-\frac{\alpha_{cj}F}{RT}(V - V_m - \tilde{\Phi}_o)\right]$$

$$\prod_k \Theta_{k,o}^{q_{kj}} P_{2n}(\eta)\eta \, d\eta \ . \qquad \text{(B-23)}$$

The coupled equations 19 and 23 govern the distributions of the potential $\tilde{\Phi}_o$ and the surface concentration of species i , $\Theta_{i,o}$. The parameters are A_j , $c^*_{i,ref}$, D^*_i , N , p_{kj} , q_{kj} , s_{ij}/n_j , ΔU_j , V_m , α_{aj} , and α_{cj} .

Solution Technique

The surface concentration and potential distributions can be approximated by calculated values at a finite number of mesh points, mp ; these distributions can then be used to determine the current distribution.

First, since the number of unknowns must equal the number of independent governing equations, let us count the number of unknowns. V , $\Theta_{i,o}$, and $\tilde{\Phi}_o^*$ are the unknown dependent variables and, since there are nc minor components, there are $(nc + 1)mp + 1$ unknowns. The independent governing equations for the unknowns are equations 19, of which there are nc , and equation 23. Thus, there are $(nc + 1)mp$ governing equations; therefore, since the unknowns outnumber the governing equations by one, we must set one of the unknowns. For convenience, the surface concentration of the principal reactant at the center of the disk can be set.

In the program CURDMR, equations 19 and 23 are decoupled and solved separately in an iterative manner. The first step is to set the concentration of the principal reactant at the center of the disk and solve equations 19 for $V - \tilde{\Phi}_o(r = 0)$ and the surface concentration of the other minor species at the center of the disk. Then, assuming that $V - \tilde{\Phi}_o(r = 0)$ applies across the disk, solve equations 19 at each mesh point for the surface concentration of the minor species from which the current distribution can be obtained according to the Butler-Volmer equation (see equation 1-10). Equation 10 is then integrated by Gauss-Legendre quadrature to obtain a finite number of B's which are used in equation 12 to obtain $\tilde{\Phi}_o^*$. The electrode potential V and, consequently, a new $V - \tilde{\Phi}_o$ distribution are then obtained in such a way that $V - \tilde{\Phi}_o(r = 0)$ remains fixed. The overall process is repeated for $r > 0$ until convergence is achieved.

Program Discussion

The program calculates the electrode potential V, the local solution potential $\tilde{\Phi}_o$, and the local surface concentrations $\Theta_{i,o}$, which (according to equation 1-10) can then be used to calculate the local current density. These distributions are approximated by solving the governing equations at LMAX equally spaced mesh points.

The governing equation for the surface concentration of species i (see equation 17) at mesh point ℓ for $2 \leq \ell \leq$ LMAX can be written as[35]

$$F_i = \frac{\Gamma(4/3)}{N} \frac{D_i^{*2/3}}{c_{i,ref}^*} \frac{2\, h^{1/3}}{3\, \zeta_\ell^{1/3}} \frac{n_m^2}{s_{Rm}^2} \sum_{j=1}^{NR} \frac{s_{ij}}{n_j} J_j'$$

$$\left\{ \prod_k \Theta_{k,o,\ell}^{p_{kj}} \exp\left[\alpha_{aj}(E_\ell + DEC_j)\right] \right.$$

$$\left. - \prod_k \Theta_{k,o,\ell}^{q_{kj}} \exp\left[-\alpha_{cj}(E_\ell + DEC_j)\right] \right\}$$

$$- \frac{2\, h^{1/3}}{3\, \zeta_\ell^{1/3}} (\Theta_{i,\infty} - \Theta_{i,o,1}) + \Theta_{i,o,\ell}$$

$$- \Theta_{i,o,1} b_{\ell-1} - SUM = 0 , \qquad \text{(B-24)}$$

where

$$E_\ell = F(V - \tilde{\Phi}_{o,\ell})/RT , \qquad \text{(B-25)}$$

$$DEC_j = -FU_{j,ref}/RT , \qquad \text{(B-26)}$$

$$a_n = 2n^{2/3} - (n+1)^{2/3} - (n-1)^{2/3} , \qquad \text{(B-27)}$$

$$b_n = n^{2/3} - (n-1)^{2/3} , \qquad \text{(B-28)}$$

$$h = 1/(\text{LMAX} - 1) , \qquad \text{(B-29)}$$

$$\zeta_\ell^{1/3} = r_\ell / r_o , \qquad \text{(B-30)}$$

$$\text{SUM} = 0 \quad \text{for} \quad \ell = 2 , \qquad \text{(B-31)}$$

and

$$\text{SUM} = \sum_{k=2}^{\ell-1} \Theta_{i,o,k} a_{\ell-k} \quad \text{for} \quad 3 \leq \ell \leq \text{LMAX} . \qquad \text{(B-32)}$$

At the center of the disk ($\ell = 1$), equation 24 applys with the last 3 terms set equal to zero. Once the concentration of the principal reactant at the center of the disk $\Theta_{R,o,1}$ is specified, E_1 and $\Theta_{i,o,1}$ for $i \neq R$ remain to be determined. The subroutine CENTER solves equation 24 for these unknowns by multidimensional Newton-Raphson iteration.[99] That is, it is assumed that

$$F_i(x_k) = F_i(x_k^o) + \sum_k \left.\frac{\partial F_i}{\partial x_k}\right|_{x_k = x_k^o} (x_k - x_k^o) \qquad \text{(B-33)}$$

or, if $F_i(x_k) = 0$,

$$\sum_k \left.\frac{\partial F_i}{\partial x_k}\right|_{x_k = x_k^o} x_k = -F_i(x_k^o) + \sum_k \left.\frac{\partial F_i(x_k)}{\partial x_k}\right|_{x_k = x_k^o} x_k^o , \qquad \text{(B-34)}$$

where x_k represents an unknown dependent variable and the superscript o designates a trial value. Solving a set of equations for nc unknowns can be carried out by solving

$$\underline{\underline{B}}\ \underline{x} = \underline{d}\ , \tag{B-35}$$

where

$$\underline{\underline{B}} = \begin{bmatrix} \frac{\partial F_1^o}{\partial x_1} & \cdots & \frac{\partial F_1^o}{\partial x_{nc}} \\ \vdots & & \\ \frac{\partial F_{nc}^o}{\partial x_1} & & \frac{\partial F_{nc}^o}{\partial x_{nc}} \end{bmatrix}, \tag{B-36}$$

$$\underline{x} = \begin{bmatrix} x_1 \\ \vdots \\ x_{nc} \end{bmatrix}, \tag{B-37}$$

and

$$\underline{d} = \begin{bmatrix} -F_1^o + \frac{\partial F_1^o}{\partial x_1} x_1^o \\ \vdots \\ -F_{nc}^o + \frac{\partial F_{nc}^o}{\partial x_{nc}} x_{nc}^o \end{bmatrix}. \tag{B-38}$$

Once E_1 and $\Theta_{i,o,1}$ are known, the program enters the main iteration loop, where it is assumed initially that E_1 applies at each mesh point. The subroutine SURF then solves equation 24 for $\Theta_{i,o,\ell}$ for $2 \leq \ell \leq$ LMAX, again by iteration at each mesh point. The procedure described in the previous section of this appendix and chapter 1 is then carried out until overall convergence is obtained.

Once overall convergence is achieved, $\tilde{\Phi}_{re}$ can be predicted according to equation 1-1, where $M_{2n}(\xi)$ is determined by the function subprogram FUNM (see Miksis[100]).

In addition, the converged potential distribution $\tilde{\Phi}_o$ can be compared to that predicted for a uniform current density, which can be obtained either from the series solution according to equation 12 or (as it is in the program) from an expression presented by Nanis and Kesselman[41] as corrected by Pierini:[101]

$$\tilde{\Phi}_o(r) = \frac{2i_{m,lim} r_o}{\pi \kappa_\infty} E\left[\left(\frac{r}{r_o}\right)^2\right], \qquad \text{(B-39)}$$

where E is the complete elliptic integral of the second kind.

Program Listing

The following is a partial list of the symbols used in the program:

AN	N
AVG	$i_{avg}/i_{m,lim}$
C(I,L)	$\Theta_{i,o,\ell}$
CB(I)	$c_{i,\infty}$, mole/ℓ
CDATA(I)	$c_{i,data}$, mole/ℓ
CINF(I)	$\Theta_{i,\infty}$
COND	κ_∞ , $\Omega^{-1}cm^{-1}$
CREF(I)	$c_{i,ref}$, mole/ℓ
CSUP	concentration of the supporting electrolyte, mole/ℓ

CRØ	$\Theta_{R,o,1}$
CUG(I)	i_T^* at X(I)
CUR(L)	$i_{T,\ell}^*$ through statement number 22 then $i_{T,\ell}/i_{m,lim}$
CURJ(J,L)	$i_{j,\ell}^*$ through statement number 22 then $i_{j,\ell}/i_{m,lim}$
CUR1L	$i_{m,lim}$, A/cm^2
DEC(J)	$-FU_{j,ref}/RT$
DELTAP	δ (see equation 1-13)
DELTAU	ΔU_s , V
E(L)	$F(V - \tilde{\Phi}_{o,\ell})/RT$
IH	1/2 the number of Gauss-Legendre quadrature points
LMAX	number of equally spaced mesh points
NC	number of components
NMAX	number of terms in the potential series
NR	number of reactions
RHO	ρ_o , g/cm^3
RNEF	n_{re}
RIODAT(J)	$i_{oj,data}$, A/cm^2
RIOREF(J)	$i_{oj,ref} = i_{oj,data}\left(\frac{c_{i,ref}}{c_{i,data}}\right)^{\gamma_{ij}}$
RJ(J)	J_j'
RN(J)	n_j
RREF	distance of reference electrode to the axis of the disk, cm
SREF	$s_{i,re}$
TCUR	total current $I = i_{avg}\pi r_o^2$, A

TCURA	i_{avg} , A/cm^2
UTH(J)	U_j^{θ} , V
UTHR	U_{re}^{θ} , V
W(I)	Gauss-Legendre weighting factor
X(I)	Gauss-Legendre abscissa

A listing of the program CURDMR , associated subroutines, and input data follows.

```
      PROGRAM CURDMR(INPUT,OUTPUT,PUNCH,TAPE1=PUNCH)
      DIMENSION C(4,201),E(201),RN(3),CINF(3),DEC(3),ALFA(3),ALFC(3),
     1RJ(3), S(3,3),Q(3,3),O(3,3), DIF(3),      UTH(3),CB(3),REF2(3),
     2 AA(200),BB(200),CUR(201),CURJ(3,201),CUG(40),X(40),W(40),PG(21,
     1 40),PP(21,201),R(201),B(40),PM(40),AVGJ(3),CUGJ(3,40),REF1(3)
     1 ,EFF(201)
     1 ,ETAC(4,201),ETAS(4,201),UJINF(2)     ,CH2(201),A(201)
     1,IFLAG(2),PHIO(201)
     1 , RIODAT(3),RIOREF(3),GAM(3,3),CREF(3),CDATA(3),PHIINV(201)
     1 ,PHIUNI(201)
      COMMON C,E,RN,CINF,DEC,ALFA,ALFC,RJ,S,Q,O,DIF,AN,NC,NR,C1,LMAX,
     1 CUR,CURJ,CRINF,CREF,AA,BB
  101 FORMAT (6H ERROR,I4)
  102 FORMAT(///,2X,*AN=*,E10.3,3X,*CRO=*,E10.3,3X,*CRINF IN M/L=*
     1 ,E15.4,/3X,*UTHR V=*,F10.5,5X,*DAMP=*,F10.5,5X,*CREFI M=*,F10.5,
     1 5X,*NREF=*,F10.1,5X,*SREF=*,F10.1,5X,*RPM = *,F10.5,/5X,*NU=*,
     1 F10.6,5X,*RO IN CM = *,E10.4,5X,*CONC OF SUP ELECT M = *,F10.5,
     15X,*COND=*,F10.5,5X,*    VM =*,F10.5//)
  103 FORMAT (3I4)
  104 FORMAT(8F8.4,E12.4)
  105 FORMAT(2X,*LMAX=*,I3,3X,*NMAX=*,I3,3X,*IH=*,I3,//)
  106 FORMAT(2X,*NUMBER OF COMPONENTS=*,I3,3X,*NUMBER OF REACTIONS=*,I3
     1,32X,*REACTION 1*, 5X,*REACTION 2*
     1/2X,*SPECIES*,15X,*DIF*,12X,*CB M *,11X,*CREF M*, 8X,
     1                                        *CDATA M*, 8X,*S*, 4X,*GAM
     1*,8X,*S*,4X,*GAM*,
     1      /(3X,A6,A6,2X,E14.6,3X,E12.4,6X,2E12.4,5X,2F5.2, 6X,2F5.2))
  107 FORMAT( 2F15.0,A6,A6,I5,E12.4)
  108 FORMAT (6E12.9)
  109 FORMAT(/,30X,*PARAMETER*/2X,*REACTION*,12X,*UTH*,8 X,*J*
     1 ,10X,*RIODAT A/CM2*, 7X,*ALFA*,6X,*ALFC*,6X,*N*/(I5,12X,F10.5,
     1 E12.4,5 X,E12.4,3F10.1))
  110 FORMAT(7F10.0)
  111 FORMAT(//,8X,*R*,7 X,*  E   *,7 X,*CUR*,7 X,*CUR1*,6 X,*CUR2*
     1        ,8 X,*C1*,8X,*C2*,7X,*CH2 IN M/L *,4X,*EFF*,4X,*PHIO*)
  112 FORMAT(2X,4F10.5,E12.4, F10.5,2E12.4,2F10.5)
  113 FORMAT(/,2X,*AVG =*,F10.5,
     1 5 X,*BAVG=*,F10.5, 5X,*RAT1=*,F10.5,5 X,*RAT2=*,F10.5/5X,*V=*
     1 ,F10.5,                5X,*AVG1=*,F10.5,5X,*AVG2=*,
     1 E12.4,2X,*EFFAVG=*,F10.5,5X,*CELLP IN MV=*,F10.4,4X,
     1 *TCUR IN MA = *,E11.4/2X,*PHIREF IN V=*,E10.3,5X,*IMLIM IN A/CM2
     1=*,E11.4,5X,*RREF IN CM=*,F10.5,5X,*DELTAP=*,F10.5,5X,*DELTAU=*,
     1F10.5/2X,*RELDEL=*,F10.5)
  114 FORMAT(2X,*JCOUNT=*,I3//)
  115 FORMAT(//,30X,*B*/(2X,6F10.5))
  116 FORMAT(///,8X,*R*,8X,*V-PHI*,5X,*PHI*
     1                          ,5X,*ETAC1*,8X,*ETAS1*,5X,*UJINF1*
     1 ,9X,*ETAC2*,9X,*ETAS2* ,6X,*UJINF2*,5X,*PHIUNI*)
  117 FORMAT (2X,3F10.5,4E12.4,2E12.4,2X, F10.5)
  118 FORMAT(2X,2E20.5)
  121 FORMAT(1H1)
  122 FORMAT(5F10.0)
  123 FORMAT( E12.4)
      PRINT 121
      READ 103, LMAX,NMAX,IH $ IM=IH*2
      PRINT 105,LMAX,NMAX,IH
      DZ= 1.0/(LMAX-1)
      DO 1 L=1,LMAX
      Z   = (L-1)*DZ
      R(L)= Z   **(1.0/3.0)
      ETA= SQRT(1.0-R(L)*R(L))
```

```
      DO 1 N=1,NMAX
    1 PP(N,L)= P(2*N-2,ETA)
      DO 2 N=1,NMAX
    2 PM(N)=-0.636619724/P(2*N-2,0.0)**2
      IHP1= IH + 1
      READ 108, (X(I),I=IHP1,IM)
      READ 108, (W(I),I=IHP1,IM)
      DO 34 I=1,IM
      IF (I-IH)  31,31,32
   31 IR= IM - I + 1
      X(I)= 0.5 - 0.5*X(IR)
      W(I)= W(IR)
      GO TO 33
   32 X(I)= 0.5 + 0.5*X(I)
   33 XX= SQRT(1.0-X(I)**2)
      DO 34 N=1,NMAX
   34 PG(N,I) = P(2*N-2,XX)
      C1=1.11984652
      READ103,NC,NR,ICPP
      READ 104,((S(I,J),GAM(I,J),I=1,NC),ALFA(J),ALFC(J),RN(J),UTH(J),
     1 RIODAT(J),J=1,NR)
      READ 107,(DIF(I),CB(I),REF1(I),REF2(I),IFLAG(I),CDATA(I),I=1,NC)
      READ 122,RPM,RNU,R0,CSUF,RREF
      READ 110,UTHR,CREFI,RNEF,SREF,DAMP
      CRINF=CB(1)
      UTHR=UTH(1) $ CREFI=CRINF
      CREF(1)=CRINF $ CREF(2)=CDATA(2)
      RHO=.99707 $ PI=3.141592654
      F=96487.$RR=8.3143 $ T=298.15 $ DF=F/RR/T
      COND=F*DF*(1.0642E-4*CSUF-5.102E-5*CRINF)/1000.
      CRINF2=CRINF**2 $ CSUP2=CSUP**2
      COND=.011163+.030798*CRINF+.42355*CSUP-.045224*CSUP2-.135359
     1 *CRINF*CSUP
      IF(ICPP)37,37,36
   36 RMUCP=.89864+.45948*CRINF+.14068*CSUF+.027576*CSUP2+.092374*CRINF
     1 *CSUP
      RMUP=RMUCP*.01
      SOLDEN=.999+.14219*CRINF+.061374*CSUF-.0003722*CSUP2-.005536*
     1 CRINF*CSUP $ RNU=RMUP/SOLDEN
      DIF(1)=5.97E-6+3.2E-6*CRINF-6.56E-7*CSUP-3.06E-6*CRINF2-5.85
     1 E-8*CSUP2
   37 CONTINUE
      DO 13 I=1,NC
   13 CINF(I)=CB(I)/CREF(I)
      DO 14 J=1,NR
      DEC(J)=-SREF/RNEF*ALOG(CREFI/RHO)+DF*(UTHR-UTH(J))
      DO 14 I=1,NC
   14 DEC(J)=DEC(J)+S(I,J)/RN(J)*ALOG(CREF(I)/RHO)
      DEC(2)=DEC(2)-ALOG(CSUP/RHO)
      DO 10 I=1,NC $ DO 10 J=1,NR
      Q(I,J)=0(I,J)=0.0
      IF(S(I,J).LT.0.0)Q(I,J)=-S(I,J)*ALFC(J)/RN(J)+GAM(I,J)
   10 IF(S(I,J).GT.0.0)O(I,J)=S(I,J)*ALFA(J)/RN(J)+GAM(I,J)
      DO 8 J=1,NR $ RIOREF(J)=1. $ DO 7 I=1,NC
    7 RIOREF(J)=RIOREF(J)*          (CREF(I)/CDATA(I))**GAM(I,J)
      IF(J.EQ.2)RIOREF(2)=RIOREF(2)*(CSUP/1.)**.5
    8 RJ(J)=RIOREF(J)*R0*DF/CCNC*RIODAT(J)
      CK=.51023262 $ OMEGA=2.*PI*RPM/60.
      DELTA=(3.*DIF(1 )/CK/RNU)**(1./3.)*SQRT(RNU/OMEGA)
      AN=RN(1)**2*R0*DIF(1 )*CRINF*DF/S(1,1)**2/COND/DELTA*F/1000.
      QQ=(-RN(1)/S(1,1) *RJ(2)/AN/C1)*(-AN*C1/RN(1)/S(1,1) /
     1 RJ(1))**(ALFC(2)/ALFC(1))
```

```
      DELTAU=DEC(2)-DEC(1)-ALCG(QQ)/ALFC(2) $ DELTAU=DELTAU/DF
      VM=-DEC(1)/DF+ALOG(-RN(1)/S(1,1) /C1*RJ(1)/AN)/DF/ALFC(1)
    3 READ 123,CR0
      IF(CR0)4,4,5
    4 STOP
    5 JCOUNT= 0
      PRINT 102,AN,CR0,CRINF,UTHR,DAMP,CREFI,RNEF,SREF,RPM,RNU,R0,CSUP,
     1 COND,VM
      PRINT 106,NC,NR,(REF1(I),REF2(I),DIF(I),CB(I),CREF(I),
     1                                          CDATA(I),S(I,1),
     1 GAM(I,1),S(I,2),GAM(I,2) ,I=1,NC)
      PRINT 109,(J,UTH(J),RJ(J),RIODAT(J),ALFA(J),ALFC(J),RN(J),J=1,NR)
      C(1 ,1)=CR0
      CALL CENTER
      EX= 2.0/3.0
      DO 29 L=1,LMAX
      E(L)=E(1)
      A=FLOAT(L)
      AA(L)= 2.0*A**EX - (A+1.0)**EX - (A-1.0)**EX
   29 BB(L)= A**EX - (A-1.0)**EX
      B(1)= 0.0
   12 BOLD= B(1)
      JCOUNT= JCOUNT + 1
      CALL SURF
      DO 16 I=1,IM
      LI= X(I)**3/DZ + 1
   16 CUG(I)= CUR(LI)+(CUR(LI+1)-CUR(LI))*(X(I)**2-R(LI)**2)/(R(LI+1)**2
     1-R(LI)**2)
      V= E(1)
      DO 15 N=1,NMAX
      B(N)= 0.0
      DO 21 I=1,IM
   21 B(N)= B(N) + CUG(I)*X(I)*PG(N,I)*W(I)
      B(N)=-0.5*B(N)*(4*N-3)/PM(N)
   15 V= V + B(N)*PP(N,1)
      DO 18 L=2,LMAX
      PHI= V
      DO 17 N=1,NMAX
   17 PHI= PHI - B(N)*PP(N,L)
   18 E(L)= E(L) + DAMP*(PHI-E(L))
      JERR= 2
      IF (JCOUNT-100)  19,19,20
   19 IF (ABS(B(1)-BOLD) - 0.000001*ABS(B(1)))  22,22,12
   20 PRINT 101, JERR
   22 CONTINUE
      DO 23 L=1,LMAX $ CUR(L)=0.0 $ DO 23 J=1,NR
      CURJ(J,L)=CURJ(J,L)*RN(1)/C1/AN/S(1,1)
   23 CUR(L)=CUR(L)+CURJ(J,L)
      AVG=0.0
      DO 35 J=1,NR $      AVGJ(J)=0.0
      DO 30 I=1,IM $ LI=X(I)**3/DZ+1
      CUGJ(J,I)=CURJ(J,LI)+(CURJ(J,LI+1)-CURJ(J,LI))*(X(I)**2-R(LI)**2)
     1 /(R(LI+1)**2-R(LI)**2)
   30 AVGJ(J)=AVGJ(J)+X(I)*CUGJ(J,I)*W(I)
   35 AVG=AVG+AVGJ(J)
      CUR1L=S(1,1)*COND*AN/RN(1)/DF*C1/R0
                                      TCUR= AVG*CUR1L*100.*PI*R0**2
      TCURA=AVG*CUR1L
      DO 25 L=1,LMAX $ CH2(L)=C(2,L)*CREF(2)$A(L)=E(L)/DF
      PHI0(L)=V-E(L)
      PHIINV(L)=PHI0(L)/DF
      IF(L.EQ.LMAX)GOTO25
```

```
      R2=R(L)**2
      PHIUNI(L)=2.*TCURA*R0/PI/COND*ELINT2(R2)
   25 EFF(L)=CURJ(1,L)/CUR(L)
      PHIUNI(LMAX)=2.*TCURA*R0/PI/COND
      EFFAVG=AVGJ(1)/AVG
      BAVG=B(1)/0.7853981634/C1/AN/S(1,1)*RN(1) $ RAT1=CUR(1)/BAVG
      RAT2=(V-E(1))/B(1)
      PHIREF=0.
      IF(R0.GE.RREF)GOTO1000
      L=LMAX $            XI=SQRT((RREF/R0)**2-1.) $ PHIREF=0.
      DO 6N=1,NMAX
    6 PHIREF=PHIREF+B(N)*PP(N,L)*FUNM(N,XI)
 1000 CONTINUE
      CELLP=-(V-PHIREF)/DF*1000.
      DO 27 J=1,NR$UJINF(J)=0. $DO 28 I=1,NC$IF(IFLAG(I).GT.0)GOTO 28
      UJINF(J)=S(I,J)*ALOG(CB(I)/RHO)+UJINF(J)
   28 CONTINUE$UJINF(J)=-UJINF(J)/RN(J)/DF
   27 UJINF(J)=UJINF(J)+UTH(J)-UTHR+SREF/RNEF/DF*ALOG(CREFI/RHO)
      DO 26 J=1,NR
                        DO 26 L=1,LMAX $ ETAC(J,L)=0.
      DO 24 I=1,NC
      IF(IFLAG(I).GT.0)GOTO 24
      ETAC(J,L)=ETAC(J,L)+S(I,J)*ALOG(CINF(I)/C(I,L))/DF/RN(J)
   24 CONTINUE
   26 ETAS(J,L)=A(L)-ETAC(J,L)-UJINF(J)
      PRINT 111 $ PRINT112,(R(L),E(L),CUR(L),(CURJ(J,L),J=1,NR),(C(I,L)
     1 ,I=1,NC),CH2(L),EFF(L),PHI0(L),          L=1,LMAX)
      PHIREF=PHIREF/DF
      DELTAP=-RN(1)/S(1,1)*R0*DF/COND*ABS(TCURA)
      RELDEL=DELTAP/C1/AN
      PRINT 113, AVG,BAVG,RAT1,RAT2,V,       (AVGJ(J),J=1,NR),EFFAVG
     1 ,CELLF,TCUR,PHIREF, CUR1L ,RREF,DELTAF,DELTAU,RELDEL
      PRINT 114,JCOUNT
      PRINT 116 $ PRINT 117,(R(L),A(L),PHIINV(L),
     1 (ETAC(J,L),ETAS(J,L),UJINF(J),J=1,NR),PHIUNI(L),L=1,LMAX)
      PRINT 115,(B(I),I=1,NMAX)
      GO TO 3 $ END
      SUBROUTINE CENTER
      DIMENSION C(4,201),E(201),RN(3),CINF(3),CUR(201),CURJ(3,201),
     1   CREF(3),DEC(3),FF(3),BBB(4,4),ALFA(3),ALFC(3),RJ(3) ,DD(4),
     1 D(3), S(3,3),Q(3,3),P(3,3),                UTH(3),CB(3)
      COMMON C,E,RN,CINF,DEC,ALFA,ALFC,RJ,S,Q,P,D,AN,NC,NR,C1,LMAX,CUR,
     1 CURJ,CRINF,CREF
  101 FORMAT(6H ERROR,I4)
  102 FORMAT(2X,*C3 DID NOT CONVERGE*)
  109 FORMAT(5X,*DETERM=0.0 AT L=1*,I5)
  103 FORMAT(3X,*E(1) DID NOT CONVERGE*)
      EX=2./3.
      JCOUNT=0
      E(1)=-DEC(1)
      IF(.9-C(1,1))25,25,26
   26 PRODE = 1.0   $ DO 15 I=1,NC
   15 IF(Q(I,1).GT.0.0)PRODE=C(I,1)**Q(I,1)*PRODE
      E(1)=-DEC(1)-ALOG(-AN*S(1,1)*C1/RJ(1)/PRODE/RN(1)*(CINF(1)-C(1,1)
     1 )*CREF(1)/CRINF)/ALFC(1)
   25 CONTINUE
      EOLD=E(1)
      DO 22 M=1,20
      DO23 I=1,1   $ BBB(I,1 )=0.0
      FF(I)=-AN*(D(I)/D(1 ))**EX*C1*(CINF(I)-C(I,1))*CREF(I)/CRINF
      DO23 J=1,NR $ PRODAJ=PRODCJ=1.0 $ DO41 K=1,1
      IF(P(K,J).GT.0.0)PRODAJ=C(K,1)**P(K,J)*PRODAJ
```

```
 41 IF(Q(K,J).GT.0.0)PRODCJ=C(K,1)**Q(K,J)*PRODCJ
    ANODJ  =EXP (ALFA(J)*(E(1)+DEC(J)))
    CATHJ  =EXP(-   ALFC(J)*(E(1)+DEC(J)))
    BBB(I,1 )=(S(I,J)*RJ(J)/RN(J)*(ANODJ  *PRODAJ*ALFA(J)+  CATHJ  *
   1 PRODCJ*ALFC(J)))*RN(1)**2/S(1 ,1)**2 + BBB(I,1 )
 23 FF(I)=FF(I)+(S(I,J)*RJ(J)/RN(J)*(ANODJ  *PRODAJ-CATHJ  *
   1 PRODCJ))*RN(1)**2/S(1 ,1)**2
    E(1)=E(1)-FF(1)/BBB(1,1)
    IF(ABS(EOLD-E(1))-1.E-6*ABS(E(1)))24,24,22
 22 EOLD=E(1) $ PRINT 103
 24 CONTINUE
    C(2,1)=EXP(-(ALFA(2)+ALFC(2))*(E(1)+DEC(2)))**(1./P(2,2))
                    COLD=C(2,1) $ DO  10 K=1,20
    F31=RN(1)**2/S(1,1)**2*S(2,2)/RN(2)*RJ(2)*C(2,1)**P(2,2)*
   1 EXP(ALFA(2)*(E(1)+DEC(2)))
    F31C=-RN(1)**2/S(1,1)**2*S(2,2)/RN(2)*RJ(2)*EXP(-ALFC(2)*
   1 (E(1)+DEC(2)))
    F32=-AN*C1*(D(2)/D(1))**EX*CREF(2)/CRINF
                                    F3=F31+F32*(CINF(2)-C(2,1))+F31C
    F3P=F31*P(2,2)/C(2,1)-F32 $ C(2,1)=C(2,1)-F3/F3P
    IF(ABS(COLD-C(2,1))-1.E-6*ABS(C(2,1)))11,11,10
 10 COLD=C(2,1) $ PRINT 102
 11 COLD=C(2,1)
    DO 3 I=1,NC $ BBB(I,1 )=0.0
    FF(I)=-AN*(D(I)/D(1 ))**EX*C1*(CINF(I)-C(I,1))*CREF(I)/CRINF
    DO 5 K=2,NC $ BBB(I,K)=0.0
  5 IF(K.EQ.I)BBB(I,K)=AN*C1*(D(I)/D(1))**EX*CREF(I)/CRINF
    DO 3 J=1,NR $ PRODAJ=PRODCJ=1.0 $ DO 1 K=1,NC
    IF(P(K,J).GT.0.0)PRODAJ=C(K,1)**P(K,J)*PRODAJ
  1 IF(Q(K,J).GT.0.0)PRODCJ=C(K,1)**Q(K,J)*PRODCJ
    ANODJ  =EXP (ALFA(J)*(E(1)+DEC(J)))
    CATHJ  =EXP(-   ALFC(J)*(E(1)+DEC(J)))
    CURJ(J,1)=RJ(J)*(ANODJ*PRODAJ-CATHJ*PRODCJ)
    DO 4 K=2,NC
  4 BBB(I,K)=S(I,J)*RJ(J)/RN(J)*(ANODJ  *PRODAJ*P(K,J)-CATHJ
   1 *PRODCJ*Q(K,J))/C(K,1)*RN(1)**2/S(1 ,1)**2+BBB(I,K)
    BBB(I,1 )=(S(I,J)*RJ(J)/RN(J)*(ANODJ  *PRODAJ*ALFA(J)+  CATHJ  *
   1 PRODCJ*ALFC(J)))*RN(1)**2/S(1 ,1)**2 + BBB(I,1 )
  3 FF(I)=FF(I)+(S(I,J)*RJ(J)/RN(J)*(ANODJ  *PRODAJ-CATHJ  *
   1 PRODCJ))*RN(1)**2/S(1 ,1)**2
    DO 7 I=1,NC$DD(I)=-FF(I)+BBB(I,1 )*E(1)$ DO 7 K=2,NC
  7 DD(I)=DD(I)+BBB(I,K)*C(K,1)
    JCOUNT=JCOUNT+1
    CALL MATINV(NC,1,BBB,DD,DETERM)
    IF(DETERM.EQ.0.0)PRINT 109
    E(1)=DD(1 )     $ DO 9 I=2,NC
  9 C(I,1)=DD(I)    $ JERR=1
    IF(JCOUNT-10 )12,12,20
 12 IF(ABS(C(2,1)-COLD)-1.E-6*ABS(C(2,1)))21,21,11
 20 PRINT 101, JERR
 21 CUR(1)=0.0 $ DO 2 J=1,NR
  2 CUR(1)=CUR(1)+CURJ(J,1)
    RETURN $ END
    SUBROUTINE SURF
    DIMENSION C(4,201),E(201),RN(3),CINF(3),DEC(3),ALFA(3),ALFC(3),
   1RJ(3), S(3,3),Q(3,3),P(3,3) ,A(200),B(200),SUM(4),D(3) ,BBB(4,4),
   2 DD(4),FF(3),CUR(201),CURJ(3,201),CREF(3)
    COMMON C,E,RN,CINF,DEC,ALFA,ALFC,RJ,S,Q,P,D  ,AN,NC,NR,C1,NZT1,CUR
   1 ,CURJ,CRINF,CREF,A,B
101 FORMAT (17HONOT CONVERGED AT,I4)
109 FORMAT(5X,*DETERM=0.0 AT L= *,I5)
110 FORMAT(5X,4(1PE20.5))
```

```
      EX1=1./3. $ EX=2./3. $ NZT=NZT1-1 $ COLD=C(2,1)
      DZ=1./FLOAT(NZT)
      DO 2  NZ=2,NZT1 $ L=NZ
      NJ=NZ-1
      Z=FLOAT(NZ-1)*DZ
      DO 30 I=1,NC
      C(I,L)=C(I,NJ)
   30 SUM(I)=0.0
      IF (NZ .LE. 2) GO TO 42
      DO 40 I=1,NC $ DO 40 J=3,NZ
      K = NZ - J + 1
   40 SUM(I)=SUM(I)+C(I,J-1)*A(K)
   42 C2=EX*DZ**EX1 $ C3= 1./C1/AN/Z**EX1*C2
      DO 56 N=1,20
      DO 3 I=1,NC
      FF(I)=-C2*(CINF(I)-C(I,1))/Z**EX1-SUM(I)-C(I,1)*B(NJ)+C(I,L)
      DO 5 K=1,NC $ BBB(I,K)=0.0
    5 IF(K.EQ.I)BBB(I,K)=1.
      DO 3 J=1,NR $ PRODAJ=PRODCJ=1.0 $ DO 1 K=1,NC
      IF(P(K,J).GT.0.0)PRODAJ=C(K,L)**P(K,J)*PRODAJ
    1 IF(Q(K,J).GT.0.0)PRODCJ=C(K,L)**Q(K,J)*PRODCJ
      ANODJ  =EXP (ALFA(J)*(E(L)+DEC(J)))
      CATHJ  =EXP(-   ALFC(J)*(E(L)+DEC(J)))
      CURJ(J,L)=RJ(J)*(ANODJ*PRODAJ-CATHJ*PRODCJ)
      DO 4 K=1,NC
    4 BBB(I,K)=S(I,J)*RJ(J)/RN(J)*(ANODJ  *PRODAJ*P(K,J)-CATHJ
     1 *PRODCJ*Q(K,J))/C(K,L)*RN(1)**2/S(1 ,1)**2*C3/(D(I)/D(1))**EX
     1 /CREF(I)*CRINF+BBB(I,K)
    3 FF(I)=FF(I)+(S(I,J)*RJ(J)/RN(J)*(ANODJ  *PRODAJ-CATHJ  *
     1 PRODCJ))*RN(1)**2/S(1 ,1)**2*C3/(D(I)/D(1))**EX/CREF(I)*CRINF
      DO 7 I=1,NC $ DD(I)=-FF(I) $ DO 7 K=1,NC
    7 DD(I)=DD(I)+BBB(I,K)*C(K,L)
      CALL MATINV (NC,1,BBB,CC,DETERM) $ IF(DETERM.EQ.0.0)PRINT 109,L
      DO 9 I=1,NC
    9 C(I,L)=DD(I)
      IF(ABS(COLD-C(2,L))-1.E-6*ABS(C(2,L)))60,60,56
   56 COLD=C(2,L)
      PRINT 101,L
   60 CUR(L)=0.0 $ DO 2 J=1,NR
    2 CUR(L)=CUR(L)+CURJ(J,L)
      RETURN $ END
      SUBROUTINE MATINV (N,M,B,D,DETERM)
      DIMENSION B(4,4),D(4,1),JCOL(4),X(4,1)
      NM1=N-1 $ DETERM=1.0 $ DO 1 I=1,N $ JCOL(I)=I $ DO 1 K=1,M
    1 X(I,K)=D(I,K) $ DO 6 II=1,NM1 $ IP1=II+1 $ BMAX=ABS(B(II,II))
      JC=II $ DO 2 J=IP1,N $ IF(ABS(B(II,J)).LE.BMAX) GO TO 2 $ JC=J
      BMAX=ABS(B(II,J))
    2 CONTINUE $ DETERM=DETERM*B(II,JC) $ IF(DETERM.EQ.0.0) RETURN
      IF(JC.EQ.II) GO TO 4 $ JS=JCOL(JC) $ JCOL(JC)=JCOL(II)
    3 B(I,II)=SAVE $ DETERM=-DETERM
    4 DO 6 I=IP1,N $ F=B(I,II)/B(II,II) $ DO 5 J=IP1,N
    5 B(I,J)=B(I,J)-F*B(II,J) $ DO 6 K=1,M
    6 X(I,K)=X(I,K)-F*X(II,K) $ DETERM=DETERM*B(N,N)
      IF(DETERM.EQ.0.0) RETURN $ DO 7 II=2,N $ IR=N-II+2 $ IM1=IR-1
      JC=JCOL(IR) $ DO 7 K=1,M $ F=X(IR,K)/B(IR,IR) $ D(JC,K)=F
      DO 7 I=1,IM1
    7 X(I,K)=X(I,K)-B(I,IR)*F $ JC=JCOL(1) $ DO 8 K=1,M
    8 D(JC,K)=X(1,K)/B(1,1) $ RETURN $ END
      FUNCTION P(N,X)
C     CALCULATION OF LEGENDRE POLYNOMIALS
      P1= 1.0
      P2= X
```

```
      IF (N-1)  1,2,3
    1 P= P1
      RETURN
    2 P= P2
      RETURN
    3 NM1= N - 1
      DO 4 NU=1,NM1
      P=(X*FLOAT (2*NU+1)*P2-FLOAT (NU)*P1)/FLOAT (NU+1)
      P1= P2
    4 P2= P
      RETURN
      END
      FUNCTION FUNM(N,XI) $ XI2=XI**2 $ ADD= 1. $ SUM =1.
      PI2=1.5707963267948966192
      IF(ABS(XI).LT.1.) GO TO 7 $ DO 1 K=1,500
      ADD= -ADD*FLOAT(2*K+N)*FLOAT(2*K+N-1)/4./FLOAT(K)/(FLOAT(K+N)+.5)
     1 /XI2 $ SUM=SUM+ADD
    1 IF(ABS(ADD).LT.1.E-9*ABS(SUM))GOTO2
    2 FUNM=SUM/XI**(1+N)/PI2 $ IF(N.EQ.0) RETURN$ DO 3 NN=1,N
    3  FUNM=FUNM*FLOAT(NN)/FLOAT(2*NN+1) $ N2=N/2 $ IF(N.NE.2*N2)GOTO5
      DO 4 NN=1,N2
    4  FUNM=FUNM*FLOAT(NN)/(FLOAT(NN)-.5) $ RETURN
    5  FUNM=FUNM*PI2 $ IF(N2.EQ.0)RETURN $ DO 6 NN=1,N2
    6  FUNM=FUNM*(FLOAT(NN)+.5)/FLOAT(NN) $ RETURN
    7 A2=1. $ N2=N/2 $ IF(2*N2.EQ.N)GOTO 9 $ A1=-PI2
      IF(N.EQ.1)GOTO11 $ DO 9NN=3,N,2
    8  A1=A1/(1.-1./FLOAT(NN))**2 $ GOTO11
    9 A1=-1./PI2 $ IF(N.EQ.0)GOTO11 $ DO 10 NN=2,N,2
   10  A1=A1/(1.-1./FLOAT(NN))**2
   11  A1=A1*XI $ FUNM=A2+A1 $ DO 12 K=2,500,2
       A2=-A2*XI2*FLOAT(K-N-2)*FLOAT(K+N-1)-FLOAT(K*K-K)
       A1=-A1*XI2*FLOAT(K-N-1)*FLOAT(K+N)/FLOAT(K*K+K) $ ADD=A2+A1
      FUNM=FUNM+ADD
   12  IF(ABS(ADD).LT.1.E-9*ABS(FUNM)) RETURN $ RETURN $ END
      FUNCTION ELINT2(XK)
C
C        THIS ROUTINE SOLVES COMPLETE ELLIPTIC INTEGRALS OF THE SECOND
C        KIND BY USING CHEBYSHEV APPROXIMATIONS. THE MAXIMAL ERROR
C        IS 2.18E-13.
C
      DIMENSION A(8), B(8)
      DATA( A(I), I=1,8 ) / 1.0, 4.43147193467733E-01,
     15.68115681053803E-02, 2.21862206993846E-02, 1.56847700239786E-02,
     21.92284389022977E-02, 1.21819481486695E-02, 1.55618744745296E-03 /
      DATA( B(I), I=1,8 ) / 0.0, 2.49999998448655E-01,
     19.37488062098189E-02, 5.84950297066166E-02, 4.09074821593164E-02,
     22.35091602564984E-02, 6.45682247315060E-03, 3.78886487349367E-04 /
      X=1.-XK*XK
      SUM1= A(8)
      SUM2= B(8)
      DO1 I=1,7
      J = 8-I
      SUM1= X*SUM1+ A(J)
      SUM2= X*SUM2+ B(J)
    1 CONTINUE
      ELINT2=SUM1-ALOG(X)*SUM2
      RETURN
      END
```

```
  41  21  20
3877241751-21160840707-11926975807-12681521850-13419940908-14137792044-1
4830758017-15494671251-16125538897-16719566846-17273182552-17783056514-1
8246122308-18659595032-19020988070-19328128083-19579168192-19772599500-1
9907262387-19982377097-1
7750594798-27703981816-27611036190-27472316906-27288658240-27061164739-2
6791204582-26480401346-26130624249-25743976910-25322784698-24869580764-2
4387090819-23878216797-23346019528-22793700698-22224584919-21642105838-2
1049828453-24521277099-3
   2   2   1
  -1.     0.42   0.       0.       1.5      .5       2.        .337        3.00E-3
  0.     0.      0.5      .25      0.       .5       1.        0.0         5.00E-6
  .0000075       .001482        CU++=1                    1.E-1
  .000038       .0000000004155  H2                     8.310E-4
 2250.     .010795   78.996     1.          5.0
  .337      .05      2.         -1.          .5
      9. E-1
      9.5E-1
     10.0E-1
     11.0E-1
     12.0E-1
```

Appendix C. Standard Electrode Potentials

Purpose

This appendix presents expressions and values for standard electrode potentials of copper and iron electrode reactions in an aqueous, acidic copper chloride solution containing iron and a value for the equilibrium constant for the plane reaction (see equation 2-5).

Electrode Reactions

Standard electrode potentials for copper reactions in an aqueous chloride solution,

$$Cu + 3Cl^- \rightarrow CuCl_3^{2-} + e^- \qquad (C-1)$$

and

$$CuCl_3^{2-} \rightarrow CuCl^+ + 2Cl^- + e^- , \qquad (C-2)$$

are not tabulated in a convenient reference. Consequently, they must be calculated from stability constant data.

The stability constants needed in this case are those for the formation of the complex ions $CuCl_3^{2-}$ and $CuCl^+$ from cuprous, cupric, and chloride ions:

$$Cu^+ + 3Cl^- \rightleftarrows CuCl_3^{2-} \qquad (C-3)$$

and

$$Cu^{2+} + Cl^- \rightleftarrows CuCl^+ . \qquad (C-4)$$

The stability constant for reaction 3 is

$$\beta_{\text{cuprous}} = \frac{a_{CuCl_3^{2-}}}{a_{Cu^+} a_{Cl^-}^3} \qquad \text{(C-5)}$$

and that for reaction 4 is

$$\beta_{\text{cupric}} = \frac{a_{CuCl^+}}{a_{Cu^{++}} a_{Cl^-}} . \qquad \text{(C-6)}$$

The symbol a_i represents the relative activity of species i and for dilute solutions is defined by

$$a_i = \lambda_i / \lambda_i^{\theta} , \qquad \text{(C-7)}$$

where λ_i is the absolute activity of species i and λ_i^{θ} is a quantity used to specify the infinitely dilute solution secondary reference state of species i.

The absolute activity of species i in solution can be written as[22]

$$\lambda_i = m_i \gamma_i \lambda_i^{\theta} , \qquad \text{(C-8)}$$

where m_i and γ_i are the molality and activity coefficient of component i, respectively. The absolute activity is also related to the electrochemical potential of species i :

$$\mu_i = RT \ln \lambda_i \ . \qquad \text{(C-9)}$$

At equilibrium, the electrochemical potentials of the components in reactions 3 and 4 are related:[22]

$$\mu_{Cu^+} + 3\mu_{Cl^-} = \mu_{CuCl_3^{2-}} \qquad \text{(C-10)}$$

and

$$\mu_{Cu^{++}} + \mu_{Cl^-} = \mu_{CuCl^+} \ . \qquad \text{(C-11)}$$

These equations together with equations 7 and 9 lead to the following expressions for the stability constants in terms of the secondary reference state quantities:

$$\beta_{cuprous} = \frac{\lambda^{\theta}_{Cu^+} \lambda^{\theta^3}_{Cl^-}}{\lambda^{\theta}_{CuCl_3^{2-}}} \qquad \text{(C-12)}$$

and

$$\beta_{cupric} = \frac{\lambda^{\theta}_{Cu^{++}} \lambda^{\theta}_{Cl^-}}{\lambda^{\theta}_{CuCl^+}} \ . \qquad \text{(C-13)}$$

To utilize the above expressions, equations for the standard electrode potentials for reactions 1 and 2 in terms of tabulated standard electrode potentials must be developed. This can be accomplished by considering the following electrochemical cell:

$$\underset{\alpha}{Pt(s),H_2(g)} \;|\; \underset{\delta}{HCl,CuCl_3^{2-}, \text{ and } CuCl^+ \text{ in } H_2O} \;|\; \underset{\beta'}{Cu(s)} \;|\; \underset{\alpha'}{Pt(s)} \;, \tag{C-14}$$

where the hydrogen reaction,

$$H_2 \rightarrow 2H^+ + 2e^- \;, \tag{C-15}$$

occurs at the left electrode and reactions 1 and 2 occur at the right electrode. An expression for the standard electrode potential for this cell, when reactions 1 and 15 occur, is (see reference 22 for a discussion of this technique)

$$FU^{\theta}_{Cu/CuCl_3^{2-}} = \frac{1}{2}\mu^*_{H_2} + RT \ln\left(\frac{\lambda^{\theta}_{CuCl_3^{2-}}}{\lambda^{\theta 3}_{Cl^-}\lambda^{\theta}_{H^+}}\right) - \mu^o_{Cu} \;, \tag{C-16}$$

where F is Faraday's constant, $\mu^*_{H_2}$ is the chemical potential of hydrogen in the ideal gas state, and μ^o_{Cu} is the chemical potential of pure copper. Subtraction of FU^{θ}_{Cu/Cu^+}, given as entry 10 in table 20-1 of reference 22,

$$FU^{\theta}_{Cu/Cu^+} = \frac{1}{2}\mu^*_{H_2} - \mu^o_{Cu} + RT \ln\left(\frac{\lambda^{\theta}_{Cu^+}}{\lambda^{\theta}_{H^+}}\right) \;, \tag{C-17}$$

from both sides of equation 16 yields the desired relationship between the standard electrode potentials and the cuprous species stability constant,

$$FU^{\theta}_{Cu/CuCl_3^{2-}} = FU^{\theta}_{Cu/Cu^{+}} - RT \ln \beta_{cuprous} . \qquad (C\text{-}18)$$

For reactions 2 and 15,

$$FU^{\theta}_{CuCl_3^{2-}/CuCl^{+}} = \frac{1}{2} \mu^{*}_{H_2} + RT \ln \left(\frac{\lambda^{\theta}_{CuCl^{+}} \lambda^{\theta 2}_{Cl^{-}}}{\lambda^{\theta}_{CuCl_3^{2-}} \lambda^{\theta}_{H^{+}}} \right), \qquad (C\text{-}19)$$

and, by using the above mentioned table,

$$FU^{\theta}_{CuCl_3^{2-}/CuCl^{+}} = FU^{\theta}_{Cu^{+}/Cu^{++}} + RT \ln \left(\frac{\lambda^{\theta}_{CuCl^{+}} \lambda^{\theta 2}_{Cl^{-}} \lambda^{\theta}_{Cu^{+}}}{\lambda^{\theta}_{CuCl_3^{2-}} \lambda^{\theta}_{Cu^{++}}} \right), \qquad (C\text{-}20)$$

which simplifies to

$$FU^{\theta}_{CuCl_3^{2-}/CuCl^{+}} = FU^{\theta}_{Cu^{+}/Cu^{++}} + RT \ln \left(\frac{\beta_{cuprous}}{\beta_{cupric}} \right) . \qquad (C\text{-}21)$$

To complete consideration of copper electrode reactions in a chloride solution, consider the electrode reaction

$$Cu + Cl^{-} \rightarrow CuCl^{+} + 2e^{-} , \qquad (C\text{-}22)$$

whose standard electrode potential expression, determined in the manner described above, is

$$FU^{\theta}_{Cu/CuCl^{+}} = \frac{1}{2}\,\mu^{*}_{H_2} + RT\,\ln\left(\frac{\lambda^{\theta}_{CuCl^{+}}}{\lambda^{\theta}_{Cl^{-}}\,\lambda^{\theta}_{H^{+}}}\right) - \frac{1}{2}\,\mu^{o}_{Cu} \quad . \qquad (C\text{-}23)$$

Comparison of this equation to the sum of equations 16 and 19 reveals that

$$U^{\theta}_{Cu/CuCl^{+}} = \frac{1}{2}\left(U^{\theta}_{Cu/CuCl_3^{2-}} + U^{\theta}_{CuCl_3^{2-}/CuCl^{+}}\right) \quad . \qquad (C\text{-}24)$$

Similar treatment for reactions involving iron in an aqueous chloride solution yields the expressions given in table C-1, which can be used to show that

$$FU^{\theta}_{Fe/FeCl^{+}} = FU^{\theta}_{Fe/Fe^{2+}} - \frac{1}{2}\,RT\,\ln\,\beta_{ferrous} \qquad (C\text{-}25)$$

and

$$FU^{\theta}_{FeCl^{+}/FeCl^{2+}} = FU^{\theta}_{Fe^{++}/Fe^{+++}} - RT\,\ln\left(\frac{\beta_{ferric}}{\beta_{ferrous}}\right) , \qquad (C\text{-}26)$$

where

$$\beta_{ferrous} = \frac{a_{FeCl^{+}}}{a_{Fe^{2+}}\,a_{Cl^{-}}} = \frac{\lambda^{\theta}_{Fe^{2+}}\,\lambda^{\theta}_{Cl^{-}}}{\lambda^{\theta}_{FeCl^{+}}} \qquad (C\text{-}27)$$

and

$$\beta_{ferric} = \frac{a_{FeCl^{2+}}}{a_{Fe^{3+}}\,a_{Cl^{-}}} = \frac{\lambda^{\theta}_{Fe^{3+}}\,\lambda^{\theta}_{Cl^{-}}}{\lambda^{\theta}_{FeCl^{2+}}} ; \qquad (C\text{-}28)$$

Table C-1. Standard Electrode Potentials

Reaction	FU^{θ}	U^{θ}, volt[a]
1. $FeCl^{+} \rightarrow FeCl^{2+} + e^{-}$	$\frac{1}{2}\mu^{*}_{H_2} + RT \ln\left(\frac{\lambda^{\theta}_{FeCl^{2+}}}{\lambda^{\theta}_{H^{+}}\lambda^{\theta}_{FeCl^{+}}}\right)$	0.745
2. $CuCl_3^{2-} \rightarrow CuCl^{+} + 2Cl^{-} + e^{-}$	$\frac{1}{2}\mu^{*}_{H_2} + RT \ln\left(\frac{\lambda^{\theta}_{CuCl^{+}}\lambda^{\theta 2}_{Cl^{-}}}{\lambda^{\theta}_{CuCl_3^{2-}}\lambda^{\theta}_{H^{+}}}\right)$	0.438
3. $Cu + Cl^{-} \rightarrow CuCl^{+} + 2e^{-}$	$\frac{1}{2}\mu^{*}_{H_2} + RT \ln\left(\frac{\lambda^{\theta}_{CuCl^{+}}}{\lambda^{\theta}_{Cl^{-}}\lambda^{\theta}_{H^{+}}}\right) - \frac{1}{2}\mu^{o}_{Cu}$	0.3355
4. $Cu + 3Cl^{-} \rightarrow CuCl_3^{2-} + e^{-}$	$\frac{1}{2}\mu^{*}_{H_2} + RT \ln\left(\frac{\lambda^{\theta}_{CuCl_3^{2-}}}{\lambda^{\theta 3}_{Cl^{-}}\lambda^{\theta}_{H^{+}}}\right) - \mu^{o}_{Cu}$	0.233
5. $Fe + Cl^{-} \rightarrow FeCl^{2+} + 3e^{-}$	$\frac{1}{2}\mu^{*}_{H_2} + RT \ln\left(\frac{\lambda^{\theta 1/3}_{FeCl^{2+}}}{\lambda^{\theta 1/3}_{Cl^{-}}\lambda^{\theta}_{H^{+}}}\right) - \frac{1}{3}\mu^{o}_{Fe}$	-0.0523
6. $Fe + Cl^{-} \rightarrow FeCl^{+} + 2e^{-}$	$\frac{1}{2}\mu^{*}_{H_2} + RT \ln\left(\frac{\lambda^{\theta 1/2}_{FeCl^{+}}}{\lambda^{\theta 1/2}_{Cl^{-}}\lambda^{\theta}_{H^{+}}}\right) - \frac{1}{2}\mu^{o}_{Fe}$	-0.451

[a] At 298.15 K and 1 atmosphere.

also, from table C-1,

$$U^{\theta}_{Fe/FeCl^{2+}} = \frac{1}{3}\left(U^{\theta}_{FeCl^{+}/FeCl^{2+}} + 2U^{\theta}_{Fe/FeCl^{+}}\right) . \qquad (C-29)$$

The stability constant data tabulated by Sillén and Martell[62] (see table C-2) can be used together with the appropriate expression from above and the necessary standard electrode potential from table 20-1 or 20-2 of reference 22 to complete the determination of the desired standard electrode potentials, as given in table C-1.

Equilibrium Constant for the Plane Reaction

The equilibrium constant for the plane reaction (see equation 2-5) can be written as

$$K = \frac{a_{CuCl^{+}}\, a_{FeCl^{+}}\, a^{2}_{Cl^{-}}}{a_{CuCl_3^{2-}}\, a_{FeCl^{2+}}} = \frac{\lambda^{\theta}_{CuCl_3^{2-}}\, \lambda^{\theta}_{FeCl^{2+}}}{\lambda^{\theta}_{CuCl^{+}}\, \lambda^{\theta}_{FeCl^{+}}\, \lambda^{\theta 2}_{Cl^{-}}} , \qquad (C-30)$$

or, according to table C-1, as

$$\ln K = \frac{F}{RT}\left(U^{\theta}_{FeCl^{+}/FeCl^{2+}} - U^{\theta}_{CuCl_3^{2-}/CuCl^{+}}\right) , \qquad (C-31)$$

which at 298.15 K yields

$$K = 1.55\times10^{5}\ (kg/mol)^{2} . \qquad (C-32)$$

Table C-2. Stability Constants from Sillén and Martell[62]

Species	Temperature(°C)	$\ln \beta_i$	$(\ln \beta_i)_{avg}$
$CuCl_2^-$	25	12.76	
		10.89	
		11.38	
$CuCl_3^{2-}$		9.74	
		11.30[a]	
$CuCl_3^{2-}$	25		11.21[b]
$CuCl^+$	25	0.12	0.12
$FeCl^+$	20	0.829	0.829
$FeCl^{2+}$	25	1.11	
		2.99	
		1.40	
		0.829	
		3.40	
		1.40	
$FeCl^{2+}$	25		1.85

[a] This value is from Trainham.[102]

[b] The stability constants for both cuprous species ($CuCl_3^{2-}$ and $CuCl_2^-$) are included in the average because of the uncertainty in establishing which is prominent in solution; however, Hurlen[64] presents data which support the view that $CuCl_3^{2-}$ is the prominent species.

Appendix D. Solution Technique for Chapter 2

Purpose

The purpose of this appendix is to discuss the solution technique used to solve the governing equations for the physical phenomena modeled in chapter 2.

Governing Equations

The physical problem discussed in chapter 2 is modeled as a boundary value problem consisting of a set of coupled, nonlinear ordinary differential equations with associated boundary conditions.

The unknowns of the problem are the reaction plane position L, $c_i(\xi)$, and $\Phi(\xi)$, where ξ is the dimensionless normal distance from the electrode (see equation 2-7). The reaction plane position is an unknown constant which, for convenience, can be treated as an unknown function of position whose governing equation is

$$\frac{dL}{dy} = 0. \qquad \text{(D-1)}$$

This numerical technique is convenient because it enables us to use the subroutine BAND listed in Appendix C of reference 22 without modification to account for the unknown constant L. Equation 2-6 is the governing material balance equation for each of the species of interest. The electroneutrality condition (see equation 2-9) governs the potential distribution (see reference 22).

The continuous concentration and potential distributions can be approximated by a set of values at a finite number of mesh points

nj , and the governing equations approximated at each point by finite-difference representations. The resulting set of coupled finite-difference equations can then be solved by the subroutine BAND.

It should be noted that since the reaction plane position is an unknown, the mesh interval in one of the regions shown in figure 2-1 (region 1 in this work) is also unknown; and, consequently, the governing equations there must be programmed accordingly.

Boundary Conditions

The schematic drawing in figure 1 helps one visualize the structure of the governing equations and the boundary conditions that must be set.

Let us first consider the conditions in the bulk solution. Since the electrolytic solution considered in chapter 2 consists of 5 elemental species H , O , Cu , Fe , and Cl , we must set the bulk concentration of 5 species of interest to specify the system. There are, however, 6 species of interest in the bulk solution: H^+ , dissolved H_2 , $CuCl^+$, $FeCl^{2+}$, $FeCl^+$, and Cl^- ; but, since the electroneutrality condition must hold, only 4 of the 5 ionic species bulk concentrations can be set. The governing equation for the potential in solution is assumed to be Possion's equation, which can be replaced by the electroneutrality condition (see reference 22). That is, a second order differential equation in Φ and its boundary conditions are replaced by an alegebric equation, $\sum_i z_i c_i = 0$. Finally, since only potential differences are significant,

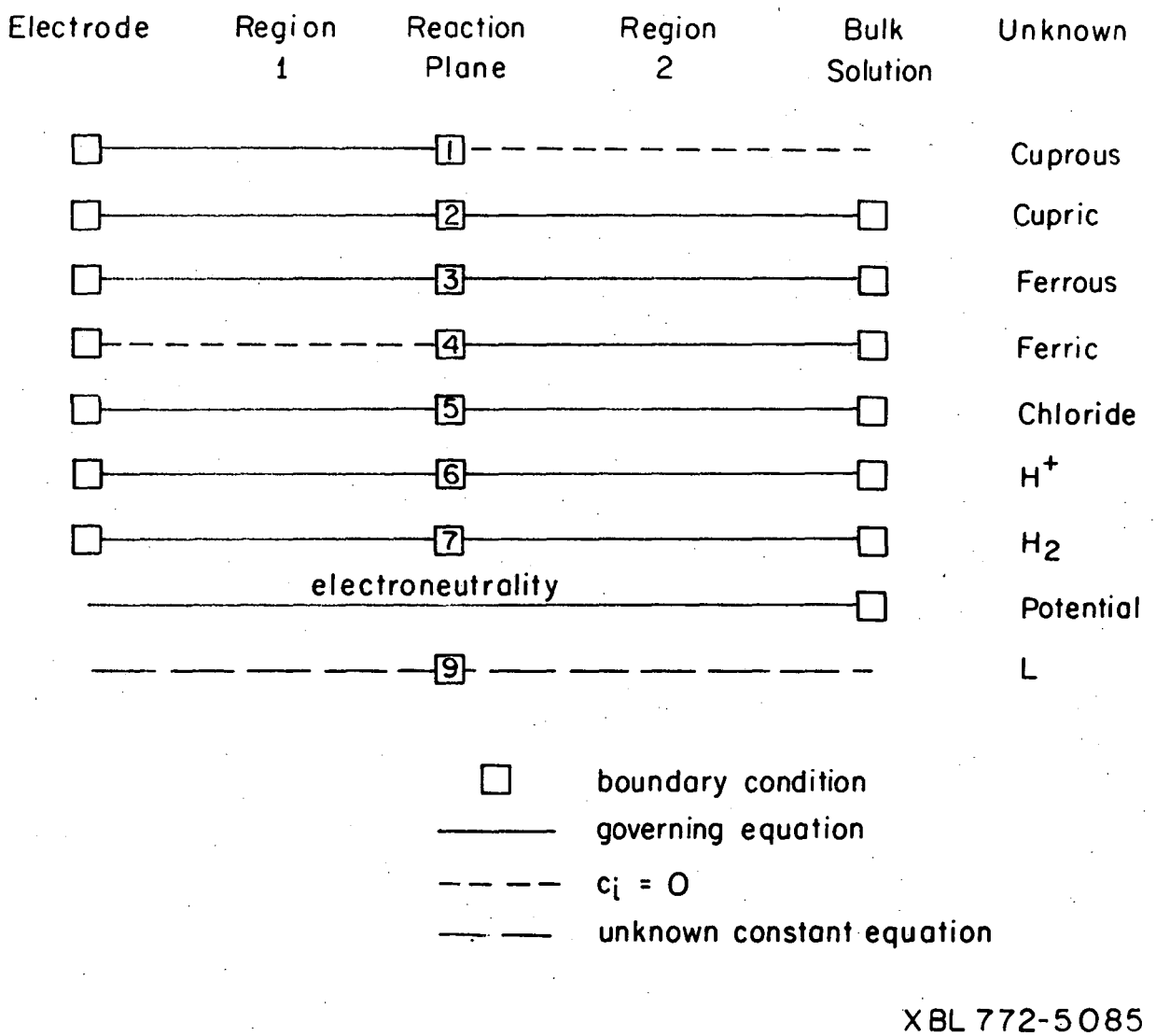

Figure D-1. A schematic representation of the structure of the governing equations and boundary conditions for the reaction plane problem. The numbers on the reaction plane boundary conditions refer to the conditions discussed in the text.

the potential Φ can arbitrarily be set equal to zero in the bulk solution.

For notational convenience, let the species of interest be represented by numbers: cuprous -1, cupric -2, ferrous -3, ferric -4, chloride -5, H^+ -6, and H_2 -7.

The conditions at the reaction plane are (see figure 1):

1. The flux of the cuprous species is equal in magnitude but opposite in sign to that of the ferric species:

$$N_4^2 + N_1^1 = 0 \ , \qquad \text{(D-2)}$$

where the superscript refers to the region.

2. The net flux of elemental copper is continuous:

$$N_2^2 - N_2^1 - N_1^1 = 0 \ . \qquad \text{(D-3)}$$

3. The net flux of elemental iron is continous:

$$N_4^2 + N_3^2 - N_3^1 = 0 \ . \qquad \text{(D-4)}$$

4. The concentration of the ferric species is set equal to zero:

$$c_4 = 0 \ . \qquad \text{(D-5)}$$

5. The net flux of elemental chlorine is continuous:

$$N_5^2 - N_5^1 + N_4^2 + N_3^2 - N_3^1 + N_2^2 - N_2^1 - 3N_1^1 = 0 \ , \qquad \text{(D-6)}$$

which, by using the copper and iron balance, simplifies to

$$N_5^2 - N_5^1 - 2N_1^1 = 0 \ . \qquad \text{(D-7)}$$

6. The flux of H^+ is continuous:

$$N_6^2 - N_6^1 = 0 \ . \qquad \text{(D-8)}$$

7. The flux of dissolved H_2 is continuous:

$$N_7^2 - N_7^1 = 0 \ . \qquad \text{(D-9)}$$

9. The concentration of cuprous is zero:

$$c_1 = 0 \ . \qquad \text{(D-10)}$$

Note that the electroneutrality condition, which can be regarded as the governing equation for the potential Φ, applies throughout the field. Also, note that setting the concentration of the cuprous and the ferric species equal to zero, conditions 9 and 4, provides the infinitely large equilibrium constant approximation for the reaction at the plane (see equation 2-5).

The boundary conditions at the electrode consist of setting the normal component of the flux of species i equal to its reaction rate there, which may be zero, as discussed in chapter 2.

Solution Technique

The boundary value problem used to model the physical phenomena considered in chapter 2 is solved by Newman's finite-difference method.[22] Highlights of the application of that technique to the present problem as outlined in the previous section of this appendix will be sketched in this section.

Specification of the bulk conditions in a form appropriate for Newman's method is simple and straightforward (see Appendix C of reference 22).

In region 2, the nonlinear, governing finite-difference equations can be programmed easily but do require linearization, which is a process that can be illustrated by considering F_i to be a nonlinear function of the unknowns at mesh points $j - 1$, j, and $j + 1$. Then, if $F_i = 0$, a linear expression for the unknowns is

$$\sum_{k=1}^{n} \sum_{\ell=j-1}^{j+1} \left.\frac{\partial F_i}{\partial c_{k,\ell}}\right|_{c_{k,\ell}=c^o_{k,\ell}} c_{k,\ell} = -F_i^o + \sum_{k=1}^{n} \sum_{\ell=j-1}^{j+1} \left.\frac{\partial F_i}{\partial c_{k,\ell}}\right|_{c_{k,\ell}=c^o_{k,\ell}} c^o_{k,\ell} , \qquad \text{(D-11)}$$

where n is the number of unknowns and the superscript o designates a trial value. The derivatives for unknown k in equation i at mesh points $j - 1$, j, and $j + 1$ are the coefficients $A_{i,k}$, $B_{i,k}$, and $D_{i,k}$, respectively, and the right side of equation i is C_i.

The flux conditions at the plane can be implemented simply by first forming the difference between the flux of species i in regions 1 and 2, $N_i^2 - N_i^1$, and then determining $A_{i,k}$, $B_{i,k}$, $D_{i,k}$, and G_i for this difference. These elements can then be used to form the appropriate elements for the flux conditions at the plane.

For example, consider the copper balance at the plane (see equation 3). The elements for this condition are

$$A_{2,k} = A_{1,k} + A_{2,k} , \qquad \text{(D-12)}$$

$$B_{2,k} = B_{1,k} + B_{2,k} , \qquad \text{(D-13)}$$

$$D_{2,k} = D_{1,k} + D_{2,k} , \qquad \text{(D-14)}$$

and

$$G_2 = G_1 + G_2 . \qquad \text{(D-15)}$$

In other words, the copper balance can be generated by simply adding the flux difference expressions for species 1 and 2, since N_1^2 is zero.

Next, consider programming the conditions at the plane accurate to order h^2, where h is the dimensionless mesh interval. To do this, introduce image points in regions 1 and 2:

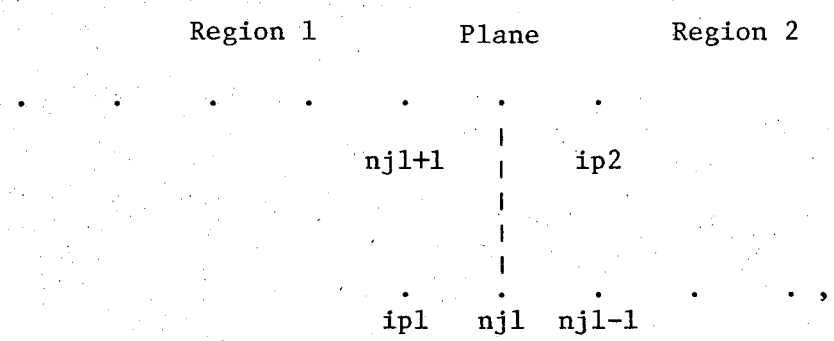

where ipl , and ip2 refer to the image points in regions 1 and 2 and njl is the mesh point at which the plane exists. Note that the mesh intervals in the two regions are equally spaced but not necessarily equal.

The interior image points require special treatment for the BAND subroutine used here. In essence, at mesh point njl the governing transport equations in regions 1 and 2 are programmed using their respective image points, electroneutrality is specified, and the reaction plane conditions are programmed using the 5 mesh points ip2 , njl-1 , njl , njl+1 , ipl ; also, electroneutrality is specified at mesh points ip2 and ipl. The governing equations for the unknowns at the 5 mesh points can be written compactly as

$$\begin{bmatrix} \underline{\underline{0}} & \underline{\underline{AT2}} & \underline{\underline{BT2}} & \underline{\underline{0}} & \underline{\underline{DT2I1}} \\ \underline{\underline{AT1I2}} & \underline{\underline{0}} & \underline{\underline{BT1}} & \underline{\underline{DT1}} & \underline{\underline{0}} \\ \underline{\underline{AFI2}} & \underline{\underline{A}} & \underline{\underline{B}} & \underline{\underline{D}} & \underline{\underline{DFI1}} \end{bmatrix} \begin{Bmatrix} \underline{c}_{ip2} \\ \underline{c}_{njl-1} \\ \underline{c}_{njl} \\ \underline{c}_{njl+1} \\ \underline{c}_{ipl} \end{Bmatrix} = \begin{Bmatrix} \underline{\underline{GT2}} \\ \underline{\underline{GT1}} \\ \underline{\underline{G}} \end{Bmatrix} \quad \text{(D-16)}$$

However, since BAND cannot handle automatically interior image points, the matrices $\underline{\underline{AFI2}}$ and $\underline{\underline{DFI1}}$ must be made null and $\underline{A}$, $\underline{B}$, $\underline{D}$, and $\underline{G}$ modified accordingly before calling BAND. This is done by using the elements on the diagonals of the upper triangular matrices $\underline{\underline{AT1I2}}$ and $\underline{\underline{DT2I1}}$ as pivotal elements to zero the elements of the matrices $\underline{\underline{AFI2}}$ and $\underline{\underline{DFI1}}$ in Gauss elimination fashion. The solution technique then proceeds as usual.

Once new values for the unknowns at each normal mesh point are calculated, the unknowns at the interior image points can be obtained from

$$\begin{bmatrix} \underline{\underline{0}} & \underline{\underline{DT2I1}} \\ \underline{\underline{AT1I2}} & \underline{\underline{0}} \end{bmatrix} \begin{Bmatrix} \underline{c}_{ip2} \\ \underline{c}_{ip1} \end{Bmatrix}$$

$$= \begin{Bmatrix} \underline{GT2'} - \underline{\underline{AT2'}}\, \underline{c}_{nj1-1} - \underline{\underline{BT2'}}\, \underline{c}_{nj1} \\ \underline{GT1'} - \underline{\underline{DT1'}}\, \underline{c}_{nj1+1} - \underline{\underline{BT1'}}\, \underline{c}_{nj1} \end{Bmatrix}, \qquad \text{(D-17)}$$

where the primes designate the modified vectors and arrays determined as described above.

Program Listing

The program PLANE, necessary subroutines, and input data are listed on the following pages.

```
      PROGRAM PLANE (INPUT,OUTPUT,PUNCH,TAPE1=PUNCH)
      DIMENSION A(9,9),B(9,9),C(9,203),D(9,19),G(9), X(9,9),Y(9,9),U(9),
     1V(203),DIF(7),Z(7),S(7,4),CIN(9),REF1(7),REF2(7),CIR(7),
     1          QI(4),QA(4,7),XIP(203),XI(203),RK(203),DP(203)
     1 ,P(9,203),CIP1(8),CIP2(8),GT1(9),GT2(9),AT2(9,9),AFI2(9,9),
     1 AT1I2(9,9),BT1(9,9),BT2(9,9),DT1(9,9),DT2I1(9,9),DFI1(9,9)
      COMMON A,B,C,D,G,X,Y,N,NJ
      TOL=1.E-6
      N=9 $ NM1=N-1 $ NM2=N-2 $ ICO=1 $ ICU=2 $ IFO=3 $ IFI=4
      ICL=5 $ IHP=6 $ IPH=8 $ IL=9 $ IR=ICU $ NR=4 $ IH2=7
      DO 36 I=1,NM2
   36 CIR(I)=1.0
  100 FORMAT(2I4,2F10.0,3I4)
  101 FORMAT(3F15.0,A6,A6)
  102 FORMAT(2X,*NJ= *,I3,3X,*NJ1= *,I3,3X,*H2= *,F5.4,15X,*REACTION 1*
     1  ,8 X,*REACTION 2*,8 X,*REACTION 3*,8 X,*REACTION 4*/3X,
     1 *SPECIES*,16X,
     2*U*,8 X,*DIF*,11X,*Z*,4X,*S*,12X,*Z*,4X,*S*     ,12X,*Z*,4X,*S*
     1 ,12X,*Z*,4X,*S*
     3  /(3X,A6,A6,6X,2E10.3,5X,2F5.1,8 X,2F5.1,8 X,2F5.1,8 X,2F5.1))
  104 FORMAT(6F10.0,F15.0,F5.0)
  105 FORMAT(2X,*SPECIES*,10X,*CINF*,10X,*CZERO*,20X,*AMP*,10X,*MIGR*)
  106 FORMAT(5X,*THE NEXT RUN DID NOT CONVERGE*)
  107 FORMAT(1H0,50X,2E14.7/(3X,A6,A6,2E14.7))
  108 FORMAT(1H0, 5X,*L = *,E16.10,3X,*L (IN CM)=*,E16.10,3X,*ZMAX=*,
     1 E16.10,3X,*ZMAX(IN CM)=*,E16.10,3X,*RPM=*,E15.6)
  109 FORMAT(3X,*RI01=*,E12.5,3X,*RI02=*,E12.5,3X,*RI03=*,E12.5,3X,
     1  *E1=*,E12.5,3X,*E2=*,E12.5,3X*E3=*,E12.5
     1 ,3X,*E =*,E12.5                    /3X,*R1A=*,E12.5,3X,*R2A=*,
     2  E12.5,3X,*R3A=*,E12.5,3X,*R1C=*,E12.5,3X,*R2C=*,E12.5,3X,*R3C=*
     1,E12.5,2X,*TOL=*,E10.4)
  110 FORMAT(1H0,3X,* I1=*,E15.6,3X,* I2=*,E15.6,3X,* I3=*,E15.6,3X,
     1 *I4=*,E15.6
     1 /  2X,*IT=*,E15.6,3X,*EFF=*,E15.6)
  111 FORMAT(3X,*VMPTO=*,E15.6,3X,*VMPO=*,E15.6,3X,* ILO=*,E15.6,3X,
     U *PTO=*,E15.6/3X,*RP=*,E15.6,3X,*CRR=*,E15.6,3X,*KAPPA=*,E15.6,
     1 2X,*ALNCRR=*,F10.5,2X,*ALNCO=*,F10.5,2X,*ALNCL=*,F10.5////)
  112 FORMAT(10F8.4)
  113 FORMAT(1H1)
  114 FORMAT(/2X,*IMAGE POINT IN REGION 1*/(2X,6F8.4,2X,E10.4,2X,F8.4))
  115 FORMAT(/2X,*IMAGE POINT IN REGION 2*/(2X,6F8.4,2X,E10.4,2X,F8.4))
  797 FORMAT(2X,6F8.4,2X,E10.4,2F8.4)
  798 FORMAT(1H0,I4)
  799 FORMAT(2X,6F8.4,2X,E10.4,2X,5F8.4,2X,E10.4)
  800 FORMAT(6F7.4,E10.4,3F7.4)
  801 FORMAT(2X,  E16.10)
      PRINT 113
      READ 101,(U(I),DIF(I),Z(I),     REF1(I),REF2(I),I=1,NM2)
      READ 104,( CIN(I),I=1,NM1)
      DO 38 I=1,NM2 $ IF(I.NE.ICL)CIN(ICL)=CIN(ICL)+Z(I)*CIN(I)
      DO 38 KR=1,NR
   38 S(I,KR)=0.0
      S(ICU,2)=-1.0$ S(ICO,2)= 1.0
      S(ICL,2)=S(ICU,2)*(Z(ICU)-2.)+S(ICO,2)*(Z(ICO)-1.0)
                       S(ICO,1)= -1.0  $  S(ICL,1)=S(ICO,1)*(Z(ICO)-1.)
      S(IFO,3)=-1.0  $  S(ICL,3)=S(IFO,3)*(Z(IFO)-2.0)
      S(IHP,4)=-1. $ S(IH2,4)=0.5
      F= 96487.
      ALFAA1=ALFAA2=ALFAC1=ALFAC2=0.5
      ALFAA3=1.5  $  ALFAC3=0.5 $ ALFAA4=ALFAC4=0.5
      RI01=5.E-3*CIR(ICO)**ALFAA1*CIR(ICL)**(3.*ALFAC1)
```

```
      RI02=1.E-3*CIR(ICO)**ALFAC2*CIR(ICU)**ALFAA2*CIR(ICL)**(2.*ALFAA2)
      RI03=1.E-3*CIR(IFO)**(0.5*ALFAA3)*CIR(ICL)**(0.5*ALFAC3)
      RI04=5.89E-7*CIR(IHP)**ALFAC4*CIR(IH2)**(0.5*ALFAA4)
      U1TH=0.233  $  U2TH=0.436  $  U3TH=-0.451$ U4TH=0.
      T=298.15  $  R=8.3143  $  FF=F/R/T  $  RHO=.99707
      RPM=2500.
      PI=3.1415926535
      OMEGA=RPM*2.*PI/60. $ RNU=.010049 $ DDELT=.8929795117
      AA=.51023262
      DELTA =1./              (AA*RNU/3./DIF(IR))**(1./3.)/
     1  SQRT(OMEGA/RNU)
      RN1=RN2=1.0  $  RN3=2.0  $ RN4=1.
   12 READ 100,NJ,NJ1,H2,E,IPUNCH,IGUESS,IREAD
      IF(NJ1.EQ.0)STOP
      NOTCON=0
      E1=E+ALOG(CIR(ICL)**3/CIR(ICO)/RHO**2)/FF-   ALOG(1./RHO)/FF
      E2=E+U1TH-U2TH-ALOG(CIR(ICU)*CIR(ICL)**2/CIR(ICO)/RHO**2)/FF
     1 -   ALOG(1./RHO)/FF
      E3=E+U1TH-U3TH+0.5*ALOG(CIR(ICL)/CIR(IFO))/FF-ALOG(1./RHO)/FF
      E4=E+U1TH-U4TH+ALOG((CIR(IH2)/RHO)**0.5/CIR(IHP)*RHO)/FF
     1 -ALOG(1./RHO)/FF
      R1A=RI01/RN1/CIR(ICL)**3*EXP(ALFAA1*FF*E1)/F*1000.*DELTA
      R2A=RI02/RN2/CIR(ICO)*EXP(ALFAA2*FF*E2)/F*1000.*DELTA
      R3A=RI03/RN3/CIR(ICL)*EXP(ALFAA3*FF*E3)/F*1000.*DELTA
      R4A=RI04/RN4/CIR(IH2)**0.5*EXP(ALFAA4*FF*E4)/F*1000.*DELTA
      R1C=RI01/RN1/CIR(ICO)*EXP(-ALFAC1*FF*E1)/F*1000.*DELTA
      R2C=RI02/RN2/CIR(ICL)**2/CIR(ICU)*EXP(-ALFAC2*FF*E2)/F*DELTA
     1 *1000.
      R3C=RI03/RN3/CIR(IFO)*EXP(-ALFAC3*FF*E3)/F*1000.*DELTA
      R4C=RI04/RN4/CIR(IHP)*EXP(-ALFAC4*FF*E4)/F*1000.*DELTA
      QLP=FLOAT(NJ1-1)
      QNP= FLOAT(NJ-NJ1-1)
      IF (IREAD.EQ.1)GO TO 61
C     SET UP PROFILES
      C(ICL,NJ-1)=CIN(ICL)
      CR0=(R2A*DIF(2)/DIF(1)*CIN(2)
     1                      +CIF(2)*CIN(2)/DDELT+DIF(4)*CIN(4)/DDELT)
     1 /(R2C*C(ICL,NJ-1)**2+R2A*DIF(2)/DIF(1)+DIF(2)/DDELT)
      CICOD=DIF(ICU)/DIF(ICO)*(CIN(ICU)-CR0)
      CIFOD=CIN(IFO)+DIF(IFI)/DIF(IFO)*CIN(IFI)
      CIN(IL)=DDELT/(1.+DIF(IFI)*CIN(IFI)/DIF(ICU)/(CIN(ICU)-CR0))
      DO 40 I=1,N  $  DO 40 J=1,NJ
   40 C(I,J)=CIN(I)
C     IMPROVE PROFILES
      DO 1 J=1,NJ
      C(IFI,J)= CIN(IFI)*(1.-EXP(FLOAT(J-NJ1)*H2))
      C(IFO,J)=(CIN(IFO)*(QLP-FLOAT(J-1))+CIFOD*FLOAT(J-1))/QLP
      IF(J.LE.NJ1) GO TO 1 $ C(IFI,J)=0.0
      C(IFO,J)=CIFOD
      C(ICU,J)=CR0+(CIN(ICU)-CR0)*FLOAT(NJ-J-1)/QNP
      C(ICO,J)=CICOD*(FLOAT(J-1)-QLP)/QNP
    1 CONTINUE
      IF (IGUESS.EQ.1) GO TO 60
   61 IF(IREAD.EQ.1)READ 800,((P(I,J),I=1,N),XI(J),J=1,NJ)
      DO 55 I=1,N $ DO 55 J=1,NJ
   55 C(I,J)=P(I,J)
   60 CONTINUE
      DO 47 I=1,NM1 $ CIP1(I)=(C(I,NJ1)-C(I,NJ1-1))   +C(I,NJ1)
   47 CIP2(I)=C(I,NJ1)+(C(I,NJ1)-C(I,NJ1+1))
      PRINT 102,NJ,NJ1,H2,(REF1(I),REF2(I),U(I),DIF(I),Z(I),S(I,1),Z(I),
     1  S(I,2),Z(I),S(I,3),Z(I),S(I,4),I=1,NM2)
      PRINT 109,RI01,RI02,RI03,E1,E2,E3,E,R1A,R2A,R3A,R1C,R2C,R3C,TOL
```

```
      DO 44 I=1,NJ $ DP(I)=0.0
      XIP(I)=0.0 $ XI(I)=0.0
   44 RK(I)=0.0
      JCOUNT= 0
      AMP= 0.0
    2 JCOUNT = JCOUNT + 1
      J= 0
      DO 3 I=1,N
      DO 3 K=1,N
      Y(I,K)=0.0
    3 X(I,K)=0.0
    4 J = J + 1
      DO 5 I=1,N $ G(I)=0.
      DO 5 K=1,N
      A(I,K)=0.0
      B(I,K)=0.0
    5 D(I,K)=0.0
      IF(J-NJ1) 30, 8,31
   30 B(IL,IL)=1.0 $ D(IL,IL)=-1.0 $ GO TO 32
   31 B(IL,IL)=1.0 $ A(IL,IL)=-1.0
   32 CONTINUE
C     BOUNDARY CONDITION AT INFINITY
      IF(J-1) 6,6,8
    6 DO 7 I=1,NM1
      B(I,I)=1.0
    7 G(I)= CIN(I)
      CALL BAND(J)
      GO TO 4
C     ELECTRONEUTRALITY CONDITION
    8 DO 9 K=1,NM2
    9 B(IPH,K) = Z(K)
      IF(C(IH2,J).LT.0.)C(IH2,J)=1.E-10
      IF(C(IFO,J) . LT. 0.0)  C(IFO,J) = 0.00001
      IF(J-NJ1)10,14,16
C      MATERIAL BALANCE REGION 2
   10 V(J) = 3.0*DIF(IR )*( H2* FLOAT(NJ1-J)   + C(IL,NJ1))**2
      DO 13 I=1,NM2 $ IF(I.EQ.ICO)GOTO13
      CONST   = Z(I)*U(I)*F/DIF(I)
      IF(NJ1-J)26,26,27
   26 PP=CONST*(CIP1(IPH)-C(IPH,J-1))/2. $ PPP=CONST*(CIP1(IPH)
     1 +C(IPH,J-1)-2.*C(IPH,J)) $ CP=(CIP1(I)-C(I,J-1))/2. $ GO TO 28
   27 PP = CONST   *(C(IPH,J+1)-C(IPH,J-1))/2.0
      PPP = CONST   *(C(IPH,J+1)+C(IPH,J-1)-2.0*C(IPH,J))
      CP = (C(I,J+1)-C(I,J-1))/2.0
   28 A(I,I)= -1.0 + PP/2.0-H2*V(J)/DIF(I)/2.0
      B(I,I)= 2.0 -PPP
      D(I,I)= -1.0-PP/2.0 + H2*V(J)/DIF(I)/2.0
      B(I,IL)=6.0/DIF(I)*DIF(IR)*CP*(H2*FLOAT(NJ1-J)+C(IL,J))*H2
      A(I,IPH) = CONST   *(CP/2.0-C(I,J))
      B(I,IPH) = CONST   *2.0*C(I,J)
      D(I,IPH) = -CONST   *(CP/2.0 + C(I,J))
      G(I) = -PPP*C(I,J) - PP*CP +B(I,IL)*C(IL,J)
   13 CONTINUE
      IF(J.EQ.NJ1)GO TO 49
      B(ICC,ICO) = 1.0
      CALL BAND(J)
      GO TO 4
C      BOUNDARY CONDITIONS AT REACTION PLANE
   14 DO 59 I=1,N
      GT1(I)=0. $ GT2(I)=0.
      DO 59 K=1,N
       AT2(I,K)=0.$ AFI2(I,K)=0. $ AT1I2(I,K)=0. $ BT1(I,K)=0.
```

```
      BT2(I,K)=0. $ DT1(I,K)=0. $ DT2I1(I,K)=0.
   59 DFI1(I,K)=0.
      DO 48 K=1,NM2 $ DT2I1(IPH,K)=Z(K)
   48 AT1I2(IPH,K)=Z(K) $ GO TO 10
   49 DO 50 I=1,NM2 $ AT2(I,I)=A(I,I)$BT2(I,I)=B(I,I)
      DT2I1(I,I)=D(I,I) $BT2(I,IL)=B(I,IL) $ AT2(I,IPH)=A(I,IPH)
      DT2I1(I,IPH)=D(I,IPH) $ BT2(I,IPH)=B(I,IPH)
   50 GT2(I)=G(I) $ DT2I1(ICO,ICO)=1. $ GO TO 16
   51 DO 52 I=1,NM2 $ IF(I.EQ.IFI)GO TO 52
      DT1(I,I)=D(I,I) $ BT1(I,I)=B(I,I)
      AT1I2(I,I)=A(I,I) $  BT1(I,IL)=B(I,IL)
      DT1(I,IPH)=D(I,IPH) $ BT1(I,IPH)=B(I,IPH) $ AT1I2(I,IPH)=A(I,IPH)
      GT1(I)=G(I)
   52 CONTINUE $ AT1I2(IFI,IFI)=1.
      DO 15 I=1,NM2
      A(I,I) = DIF(I)*C(IL, J )/QNP     $ DFI1(I,I)=-A(I,I)
      B(I,I)=-Z(I)*F*U(I)*(C(IL,J)/QNP    *(CIP1(IPH)-C(IPH,J-1))
     1 -H2*(C(IPH,J+1)-CIP2(IPH)))
      D(I,I) = DIF(I)*H2     $ AFI2(I,I  )=-D(I,I  )
      B(I,IL)=-DIF(I)    /QNP*(CIP1(I)-C(I,J-1))-Z(I)*F*U(I)
     1 *C(I,J)    /QNP*(CIP1(IPH)-C(IPH,J-1))
      A(I,IPH)=Z(I)*F*U(I)*C(I,J)*C(IL,J)/QNP    $DFI1(I,IPH)=-A(I,IPH)
      B(I,IPH)=0.
      D(I,IPH)=Z(I)*F*U(I)*C(I,J)*H2    $AFI2(I,IPH)=-D(I,IPH)
   15 G(I) = B(I,IL)*C(IL,NJ1)+A(I,IPH)*C(IPH,J-1)+
     1D(I,IPH)*C(IPH,J+1)+AFI2(I,IPH)*CIP2(IPH) +DFI1(I,IPH)*CIP1(IPH)
C     EQUATION 2, TOTAL FLUX OF COPPER CONSTANT
      A(ICU,ICO)= A(ICO,ICO) $ A(ICU,IPH)=A(ICU,IPH)+A(ICO,IPH)
      B(ICU,ICO)=B(ICO,ICO) $ AFI2(ICU,IPH)=AFI2(ICU,IPH)+AFI2(ICO ,IPH)
      D(ICU,ICO)=D(ICO,ICO) $ D(ICU,IPH)=D(ICU,IPH)+D(ICO,IPH)
      G(ICU)=G(ICU)+G(ICO) $ B(ICU,IL)=B(ICU,IL)+B(ICO,IL)
      AFI2(ICU,ICO)=AFI2(ICO,ICO) $ DFI1(ICU,ICO)=DFI1(ICO,ICO)
      DFI1(ICU,IPH)=DFI1(ICU,IPH)+DFI1(ICO,IPH)
C     EQUATION 3, TOTAL FLUX OF IRON IS A CONSTANT
      A(IFO,IFI)=A(IFI,IFI) $ A(IFO,IPH)=A(IFO,IPH)+A(IFI,IPH)
      B(IFO,IFI)=B(IFI,IFI) $ AFI2(IFO,IPH)=AFI2(IFO,IPH)+AFI2(IFI,IPH)
      D(IFO,IFI)=D(IFI,IFI) $ D(IFO,IPH)=D(IFO,IPH)+D(IFI,IPH)
      G(IFO)=G(IFO)+G(IFI) $ B(IFO,IL)=B(IFO,IL)+B(IFI,IL)
      AFI2(IFO,IFI)=AFI2(IFI,IFI) $ DFI1(IFO,IFI)=DFI1(IFI,IFI)
      DFI1(IFO,IPH)=DFI1(IFO,IPH)+DFI1(IFI,IPH)
C     TOTAL FLUX OF CHLORINE ATOMS IS CONSTANT
      ECL=Z(IFO)+Z(ICU)-Z(IFI)-Z(ICO)
      DO 37 K=1,N
      A(ICL,K)= A(ICL,K) + ECL*A(ICO,K)
      AFI2(ICL,K)=AFI2(ICL,K)+ECL*AFI2(ICO,K)
      B(ICL,K)= B(ICL,K) + ECL*B(ICO,K)
      DFI1(ICL,K)=DFI1(ICL,K)+ECL*DFI1(ICO,K)
   37 D(ICL,K)= D(ICL,K) + ECL*D(ICO,K)
      G(ICL)= G(ICL) + ECL*G(ICO)
C     EQUATION 1, REACTION RATE EXPRESSION
      A(ICO,IFI)=-A(IFI,IFI)$A(ICO,IPH)=A(ICO,IPH)-A(IFI,IPH)
      B(ICO,IFI)=-B(IFI,IFI)
      D(ICO,IFI)=-D(IFI,IFI)$D(ICO,IPH)=D(ICO,IPH)-D(IFI,IPH)
      G(ICO)=G(ICO)-G(IFI) $  B(ICO,IL)=B(ICO,IL)-B(IFI,IL)
      DFI1(ICO,IFI)=-DFI1(IFI,IFI) $ AFI2(ICO,IFI)=-AFI2(IFI,IFI)
      AFI2(ICO,IPH)=AFI2(ICO,IPH)-AFI2(IFI,IPH)
       DFI1(ICO,IPH)=DFI1(ICO,IPH)-DFI1(IFI,IPH)
C     EQUATION  9, CONCENTRATION OF CUPROUS SPECIES IS ZERO
C     PIN THE POSITION OF THE THE PLANE IF NECESSARY.
      IF(JCOUNT-0)23,23,24
   23 B(IL,IL)=1.0 $ G(IL)=C(IL,J) $ GO TO 25
   24 B(IL,ICO)=1.0
```

```
   25 CONTINUE
C     EQUATION 4, CONCENTRATION OF FERRIC SPECIES IS ZERO
      A(IFI,IFI)=0.0 $ D(IFI,IFI)=0.0 $ B(IFI,IL)=0.0 $ G(IFI)=0.0
      A(IFI,IPH)=0.0 $ D(IFI,IPH)=0.0 $ DFI1(IFI,IFI)=0.
      DFI1(IFI,IPH)=0. $ AFI2(IFI,IFI)=0. $ AFI2(IFI,IPH)=0.
      B(IFI,IFI) = 1.0
      DO 53 I=1,NM2 $ RAT=AT1I2(IPH,I)/AT1I2(I,I)
      AT1I2(IPH,IPH)=AT1I2(IPH,IPH)-RAT*AT1I2(I,IPH)
      CAT=DT2I1(IPH,I)/DT2I1(I,I)
      DT2I1(IPH,IPH)=DT2I1(IPH,IPH)-CAT*DT2I1(I,IPH)
      GT1(IPH)=GT1(IPH)-RAT*GT1(I) $ GT2(IPH)=GT2(IPH)-CAT*GT2(I)
      DO 53 K=1,N $ BT1(IPH,K)=BT1(IPH,K)-RAT*BT1(I,K)
      DT1(IPH,K)=DT1(IPH,K)-RAT*DT1(I,K)
      AT2(IPH,K)=AT2(IPH,K)-CAT*AT2(I,K)
   53 BT2(IPH,K)=BT2(IPH,K)-CAT*BT2(I,K)
      DO 58 K=1,NM1 $ DO 58 I=1,N    $ RAT=AFI2(I,K)/AT1I2(K,K)
      CAT=DFI1(I,K)/DT2I1(K,K)
      G(I)=G(I)-RAT*GT1(K)-CAT*GT2(K)
      DO 58 L=K,N
      AFI2(I,L)=AFI2(I,L)-AT1I2(K,L)*RAT
      DFI1(I,L)=DFI1(I,L)-DT2I1(K,L)*CAT
      A(I,L)=A(I,L)-AT2(K,L)*CAT $ B(I,L)=B(I,L)-BT1(K,L)*RAT-BT2(K,L)
     1 *CAT
   58 D(I,L)=D(I,L)-DT1(K,L)*RAT
      CALL BAND(J)
      GO TO 4
   16 IF(J.EQ.NJ) GO TO 18
C      MATERIAL BALANCE REGION 1
      V(J)=3.0*DIF(IR)*C(IL,J)*(C(IL,J)*FLOAT(NJ-J-1)/QNP)**2
      DO 17 I=1,NM2 $ IF(I.EQ.IFI)GOTO17
      CONST    = Z(I)*U(I)*F/DIF(I)
      IF(J-NJ1)29,29,33
   29 PP=CONST*(C(IPH,J+1)-CIP2(IPH))/2. $ PPP=CONST*(C(IPH,J+1)
     1 +CIP2(IPH)-2.*C(IPH,J)) $ CP=(C(I,J+1)-CIP2(I))/2. $ GO TO 45
   33 PP = CONST    *(C(IPH,J+1)-C(IPH,J-1))/2.0
      PPP = CONST    *(C(IPH,J+1)+C(IPH,J-1)-2.0*C(IPH,J))
      CP = (C(I,J+1)-C(I,J-1))/2.0
   45 A(I,I) = -1.0 + PP/2.0 - V(J)/DIF(I)/QNP/2.0
      B(I,I) = 2.0 - PPP
      D(I,I) = -1.0 - PP/2.0 + V(J)/DIF(I)/QNP/2.0
      A(I,IPH) = CONST    *(CP/2.0 - C(I,J))
      B(I,IPH) = CONST    *2.0*C(I,J)
      D(I,IPH) = -CONST    *(CP/2.0 + C(I,J))
      B(I,IL)=3.0*V(J)*CF/DIF(1)/QNP/C(IL,J)
      G(I) = -PPP*C(I,J) - PP*CP + B(I,IL)*C(IL,J)
   17 CONTINUE
      IF(J.EQ.NJ1)GO TO 51
      B(IFI,IFI) = 1.0
      CALL BAND(J)
      GO TO 4
C     BOUNDARY CONDITION AT THE ELECTRODE
   18 DO 19 I = 1,NM2
      CP=DIF(I)*(C(I,J)-C(I,J-2))/2./C(IL,J-1)*QNP
      PP = Z(I)*U(I)*F*(C(IPH,NJ)-C(IPH,NJ-2))/2.0/C(IL,J)*QNP
      Y(I,I)=-DIF(I)/2.0/C(IL,J)*QNP
      A(I,I) = PP
      B(I,I)=-Y(I,I)
      Y(I,IPH)=-Z(I)*U(I)*C(I,J-1)*F/2./C(IL,J)*QNP
      B(I,IPH) = -Y(I,IPH)
      B(I,IL)=-PP*C(I,J-1)/C(IL,J)-CP/C(IL,J)
   19 G(I)=-CP
      DO 35 K=1,NR$ GI(K)=0.0 $ DO  35 I=1,NM2
```

```
35 QA(K,I)=0.0
   QA(1,5)=R1A*3.*C(5,J-1)**2
   QA(1,1)=-R1C  $ QI(1)=QA(1,5)*C(5,J-1)/1.5
   QA(2,2)=-R2C*C(ICL,J-1)**2 $ QA(2,1)=R2A
   QA(2,5)=2.*QA(2,2)*C(2,J-1)/C(ICL,J-1)
   QI(2)=QA(2,5)*C(ICL,J-1)
   R3T=1./(1.-R3A*C(5,J-1)/(R1A*C(5,J-1)**3-R1C*C(1,J-1)))
   R3TT=1./(R1A*C(5,J-1)**3-R1C*C(1,J-1))
   QA(3,3)=-R3C*R3T
   QA(3,1)=-R3C*C(3,J-1)*R3T**2*R3A*C(5,J-1)*R3TT**2*R1C
   QA(3,5)= R3C*C(3,J-1)*R3T**2*(R3A*C(5,J-1)*R3TT**2*3.*R1A
  1 *C(5,J-1)**2-R3A*R3TT)
   QI(3)= -QA(3,1)*C(1,J-1)-QA(3,5)*C(5,J-1)
   IF(ABS(S(IH2,4)).LT..4)GOTO57
   QA(4,IH2)=R4A*0.5/C(IH2,J-1)**0.5 $ QA(4,IHP)=-R4C
   QI(4)=-R4A*0.5*C(IH2,J-1)**0.5
57 CONTINUE
   DO 34 I=1,NM2 $ DO 34 K=1,NR$ G(I)=G(I)+S(I,K)*QI(K)
   DO 34 II=1,NM2
34 A(I,II)=A(I,II)+S(I,K)*QA(K,II)
   CALL BAND(J)
   DO 54 I=1,NM1 $ DO 54 K=1,N
   GT2(I)=GT2(I)-AT2(I,K)*C(K,NJ1-1)-BT2(I,K)*C(K,NJ1)
54 GT1(I)=GT1(I)-DT1(I,K)*C(K,NJ1+1)-BT1(I,K)*C(K,NJ1)
   DO 56 II=2,NM1 $ IR=NM1-II+2 $ IM1=IR-1
   RATI1=GT2(IR)/DT2I1(IR,IR)$CIP1(IR)=RATI1
   RATI2=GT1(IR)/AT1I2(IR,IR) $ CIP2(IR)=RATI2 $ DO 56 I=1,IM1
    GT2(I)=GT2(I)-DT2I1(I,IR)*RATI1
56 GT1(I)=GT1(I)-AT1I2(I,IR)*RATI2 $CIP1(1)=GT2(1)/DT2I1(1,1)
    CIP2(1)=GT1(1)/AT1I2(1,1)
   ZMAX=H2*FLOAT(NJ1-1)+C(IL,NJ)
   DO 39 J=1,NJ  $XIP(J)=H2*FLOAT(J-1)
   IF(J.GE.NJ1)XIP(J)=C(IL,NJ1)/QNP*FLOAT(J-NJ1)+H2*FLOAT(NJ1-1)
39 XI(J)=ZMAX-XIP(J)
   DO 43 J=1,NJ
   IF(J.EQ.1.OR.J.EQ.NJ)GO TO 43
   SUMKC=0.0 $ DO 42 I=1,NM2
42 SUMKC=SUMKC+Z(I)**2*U(I)*C(I,J) $ RK(J)=SUMKC*F**2/1000.
   SUMDP=0.0
   DO 41 I=1,NM2
   DC = (C(I,J+1)-C(I,J-1))/2.0/H2
   IF(J.EQ.NJ1)DC=(C(I,J+1)-C(I,J))/C(IL,J)*QNP
   IF(J.GT.NJ1)DC=DC*H2/C(IL,NJ1)*QNP
41 SUMDP=SUMDP+Z(I)*DIF(I)*DC $ CP(J)= F/RK(J)*SUMDP /1000./DELTA
43 CONTINUE
   AMPO = AMP
   CR0=C(IR,NJ-1)
   AMP = (Z(IR )*U(IR )*F*CR0*(C(IPH,NJ-2) - C(IPH,NJ))+
  1DIF(IR )*(C(IR ,NJ-2) - C(IR ,NJ)))*QNP/C(IL,NJ1)/2.0/
  1(CIN(IR )-CR0)/DIF(IR )
   IF( ABS(AMP-AMPO) - TOL     * ABS(AMP)) 22,22,20
20 IF(JCOUNT-20)2,2,21
21 PRINT 106
   NOTCON=1
22 PRINT 798,JCOUNT
   PRINT 105
   EMIGR = AMP/1.1198
   AMP=EMIGR*(1.-CR0/CIN(IR))
   PRINT 107,AMP,EMIGR,(REF1(I),REF2(I),C(I,1),C(I,NJ-1),I=1,NM2)
   ZMAX=H2*FLOAT(NJ1-1)+C(IL,NJ)
   RL=C(IL,NJ1)*DELTA  $ ZZMAX=ZMAX*DELTA
   PRINT 108,C(IL,NJ1),RL,ZMAX,ZZMAX,RPM
```

```
      IF(NOTCON.EQ.1)GOTO12
      RILD=RN2*F*DIF(IR)*CIN(IR)/S(IR,2)/DELTA/DDELT/1000.
      R1=(R1A*C(ICL,NJ-1)**3-R1C*C(ICO,NJ-1))/RILD*RN1*F/1000./DELTA
      IF(ABS(S(ICO,1)).LT.0.5)R1=0.0
      R2=(R2A*C(ICO,NJ-1)-R2C*C(ICL,NJ-1)**2*C(ICU,NJ-1))/RILD*RN2*F
     1 /1000./DELTA
      R3=-R3C*C(3,NJ-1)*R3T/RILD*RN3*F/1000./DELTA
      IF(ABS(S(IFO,3)).LT.0.5)R3=0.0
      R4=(R4A*C(IH2,NJ-1)**0.5-R4C*C(IHP,NJ-1))/RILD*RN4*F/1000./DELTA
      IF(ABS(S(IH2,4)).LT.0.4)R4=0.
      RIT=R1+R2+R3+R4 $ EFF=R 1/RIT*100.
      SUM=0.0
      DO 11 I=1,NM2
   11 SUM=SUM+Z(I)**2*U(I)*CIN(I)
      RKAPPA=F**2*SUM/1000.
      PTO=RIT*RILD*ZMAX*DELTA/RKAPPA
      UNTH=0.2676 $ VMPO=E-UNTH+U1TH $ VMPTO=VMPO+C(IPH,NJ-1)-PTO
      CRR=CRO/CIN(IR)
      RP=-F*DIF(ICO)*((C(ICO,NJ1+1)-C(ICO,NJ1))/C(IL,NJ1)*QNP) /RILD
      PRINT 110,R1,R2,R3,R4,RIT,EFF
      ALNCRR=ALOG(CRR) $ ALNCO=ALOG(C(ICO,NJ-1)/CIN(ICU))
      ALNCL=ALOG(C(ICL,NJ-1)/CIN(ICL))
      PRINT 111, VMPTO,VMPO,RILD,PTO,RP,CRR,RKAPPA,ALNCRR,ALNCO,ALNCL
      PUNCH 112,VMPTO,VMPO,RIT,R1,R2,EFF,C(IL,1),ALNCL,ALNCRR,ALNCO
      IF(IPUNCH.GT.0)PUNCH 800,((C(I,J),I=1,N),XI(J),J=1,NJ)
      DO 46 I=1,N $ DO 46 J=1,NJ
   46 P(I,J)=C(I,J)
      GO TO 12
      END
      SUBROUTINE BAND(J)
      DIMENSION A(9,9),B(9,9),C(9,203),D(9,19),G(9), X(9,9),Y(9,9),
     1 E(9,10,203)
      COMMON A,B,C,D,G,X,Y,N,NJ
  101 FORMAT (15H0DETERM=0 AT J=,I4)
      IF (J-2)  1,6,8
    1 NP1= N + 1
      DO 2 I=1,N
      D(I,2*N+1)= G(I)
      DO 2 L=1,N
      LPN= L + N
    2 D(I,LPN)= X(I,L)
      CALL MATINV (N,2*N+1,DETERM)
      IF (DETERM)  4,3,4
    3 PRINT 101, J
    4 DO 5 K=1,N
      E(K,NP1,1)= D(K,2*N+1)
      DO 5 L=1,N
      E(K,L,1)= - D(K,L)
      LPN= L + N
    5 X(K,L)= - D(K,LPN)
      RETURN
    6 DO 7 I=1,N
      DO 7 K=1,N
      DO 7 L=1,N
    7 D(I,K)= D(I,K) + A(I,L)*X(L,K)
    8 IF (J-NJ)  11,9,9
    9 DO 10 I=1,N
      DO 10 L=1,N
      G(I)= G(I) - Y(I,L)*E(L,NP1,J-2)
      DO 10 M=1,N
   10 A(I,L)= A(I,L) + Y(I,M)*E(M,L,J-2)
   11 DO 12 I=1,N
```

```
      D(I,NP1)= - G(I)
      DO 12 L=1,N
      D(I,NP1)= D(I,NP1) + A(I,L)*E(L,NP1,J-1)                          \
      DO 12 K=1,N
   12 B(I,K)= B(I,K) + A(I,L)*E(L,K,J-1)
      CALL MATINV (N,NP1  ,DETERM)
      IF (DETERM)  14,13,14
   13 PRINT 101, J
   14 DO 15 K=1,N
      DO 15 M=1,NP1
   15 E(K,M,J)= - D(K,M)
      IF (J-NJ)  20,16,16
   16 DO 17 K=1,N
   17 C(K,J)= E(K,NP1,J)
      DO 18 JJ=2,NJ
      M= NJ - JJ + 1
      DO 18 K=1,N
      C(K,M)= E(K,NP1,M)
      DO 18 L=1,N
   18 C(K,M)= C(K,M) + E(K,L,M)*C(L,M+1)
      DO 19 L=1,N
      DO 19 K=1,N
   19 C(K,1)= C(K,1) + X(K,L)*C(L,3)
   20 RETURN
      END
      SUBROUTINE MATINV(N,M,DETERM)  $  COMMON A,B,C,D
      DIMENSION A(9,9),B(9,9),C(9,203),D(9,19),JCOL(9),X(9,19)
      NM1=N-1 $ DETERM=1.0 $ DO 1 I=1,N $ JCOL(I)=I $ DO 1 K=1,M
    1 X(I,K)=D(I,K) $ DO 6 II=1,NM1 $ IP1=II+1 $ BMAX=ABS(B(II,II))
      JC=II $ DO 2 J=IP1,N $ IF(ABS(B(II,J)).LE.BMAX) GO TO 2 $ JC=J
      BMAX=ABS(B(II,J))
    2 CONTINUE $ DETERM=DETERM*B(II,JC) $ IF(DETERM.EQ.0.0) RETURN
      IF(JC.EQ.II) GO TO 4 $ JS=JCOL(JC) $ JCOL(JC)=JCOL(II)
      JCOL(II)=JS $ DO 3 I=1,N $ SAVE=B(I,JC) $ B(I,JC)=B(I,II)
    3 B(I,II)=SAVE $ DETERM=-DETERM
    4 DO 6 I=IP1,N $ F=B(I,II)/B(II,II) $ DO 5 J=IP1,N
    5 B(I,J)=B(I,J)-F*B(II,J) $ DO 6 K=1,M
    6 X(I,K)=X(I,K)-F*X(II,K) $ DETERM=DETERM*B(N,N)
      IF(DETERM.EQ.0.0) RETURN $ DO 7 II=2,N $ IR=N-II+2 $ IM1=IR-1
      JC=JCOL(IR) $ DO 7 K=1,M $ F=X(IR,K)/B(IR,IR) $ D(JC,K)=F
      DO 7 I=1,IM1
    7 X(I,K)=X(I,K)-B(I,IR)*F $ JC=JCOL(1) $ DO 8 K=1,M
    8 D(JC,K)=X(1,K)/B(1,1) $ RETURN $ END
```

```
.00000000242  .000006          -2.0              CU(CL)32-
.00000000242  .0000060         1.0               CUCL+
.00000000298  .00000739         1.0              FECL+
.00000000361  .00000896         2.0              FECL++
.000000008197 .00002032        -1.0              CL-
.000000037560 .00009312        1.0               H+
.0000000153   .000038          0.0               H2
 0.0       1.5       0.0        3.0        0.          0.1       .0000000004155
 88  77  .05       -.3          1    1
 88  77  .05       -.29
 88  77  .05       -.28
 88  77  .05       -.27
 88  77  .05       -.26
 88  77  .05       -.25
```

Notation

a	0.51023262 (see reference 44)
a_i	relative activity of species i
a_i^θ	property expressing secondary reference state of species i, ℓ/mol
$a_{i,n}^\theta$	property expressing secondary reference state of species i relative to ionic species n (see equation A-15)
B_n	coefficient in the expansion for the potential, V
c_i	concentration of species i, mol/cm^3
$c_{i,o}$	local surface concentration of species i, mol/cm^3
$c_{i,ref}$	reference concentration of species i, mol/cm^3
$c_{i,\infty}$	bulk concentration of species i, mol/cm^3
D_i	diffusion coefficient of species i, cm^2/s
f_i	molar activity coefficient of species i
$f_{i,n}$	molar activity coefficient of species i relative to the ionic species n (see equation A-14)
F	Faraday's constant, 96,487 C/mol
h	dimensionless mesh size
i_{avg}	average current density, A/cm^2
i_j	local current density due to reaction j, A/cm^2
i_{LD}	limiting current density due to diffusion (see equation 2-18), A/cm^2
$i_{m,lim}$	limiting current density for the main reaction, A/cm^2
$i_{oj,ref}$	reference exchange current density, A/cm^2
i_T	total local electrode current density, A/cm^2
I	total current, A
J_j	dimensionless exchange current density

J'_j	dimensionless exchange current density (see equation B-18)
K	equilibrium constant for reaction 2-5, $(kg/mol)^2$
L	position of the reaction plane, cm
M_i	symbol for the chemical formula of species i
M_{2n}	Legendre function of imaginary argument
n_j	number of electrons transferred in reaction j
N	dimensionless limiting current density
N'	dimensionless limiting current density (see equation B-15)
N_i	normal component of the flux of species i, mol/cm^2-s
p_i	total pressure times mole fraction of component i in the vapor phase, atm
p_{ij}	anodic reaction order
P_{2n}	Legendre polynomial of order 2n
q_{ij}	cathodic reaction order
r	radial coordinate, cm
r_o	electrode radius, cm
R	universal gas constant, 8.3143 J/mol-K
s_{ij}	stoichiometric coefficient of species i in reaction j
t_i^o	transference number of species i with respect to the velocity of species o
T	absolute temperature, K
u_i	mobility of species i, cm^2-mol/J-s
$U_{j,o}$	theoretical open-circuit potential for reaction j at the composition prevailing locally at the electrode surface, relative to a reference electrode of a given kind, V
$U_{j,ref}$	theoretical open-circuit potential evaluated for reference concentrations, V
U_j^θ	standard electrode potential for reaction j, V
ΔU_j	parameter characteristic of the cathodic part of reaction j relative to a main reaction, V

V	potential of the rotating-disk electrode, V
V_m	electrode potential characteristic of the limiting-current plateau for the main reaction, V
x	dummy integration variable, cm
y	axial coordinate, cm
z	axial coordinate, cm
z_i	charge number of species i
α_{aj}	anodic transfer coefficient for reaction j
α_{cj}	cathodic transfer coefficient for reaction j
γ_{ij}	exponent in composition dependence of exchange current density
$\Gamma(4/3)$	0.89298., the gamma function of 4/3
ζ	dimensionless radial coordinate (see equation B-7)
δ	dimensionless average current density (see equation 1-13)
δ	diffusion-layer thickness, cm (see equation 2-8)
δ_d	diffusion-layer thickness, cm (see equation 1-5)
η	rotational elliptic coordinate
η_j	local total overpotential for reaction j, V
η_{cj}	local concentration overpotential for reaction j, V
η_{sj}	local surface overpotential for reaction j, V
Θ_i	dimensionless concentration of species i
κ	solution conductivity, $ohm^{-1}-cm^{-1}$
κ_∞	bulk solution conductivity, $ohm^{-1} - cm^{-1}$
λ_i	absolute activity of species i
λ_i^θ	property expressing secondary reference state, kg/mol
μ_i	electrochemical potential of species i, J/mol

ν kinematic viscosity of the solution, cm^2/s

ξ dimensionless axial coordinate (see equation 2-7)

ξ rotational elliptic coordinate

ρ_o pure solvent density, kg/cm^3

ϕ_i fugacity coefficient of gaseous species i

Φ potential in solution within the diffusion layer, V

Φ_o local solution potential adjacent to electrode surface, V

$\tilde{\Phi}$ potential in the solution outside the diffusion layer, V

$\tilde{\Phi}_o$ local potential in the bulk solution extrapolated to the electrode surface, V

Ω rotation speed of the disk, rad/s

superscripts

o pure species or trial value

* ideal-gas secondary reference state

θ secondary reference state at infinite dilution

subscripts

o at the electrode surface

m main reaction

re reference electrode

R principal reactant

s side reaction

∞ bulk solution

References

1. A. C. Riddiford, "The Rotating Disk System," Advances in Electrochemistry and Electrochemical Engineering, 4 (1966), 47-116.

2. František Opekar and Přemysl Beran, "Rotating Disk Electrodes," Journal of Electroanalytical Chemistry, 69 (1976), 1-105.

3. V. Yu. Filinovsky and Yu. V. Pleskov, "Rotating Disk and Ring-Disk Electrodes in Investigations of Surface Phenomena at the Metal-Electrolyte Interface," Progress in Surface and Membrane Science, 10 (1976), 27-113.

4. W. J. Albery and M. L. Hitchman, Ring-disc Electrodes, London: Oxford University Press, 1971.

5. Jan Robert Selman, Measurement and Interpretation of Limiting Currents, Ph.D. Dissertation, University of California, Berkeley, 1971.

6. J. Robert Selman and Charles W. Tobias, 'Mass-Transfer Measurements by the Limiting-Current Technique," Thomas B. Drew, Giles R. Cokelet, John W. Hoopes, Jr., and Theodore Vermeulen, eds., Advances in Chemical Engineering, 10, to be published.

7. Ralph White, James A. Trainham, John Newman, and Thomas W. Chapman, "Potential-Selective Deposition of Copper from Chloride Solutions Containing Iron," Journal of the Electrochemical Society, to be published.

8. Kameo Asada, Fumio Hine, Shiro Yoshizawa, and Shinzo Okada, "Mass Transfer and Current Distribution under Free Convection Conditions," Journal of the Electrochemical Society, 107 (1960), 242-246.

9. John Newman, "The Effect of Migration in Laminar Diffusion Layers," International Journal of Heat and Mass Transfer, 10 (1967), 983-997.

10. John Newman, "Current Distribution on a Rotating Disk below the Limiting Current," Journal of the Electrochemical Society, 113 (1966), 1235-1241.

11. John Newman, "The Diffusion Layer on a Rotating Disk Electrode," Journal of the Electrochemical Society, 114 (1967), 239.

12. W. R. Parrish and John Newman, "Current Distribution on a Plane Electrode below the Limiting Current," Journal of the Electrochemical Society, 116 (1969), 169-172.

13. D. H. Angell, T. Dickinson, and R. Greef, "The Potential Distribution near a Rotating-Disk Electrode," Electrochimica Acta, 13 (1968), 120-123.

14. W. J. Albery and J. Ulstrup, "The Current Distribution on a Rotating Disk Electrode," Electrochimica Acta, 13 (1968), 281-284.

15. Vinay Marathe and John Newman, "Current Distribution on a Rotating Disk Electrode," Journal of the Electrochemical Society, 116 (1969), 1704-1707.

16. Stanley Bruckenstein and Barry Miller, "An Experimental Study of Nonuniform Current Distribution at Rotating Disk Electrodes," Journal of the Electrochemical Society, 117 (1970), 1044-1048.

17. William H. Smyrl and John Newman, "Ring-Disk and Sectioned Disk Electrodes," Journal of the Electrochemical Society, 119 (1972), 212-219.

18. William H. Smyrl and John Newman, "Detection of Nonuniform Current Distribution on a Disk Electrode," Journal of the Electrochemical Society, 119 (1972), 208-212.

19. John Newman, "Engineering Design of Electrochemical Systems," Industrial and Engineering Chemistry, 60 (no. 4 , April, 1968), 12-27.

20. W. R. Parrish and John Newman, "Current Distributions on Plane, Parallel Electrodes in Channel Flow," Journal of the Electrochemical Society, 117 (1970), 43-48.

21. John Newman, "The Fundamental Principles of Current Distribution and Mass Transport in Electrochemical Cells," Allen J. Bard, ed., Electroanalytical Chemistry, 6 (1973), 187-352, New York: Marcel Dekker, Inc.

22. John S. Newman, Electrochemical Systems, Englewood Cliffs, N.J.: Prentice-Hall, Inc., 1973.

23. Peter Pierini, Peter Appel, and John Newman, "Current Distribution on a Disk Electrode for Redox Reactions," Journal of the Electrochemical Society, 123 (1976), 366-369.

24. Peter Pierini and John Newman, "Current Distribution on a Rotating Ring-Disk Electrode below the Limiting Current," Journal of the Electrochemical Society, to be published.

25. Richard Alkire and Ali Asghar Mirarefi, "The Current Distribution Within Tubular Electrodes under Laminar Flow," Journal of the Electrochemical Society, 120 (1973), 1507-1515.

26. Richard Alkire and Ali Asghar Mirarefi, "Current Distribution in a Tubular Electrode: Two Electrode Reactions," Journal of the Electrochemical Society, to be published.

27. Reinaldo Cabán and Thomas W. Chapman, "Rapid Computation of Current Distribution by Orthogonal Collocation," Journal of the Electrochemical Society, 123 (1976), 1036-1041.

28. Reinaldo Cabán and Thomas W. Chapman, "Statistical Analysis of Electrode Kinetics Measurements-Copper Deposition from $CuSO_4$-H_2SO_4 Solutions," Journal of the Electrochemical Society, to be published.

29. Philip M. Morse and Herman Feshback, Methods of Theoretical Physics, New York: McGraw Hill Book Company, Inc., 1953.

30. Daniel E. Rosner, "Reaction Rates on Partially Blocked Rotating Disk - Effect of Chemical Kinetic Limitations," Journal of the Electrochemical Society, 113 (1966), 624-625.

31. Daniel E. Rosner, "Effects of convective diffusion on the apparent kinetics of zeroth order surface-catalysed chemical reactions," Chemical Engineering Science, 21 (1966), 223-239.

32. B. Levich, "The Theory of Concentration Polarization," Acta Physicochimica U.R.S.S., 17 (1942), 257-307.

33. Heinz.Gerischer, "Eine Einführung in die Method zur Untersuchung der Kinetik von Elektrodenprozessen," Zeitschrift für Elektrochemie, 59 (1955), 604-612.

34. Paul Delahay, Double Layer and Electrode Kinetics, New York: Interscience Publishers, 1965, p. 170.

35. Andreas Acrivos and Paul L. Chambré, "Laminar Boundary Layer Flows with Surface Reactions," Industrial and Engineering Chemistry, 49 (1957), 1025-1029.

36. Charles Milton Mohr, Jr., Mass Transfer in Rotating Electrode Systems, Ph.D. Dissertation, University of California, Berkeley, 1975.

37. Limin Hsueh, Diffusion and Migration in Electrochemical Systems, Ph.D. Dissertation, University of California, Berkeley, 1968.

38. John Newman and Limin Hsueh, "Currents Limited by Gas Solubility," Industrial and Engineering Chemistry Fundamentals, 9 (1970), 677-679.

39. O. R. Brown and H. R. Thirsk, "The Rate-Determining Step in the Electrodeposition of Copper on Copper from Aqueous Cupric Sulfate Solutions," Electrochimica Acta, 10 (1965), 383-393.

40. Charles M. Mohr, Jr., and John Newman, "Mass Transfer to a Rotating Disk in Transition Flow," Journal of the Electrochemical Society, 123 (1976), 1687-1691.

41. Leonard Nanis and Wallace Kesselman, "Engineering Applications of Current and Potential Distributions in Disk Electrode Systems," Journal of the Electrochemical Society, 118 (1971), 454-461.

42. Charles K. Bon, Supersaturation at Gas-Evolving Electrodes, M.S. Thesis, University of California, Berkeley, 1970.

43. John Newman, "Resistance for Flow of Current to a Disk," Journal of the Electrochemical Society, 113 (1966), 501-502.

44. Ralph White, Charles M. Mohr, Jr., and John Newman, "The Fluid Motion Due to a Rotating Disk," Journal of the Electrochemical Society, 123 (1976), 383-385.

45. F. P. Haver and M. M. Wong, "Recovery of Copper, Iron and Sulfur from Chalcopyrite Concentrates Using a Ferric Chloride Leach," J. Metals, 23 (2), 25-29 (1971).

46. F. P. Haver, R. D. Baker, and M. M. Wong, "Improvements in Ferric Chloride Leaching of Chalcopyrite Concentrate," U.S. Bureau of Mines RI 8007, 1975, 16 pp.

47. P. R. Kruesi, E. S. Allen, and J. L. Lake, "Cymet Process - Hydrometallurgical Conversion of Base Metal Sulfides to Pure Metals," CIM Bulletin, Vol. 66, No. 734, June 1973, pp. 81-87.

48. K. N. Subramanian and P. H. Jennings, "Review of the Hydrometallurgy of Chalcopyrite Concentrates," Canadian Metallurgical Quarterly, 11(2), 387-400 (1972).

49. Carl Rampacek and James T. Dunham, "Copper Ore Processing - U.S. Practices and Trends," Mining Congress Journal, February 1976, pp. 43-50.

50. Wayne L. Chambers and Ronald W. Chambers, "Electrolytic Copper Producing Process," U.S. Patent 3,692,647, September 19, 1972.

51. K. J. Cathro, "Recovery of Copper from Chalcopyrite by Means of a Cupric Chloride Leach," International Symposium on Copper Extraction and Refining, The Metallurgical Society of AIME, New York, 1976, Vol. II, pp. 776-792.

52. W. W. Harvey and F. O. Dudas, "Hydrochloric Acid Leach Processes for Copper Concentrates," presentedat AIME Annual Meeting, Las Vegas, Nevada, February 22-26, 1976. SME-AIME Preprint No. 76-B-73.

53. G. E. Atwood and C. H. Curtis, "Hydrometallurgical Process for the Production of Copper," U.S. Patent 3,785,944, January 15, 1974.

54. T. D. Kaun, "Chloride Hydrometallurgy; A Bench Scale Process for Brass Scrap," M.S. Thesis, University of Wisconsin, Madison, 1975.

55. J. E. Dutrizac and R. J. C. MacDonald, "Ferric Ion as a Leaching Medium," Minerals Sci. Engng., 6(2), 59-100 (1974).

56. R. J. Roman and B. R. Benner, "The Dissolution of Copper Concentrates," Minerals Sci. Engng., 5(1), 3-24 (1973).

57. D. L. Jones and E. Peters, "The Leaching of Chalcopyrite with Ferric Sulphate and Ferric Chloride," International Symposium on Copper Extraction and Refining, The Metallurgical Society of AIME, New York, 1976, Vol. II, pp. 633-653.

58. W. Kunda, R. Hitesman, and H. Veltman, "Treatment of Copper Concentrate in Chloride Systems," International Symposium on Copper Extraction and Refining, The Metallurgical Society of AIME, New York, 1976, Vol. II, pp. 793-822.

59. M. M. Wong, F. P. Haver, and R. D. Baker, "Electrodeposition of Copper from Chloride Solutions," paper presented at Annual Meeting of AIME, New York, February 16-20, 1975.

60. R. F. P. Winand, P. P. Andrianne, and J. P. Dubois, "The Electrocyrstallization of Copper in Chloride Aqueous Solutions," presented at AIME Annual Meeting, Las Vegas, Nevada, February 22-26, 1976.

61. James A. Trainham and Thomas W. Chapman, "Mixed Potentials and Current Efficiency in Copper Chloride Solutions," to be submitted.

62. Lars Gunnar Sillén, and Arthur E. Martell, Stability Constants of Metal-Ion Complexes, London: The Chemical Society, Burlington House, W.1, Special Publication No. 17, 1964.

63. Marie-José Schwing-Weill, "Étude des complexes chlorés du cuivre (II) en solution aqueuse," Bulletin de la Société chimique de France No. 3 (1973), 823-830.

64. Tor Hurlen, "Electrochemical Behaviour of Copper in Acid Chloride Solution," Acta Chemica Scandinavica, 15 (1961), 1231-1238.

65. Limin Hsueh and John Newman, "The Role of Bisulfate Ions in Ionic Migration Effects," Industrial and Engineering Chemistry Fundamentals, 10 (1971), 615-620.

66. Sirôzi Hatta, "On the Absorption Velocity of Gases by Liquids. I. Absorption of Carbon Dioxide by Potassium Hydroxide," The Technology Reports of the Tôhoku Imperial University, 8 (1928), 1-25.

67. D. W. Van Krevelen and P. J. Hoftijzer, "Kinetics of Gas-Liquid Reactions Part I. General Theory," Recueil des Travaux Chimiques des Pays-Bas, 67 (1948), 563-586.

68. P. V. Danckwerts, "Absorption by Simultaneous Diffusion and Chemical Reaction," Transactions of the Faraday Society, 46 (1950), 300-304.

69. Robert H. Perry and Robert L. Pigford, "Kinetics of Gas-Liquid Reactions Simultaneous Absorption and Chemical Reaction," Industrial and Engineering Chemistry, 45 (1953), 1247-1253.

70. Donald R. Olander, "Simultaneous Mass Transfer and Equilibrium Chemical Reaction," A.I.Ch.E. Journal, 6 (1960) 233-239.

71. Thomas K. Sherwood and Robert L. Pigford, Absorption and Extraction, New York: McGraw-Hill Book Company, Inc., 1952.

72. Giovanni Astarita, Mass Transfer with Chemical Reaction, Amsterdam: Elsevier Publishing Company, 1967.

73. P. V. Danckwerts, Gas-Liquid Reactions, New York: McGraw-Hill Book Company, 1970.

74. Thomas K. Sherwood, Robert L. Pigford, and Charles R. Wilke, Mass Transfer, New York: McGraw-Hill Book Company, 1975.

75. James J. Carberry, Chemical and Catalytic Reaction Engineering, New York: McGraw-Hill Book Company, 1976.

76. S. K. Friedlander and Mitchell Litt, "Diffusion controlled reaction in a laminar boundary layer," Chemical Engineering Science, 7 (1958), 229-234.

77. A. Acrivos, "On laminar boundary layer flows with a rapid homogeneous chemical reaction," Chemical Engineering Science, 13 (1960), 57-62.

78. Veniamin G. Levich, Physicochemical Hydrodynamics, Englewood Cliffs, N.J.: Prentice-Hall, Inc., 1962, p. 345.

79. R. Byron Bird, Warren E. Stewart, and Edwin N. Lightfoot, Transport Phenomena, New York: John Wiley & Sons, Inc., 1960.

80. Andreas Acrivos, Editor, Modern Chemical Engineering, 1, New York: Reinhold Publishing Corporation, 1963.

81. Paul L. Chambré, "On the Ignition of a Moving Combustible Gas Stream," The Journal of Chemical Physics, 25 (1956), 417-421.

82. Michael Jischa, "Production Terms in Chemically Reacting Equilibrium Flows, Discussed for a Binary Mixture Laminar Boundary Layer Flow," International Journal of Heat and Mass Transfer, 16 (1973), 2261-2273.

83. G. T. Sergeev, "Distribution of Transfer Parameters During the Reaction of Surface Material of a Body and Injected Material with a Laminar Boundary Layer," Inzh.-Fiz. Zh., 23 (1972), 234-242.

84. F. Coeuret and J. J. Ronco, "Mass Transfer with Irreversible Chemical Reaction in a Laminar Boundary Layer," International Journal of Heat and Mass Transfer, 14 (1971), 2017-2024.

85. Paul L. Chambré and Jonathan D. Young, "On the Diffusion of a Chemically Reactive Species in Laminar Boundary Layer Flow," The Physics of Fluids, 1 (1958), 48-54.

86. A. V. Lykov and G. T. Sergeev, "Distribution of Heat-and Mass-Transfer Parameters in the Presence of a Reaction Front in a Laminar Boundary Layer," Inzh.-Fiz. Zh., 26 (1974), 807-819.

87. Michael Jischa, "An Integral Method for the Nonequilibrium Dissociating Laminar Flat Plate Boundary Layer," International Journal of Heat and Mass Transfer, 15 (1972), 1125-1136.

88. Yu. M. Gershenzon, V. B. Rozenshtein, A. I. Spasskii, and A. M. Kogan, "Homogeneous First-Order Reactions Under Laminar Flow Conditions," Dokl. Akad. Nauk SSSR, 205 (1972), 624-627.

89. Koretsune Ueyama, Jun-ichi Hatanaka, and Kanehiro Ogawa, "Mass Transfer in a Laminar Boundary Layer with Moving Interface," J. Chem. Eng. Jap., 5 (1972), 248-251.

90. Koretsune Ueyama, Jun-ichi Hatanaka, and Kanehiro Ogawa, "Numerical Calculation of Mass Transfer through Laminar Boundary Layer with Moving Interface," J. Chem. Eng. Jap., 5 (1972), 371-375.

91. Norbert Peters, "Analysis of a Laminar Flat Plate Boundary-Layer Diffusion Flame," International Journal of Heat and Mass Transfer, 19 (1976), 385-393.

92. R. B. Bird, W. E. Stewart, E. N. Lightfoot, and T. W. Chapman, "Lectures in Transport Phenomena," AIChE Continuing Education Series 4, New York: American Institute of Chemical Engineers, 1969.

93. John Newman, "Transport Processes in Electrolytic Solutions," Charles W. Tobias, ed., Advances in Electrochemistry and Electrochemical Engineering, 5 (1967), 87-135.

94. John Newman, "Effect of Ionic Migration on Limiting Currents," Industrial and Engineering Chemistry Fundamentals, 5 (1966), 525-529.

95. P. de Voogd, Ir. (M.Sc.) Report, T. H. Delft (1961).

96. Peter Willem Appel, Electrochemical Systems: Impedance of a Rotating Disk and Mass Transfer in Packed Beds, Ph.D. Dissertation, University of California, Berkeley, 1976.

97. Kemal Mustafa Nişancioğlu, Current Distribution and Mass Transfer in Rotating Electrode Systems, Ph.D. Dissertation, University of California, Berkeley, 1973.

98. John Newman, Chemical Engineering Thermodynamics, in preparation.

99. John S. Newman, "Temperature Computed for Distillation," Hydrocarbon Processing and Petroleum Refiner, 42 (no. 4, April 1963), 141-144.

100. Joseph John Miksis, Jr., Primary Resistances for Ring-Disk Electrodes, M.S. Thesis, University of California, Berkeley, 1975.

101. Peter Pierini, private communication, 1976.

102. James A. Trainham, private communication, 1975.

This report was done with support from the United States Energy Research and Development Administration. Any conclusions or opinions expressed in this report represent solely those of the author(s) and not necessarily those of The Regents of the University of California, the Lawrence Berkeley Laboratory or the United States Energy Research and Development Administration.

TECHNICAL INFORMATION DIVISION
LAWRENCE BERKELEY LABORATORY
UNIVERSITY OF CALIFORNIA
BERKELEY, CALIFORNIA 94720